

Washington University in St. Louis

## Washington University Open Scholarship

---

Arts & Sciences Electronic Theses and  
Dissertations

Arts & Sciences

---

Spring 5-15-2015

### Molecular and Epigenetic Regulation of Stem Cell Radiosensitivity

Keith Michael Jacobs

*Washington University in St. Louis*

Follow this and additional works at: [https://openscholarship.wustl.edu/art\\_sci\\_etds](https://openscholarship.wustl.edu/art_sci_etds)



Part of the [Biology Commons](#)

---

#### Recommended Citation

Jacobs, Keith Michael, "Molecular and Epigenetic Regulation of Stem Cell Radiosensitivity" (2015). *Arts & Sciences Electronic Theses and Dissertations*. 453.

[https://openscholarship.wustl.edu/art\\_sci\\_etds/453](https://openscholarship.wustl.edu/art_sci_etds/453)

This Dissertation is brought to you for free and open access by the Arts & Sciences at Washington University Open Scholarship. It has been accepted for inclusion in Arts & Sciences Electronic Theses and Dissertations by an authorized administrator of Washington University Open Scholarship. For more information, please contact [digital@wumail.wustl.edu](mailto:digital@wumail.wustl.edu).

WASHINGTON UNIVERSITY IN ST. LOUIS

Division of Biology and Biomedical Sciences  
Molecular Cell Biology

Dissertation Examination Committee:

Dennis Hallahan, Chair

Susana Gonzalo

Kristen Kroll

Barry Sleckman

Lila Solnica-Krezel

Molecular and Epigenetic Regulation of Stem Cell Radiosensitivity

by

Keith Michael Jacobs

A dissertation presented to the  
Graduate School of Arts & Sciences  
of Washington University in  
partial fulfillment of the  
requirements for the degree  
of Doctor of Philosophy

May 2015

St. Louis, Missouri

© 2015, Keith Michael Jacobs

## Table of Contents

List of Figures.....	iv
List of Tables.....	vii
Acknowledgments.....	viii
Abstract.....	x
Chapter 1: Introduction.....	1
1.1 Radiation Therapy.....	2
1.2 Mechanisms of Cell Death.....	7
1.3 DNA Damage Response.....	12
1.4 Stem Cells.....	14
1.5 DNA Damage-Responsive Histone Modifications.....	19
1.6 Project Summary.....	22
1.7 References.....	26
Chapter 2: Stem Cells are Radiosensitive in Contrast with Differentiated Progeny.....	38
2.1 Abstract.....	39
2.2 Methods.....	39
2.3 Introduction.....	44
2.4 Results.....	46
2.5 Discussion.....	57
2.6 References.....	60
Chapter 3: Stem Cells Exhibit an Attenuated DNA Damage Response.....	64
3.1 Abstract.....	65
3.2 Methods.....	65
3.3 Introduction.....	71
3.4 Results.....	72
3.5 Discussion.....	90
3.6 References.....	93
Chapter 4: Unique Epigenetic Regulation Contributes to Stem Cell Radiosensitivity.....	97
4.1 Abstract.....	98
4.2 Methods.....	98
4.3 Introduction.....	103
4.4 Results.....	105
4.5 Discussion.....	118
4.6 References.....	120

Chapter 5: Conclusions and Ongoing Work.....	123
5.1 Summary.....	124
5.2 Ongoing Work and Future Directions.....	125
5.3 References.....	128
Curriculum Vitae.....	130

## List of Figures

### CHAPTER 1

Figure 1.1: An overview of the DNA Damage Response.....	13
Figure 1.2: Primary stem cell culture models utilized in this study.....	25
Figure 1.3: The interrelatedness of the DDR, differentiation state and epigenetics in controlling cellular radiosensitivity.....	25

### CHAPTER 2

Figure 2.1: IR-induced apoptosis is exclusive to stem cells <i>in vivo</i> .....	47
Figure 2.2: Dose curve of IR-induced apoptosis among stem and non-stem cells <i>in vivo</i> .....	47
Figure 2.3: <i>In vivo</i> sham irradiation apoptosis negative controls.....	48
Figure 2.4: Differentiation of stem cell culture models.....	49
Figure 2.5: Differential viability of ES and ED cells following irradiation.....	50
Figure 2.6: Stem cells but not directly differentiated progeny undergo IR-induced apoptosis in culture.....	51
Figure 2.7: Clonogenic survival of cell culture models after various IR doses.....	52
Figure 2.8: Neutral comet assay on cell culture models at late timepoints.....	52
Figure 2.9: Western blots for apoptotic effectors.....	53
Figure 2.10: BrdU pulse-chase profiles labeling cell cycle progression of unirradiated stem and non-stem cells.....	54
Figure 2.11: Proliferation status of stem and non-stem cells <i>in vivo</i> .....	54
Figure 2.12: Proliferating cells exist both within and outside of the hair follicle bulge stem cell region.....	55
Figure 2.13: Apoptosis relative to proliferation status of stem and non-stem cells <i>in vivo</i> .....	55
Figure 2.14: Model of radiosensitivity relative to proliferation status within the intestinal crypt and villus.....	56
Figure 2.15: Differentially distributed radiosensitivity across the cell cycle in stem and non-stem cells.....	57

## CHAPTER 3

Figure 3.1: Absence of $\gamma$ H2AX IRIF in stem cells <i>in vivo</i> .....	74
Figure 3.2: Sham-irradiated negative controls for <i>in vivo</i> $\gamma$ H2AX IRIF.....	75
Figure 3.3: $\gamma$ H2AX induction is attenuated along DSBs in cultured stem cells.....	75
Figure 3.4: Global attenuation of IR-induced $\gamma$ H2AX in cultured stem cells is not due to reduced H2AX expression.....	76
Figure 3.5: IR-induced ATM activation is attenuated in cultured stem cells.....	76
Figure 3.6: pATM is not recruited to DSBs in cultured stem cells.....	77
Figure 3.7: IR-induced activation and recruitment of ATM IRIF is attenuated in stem cells <i>in vivo</i> .....	77
Figure 3.8: IR-induced ATR activation is attenuated in cultured stem cells.....	78
Figure 3.9: Recruitment of pDNA-PKcs to DSBs is attenuated in stem cells both in culture and <i>in vivo</i> .....	78
Figure 3.10: Rad51 recruitment to IRIF is attenuated in stem cells <i>in vivo</i> .....	79
Figure 3.11: Cell cycle profile overlays of irradiated stem and non-stem cells.....	80
Figure 3.12: BrdU pulse-chase profiles of irradiated stem and non-stem cells.....	81
Figure 3.13: Stem cells exhibit a shortened G2 checkpoint arrest.....	82
Figure 3.14: Neutral comet assay on stem and non-stem cells to measure DNA repair.....	83
Figure 3.15: Chromosome preparations from stem and non-stem cells.....	84
Figure 3.16: Cultured stem cells show more residual chromosomal aberrations than non-stem cells following irradiation.....	84
Figure 3.17: MRN complex is recruited to DSBs in cultured stem cells.....	85
Figure 3.18: Ku complex is recruited to DSBs in cultured stem cells.....	85
Figure 3.19: Apoptosis in stem cell regions <i>in vivo</i> does not require DDR components.....	87
Figure 3.20: Stem cells <i>in vivo</i> induce pan-nuclear H2AX0pS139 at late timepoints following irradiation.....	87
Figure 3.21: MST1 and JNK are activated only in cultured stem cells at late timepoints following irradiation.....	88
Figure 3.22: MST1 is nuclear translocated correlating with the onset of H2AX-pS139 in stem cell regions.....	88

Figure 3.23: pJNK is activated in stem cells <i>in vivo</i> at late timepoints following irradiation.....	89
Figure 3.24: pJNK colocalizes with H2AX-pS139 in stem cell regions.....	89

## CHAPTER 4

Figure 4.1: H2AX-pY142 persists along DSBs only in cultured stem cells.....	106
Figure 4.2: Global H2AX-pY142 is reduced following irradiation only in non-stem cells.....	106
Figure 4.3: MDC1 is not recruited to DSBs in cultured stem cells.....	107
Figure 4.4: H3K56ac is enhanced in ES cells compared to differentiated progeny.....	108
Figure 4.5: Elevated H3K56ac levels in culture cells correlates with attenuated $\gamma$ H2AX induction.....	109
Figure 4.6: Elevated H3K56ac levels in stem cell regions correlates with attenuated $\gamma$ H2AX induction.....	109
Figure 4.7: H3K56ac is reduced in non-stem but not stem cells along DSBs.....	111
Figure 4.8: Histones are not evicted from chromatin along DSBs in stem or non-stem cells.....	112
Figure 4.9: Baseline H3K56ac levels are restored along DSBs in non-stem cells within 30min of microirradiation.....	113
Figure 4.10: Expression of p300 acetyltransferase is substantially higher in stem cells as compared to non-stem cells.....	114
Figure 4.11: Elevated p300 expression corresponds with Sox2 expression in ES colonies.....	114
Figure 4.12: Elevated p300 expression corresponds with elevated H3K56ac in ES colonies....	115
Figure 4.13: siRNA knockdown of p300 transiently downregulates H3K56ac in cultured stem cells.....	115
Figure 4.14: p300 knockdown increases $\gamma$ H2AX induction in cultured stem cells following irradiation.....	116
Figure 4.15: p300 knockdown improves DNA repair in cultured stem cells.....	117
Figure 4.16: p300 knockdown reduces IR-induced apoptosis in stem cells without any effect on non-stem cells.....	117

## **List of Tables**

Table 2.1: Antibody Information Table.....	40
Table 3.1: Antibody Information Table.....	66
Table 4.1: Antibody Information Table.....	99

## **Acknowledgments**

The most important contributors to my successful completion of my graduate research are of course my PIs. My lab hierarchy was organized in a somewhat uncommon manner where I had both an overall PI that oversaw everything in the lab as well as a direct PI for my project. As overall PI for the lab, Dr. Dennis Hallahan was an excellent mentor and always went out of his way to ensure that I had all the resources and help that I needed to succeed. Also serving as Department Chair for Radiation Oncology, I was always extremely impressed with his availability for meetings or individual questions. I must especially thank him for his advice and help during my applications for postdoctoral labs and fellowships as well as taking the time to edit my dissertation.

Dr. Girdhar Sharma directly oversaw my research project from my first day in the lab. I greatly appreciate that I was able to receive a somewhat straightforward thesis project right away, which helped me remain focused and surely contributed to my timely graduation. Girdhar has taught me the vast majority of what I know about becoming a better scientist, better writer and better thinker. We have traversed the minefields of scientific politics and the manuscript submission process together, yet he has always remained determined and dedicated to my scientific success. He also has gone out of his way to promote my ability to network with important scientists who have visited. While we have had our fair share of heated discussions and disagreements, it is only because Girdhar respected my opinions enough to partake in those conversations with me. I owe much of my academic success to his mentorship and oversight.

A huge thank you also goes out to all of my friends who I met in graduate school. My time here in St. Louis was possibly the most enjoyable years of my life, and it is mostly because of having so many like-minded friends around with similar interests. Despite all the pressures and stress of graduate school, having friends and peers around to have fun and blow off steam with has been invaluable. Thank you to everyone from my DBBS class, the WUSM Musical, and all the other groups that I was a part of during my time here.

Of course, most of all I must thank my family, especially my parents. My parents have never blinked an eye at providing me with both the emotional and financial support for anything that I have wanted to do throughout my life. While not scientists themselves, they always supported my curiosity and even at times stubbornness about the need to understand everything around me. I am extremely excited for the opportunity to have them present for my thesis defense, as everything that I have developed into is because of them.

Funding for this work was provided by the Department of Radiation Oncology and NIH- R01CA174966, R01CA140220. Technical help was also provided by the Washington University School of Medicine Developmental Biology Histology Core and the Washington University Murine Embryonic Stem Cell Core.

Keith Jacobs

*Washington University in St. Louis*

*May 2015*

## ABSTRACT OF THE DISSERTATION

Molecular and Epigenetic Regulation of Stem Cell Radiosensitivity

by

Keith Michael Jacobs

Doctor of Philosophy in Biology and Biomedical Sciences

Molecular Cell Biology

Washington University in St. Louis, 2015

Professor Dennis Hallahan, Chair

Normal tissue injury resulting from ionizing radiation (IR) during cancer radiotherapy has been attributed to reduced regenerative capacity of stem cell compartments. Utilizing multiple *in vivo* tissue niches and primary culture models, we demonstrate that normal stem cells are highly radiosensitive while their isogenic, directly differentiated progeny are radioresistant. Stem cell dropout is therefore likely responsible for the resulting radiation injury in these niches. This differential radiosensitivity is independent of proliferation status, and increased IR-induced apoptosis in stem cells is more broadly distributed across the cell cycle.

We elucidate that stem cells exhibit an attenuated DDR resulting in aberrant cell cycle checkpoint activation and severely diminished DNA repair capacity despite normal sensing of DNA double strand breaks. Interestingly, while these stem cells are unable to induce  $\gamma$ H2AX foci, apoptosis induces pan-nuclear H2AX S139 phosphorylation together with activation of MST1 and JNK. This apoptotic signaling corresponds to a unique inability of stem cells to dephosphorylate H2AX-Y142 around break sites, which promotes apoptosis through JNK while inhibiting DDR signaling. By investigating these molecular responses for the first time in stem cells, we provide potential mechanisms for IR-induced apoptosis independent of DDR signaling. The abrogated DDR in stem cells is also associated with constitutively elevated histone-3 lysine-56 acetylation, which contributes to IR-induced apoptosis through restriction of the DDR and can be modulated to impart radioprotection on stem cells.

This data establishes that unique epigenetic landscapes among differing cell types can impart heterogeneity in the DDR, resulting in varying radiosensitivities and challenging prior assumptions about the ubiquitous nature of canonical DDR signaling. We thus identify pluralistic molecular and epigenetic mechanisms that collectively contribute to IR hypersensitivity in stem cells, promoting development of future therapeutic strategies for minimizing deleterious sequelae from radiotherapy.

# **CHAPTER 1**

---

## **Introduction**

## 1.1 RADIATION THERAPY

Radiation therapy is commonly used to destroy localized tumors in cancer patients. Radiation therapy utilizes ionizing radiation (IR) to kill cancer cells through the induction of damaging DNA double-strand breaks (DSBs). DSBs are more detrimental than single strand breaks because DSBs do not have an undamaged strand available to use as a repair template. DSBs may ultimately lead to chromosomal aberrations which severely impinge on genomic integrity<sup>1</sup>. Unfortunately, tumors often evolve resistance to DNA damage-induced cell death through inactivation of apoptosis pathways<sup>2,3</sup>. Additionally, cancer stem cells within many tumors are believed to be especially radioresistant<sup>4,5</sup> and can inhibit complete eradication of the tumor<sup>6</sup>. The relative radioresistance of cancer cells requires the use of increased and repeated IR doses, which often result in injury to normal tissue<sup>8</sup>.

### 1.1.1 Physics of Ionizing Radiation

Ionizing radiation is defined as radiation that imparts enough energy to cause ejection of one or more electrons from its target atoms, resulting in the localized release of energy<sup>8</sup>. The energy released per displaced electron is approximately 33eV, which is enough energy to break chemical bonds of nearby molecules. Ionizing radiation can be classified as either electromagnetic or particulate. IR induces DSBs both directly through the energy imparted from the radiation as well as indirectly by the creation of highly reactive hydroxyl radicals (reactive oxygen species or ROS) from nearby water or other molecules<sup>8,9</sup>. Only particulate radiation typically imparts enough energy to directly induce DNA breaks, while all forms of radiation can induce indirect ionization. X-rays and  $\gamma$ -rays are electromagnetic radiation, while atomic particles and heavy ions represent particulate radiation. X-rays are created by focusing the kinetic energy produced from accelerated electrons, while gamma rays emanate through natural decay of radioactive isotopes. Atomic particle radiation includes electrons, protons, alpha particles and neutrons, all of which can be used for radiation therapy. Heavy ions include the nuclei of carbon, neon, argon, or iron that have had electrons removed to create a positive charge and can be used for radiation therapy with specialized accelerators. Heavy ions are also present in outer space and are a major potential danger for astronauts during long space voyages<sup>8</sup>. Ionizing radiation is typically measured as

absorbed dose in the unit of grays (Gy), which equals 100 rad or 1 Joule of deposited energy per kilogram of tissue<sup>10</sup>. There are also measures of effective dose, to account for differing biological effects of various forms of radiation relative to their respective linear energy transfer (LET), or the average amount of energy deposited per linear unit of length. X-rays, electrons, gamma rays and protons exhibit a significantly lower LET than neutrons, alpha particles and heavy ions and therefore have a less efficient biological effect per dose<sup>8</sup>. The sievert (Sv), which equals 100 rem, is the international unit for effective dose, and a Gray is similar to a Sievert for low LET radiation<sup>11</sup>.

### **1.1.2 Cancer Radioresistance**

While radiation therapy is an often effective treatment for destroying cancer, inactivation of the apoptotic factor p53 and other evolutionary mutations impart radioresistance upon cancer cells<sup>2,3</sup>. Inactivation of DNA repair factors and the DNA Damage Response (discussed below) is often an important step in cellular transformation by promoting genomic instability and preventing the induction of programmed cell death<sup>12</sup>. While mutation of repair factors can indeed sensitize cancer cells, associated inhibition of apoptosis can promote resistance and further mutational evolution. Because of the common loss-of-function of apoptosis in cancer cells, cell death often involves other mechanisms. Cancer cells often die through mitotic catastrophe, whereby residual unrepaired DNA damage results in severe chromosomal defects following mis-segregation during mitosis, leading to delayed p53-independent apoptosis. Additionally, DNA damage may induce senescence in cancer, which does not destroy cells but stops their division and therefore can halt the proliferation of a tumor<sup>3,13</sup>.

While their existence is still debated, cancer stem cells are believed to be extremely radioresistant, thereby contributing to the overall radioresistance of tumors and promoting cancer recurrence<sup>6,14</sup>. Cancer stem cells exhibit resistance in part through elevated DNA Damage Response signaling, increased aldehyde dehydrogenase and ABC transporter activity (which are less important for radiation but can inactivate or remove chemotherapeutic drugs), a hypoxic microenvironment, increased free-radical scavengers, activation of self-renewal pathways and even potentially

reduced proliferation<sup>4-6,14-16</sup>. Unique strategies to target these mechanisms may be required in conjunction with radiation treatment in order to sufficiently destroy cancer stem cells.

### **1.1.3 Whole Body Irradiation Dosage and Mortality**

In addition to the relative radioresistance of tumors, the effectiveness of radiation therapy is also limited by clinical side effects on normal tissue. Acute clinical consequences of accidental whole-body radiation exposure such as from nuclear disasters are dosage-dependent. Doses below 2Gy are considered subclinical and may only result in a temporary drop in blood cell counts along with some mild nausea or headache. Hematopoietic injury and white blood cell loss occurs at doses of 2Gy and above, which can lead to death within 30 days from bone marrow depletion due to infection or hemorrhaging<sup>10</sup>. During this hematopoietic syndrome, rapid depletion of lymphocytes is followed by gradual reduction in granulocytes, platelets and red blood cells, leading to impaired immunity, poor wound healing and excessive bleeding. Exposure to single doses of 10Gy and above produce gastrointestinal damage and potential death within 2-3 weeks from organ failure, sepsis and internal bleeding, with symptoms including loss of nutrient absorption, severe nausea and vomiting, diarrhea, anorexia and abdominal pain. More global effects can be observed above 10Gy, with patients experiencing “fatigue syndrome” consisting of central nervous system manifestations such as fever, headache, disorientation, reduced reflexes, diminished coordination and even occasional loss of consciousness. Exposure to more than 30Gy induces cardiovascular and central nervous system failure resulting in death within a few days due to loss of blood vessel integrity and brain swelling/inflammation. All of these doses also induce nausea and vomiting within the first 12 hours following exposure<sup>11</sup>.

#### **1.1.3.1 Linear No-Threshold Hypothesis**

Exposure to doses below 1Gy does not result in any significant risk of tissue injury, although continued exposure does increase cancer risk in a dose-dependent manner<sup>11,17,18</sup>. The linear no-threshold (LNT) hypothesis proposes that any and all doses of radiation pose some cancer risk, and therefore no “safe” levels of radiation exist<sup>17,18</sup>.

This hypothesis is faulty however, and acute doses below 100mSv or continued exposure below 500mSv fails to promote any increased cancer risk. In contrast, strong evidence exists for beneficial effects of exposure to very low levels of radiation, known as hormesis. Radiation hormesis develops within hours of exposure and its effects can last up to months, including reduction of reactive oxygen species, death of previously damaged cells, immune stimulation, and modification of cell cycle parameters including senescence. These adaptive mechanisms all combine to protect long term genomic integrity and reduce the risk of future carcinogenesis<sup>17,19</sup>.

#### **1.1.4 Chronic and late effects of radiation injury**

Consequences of localized normal tissue injury include both acute and chronic sequelae such as hematopoietic dysfunction<sup>20</sup>, cognitive impairment<sup>21,22</sup>, infertility<sup>23</sup>, intestinal epithelial erosion<sup>24,25</sup> and hair loss<sup>26</sup>. These pathologies result from deficient tissue regeneration following normal cell turnover and thus have been attributed to the depletion of regenerative stem cell compartments<sup>7,27,28</sup>. The timing of the clinical onset of these symptoms is therefore dictated by the turnover rate of the affected tissue, with early consequences presenting only days or weeks following irradiation in rapidly dividing tissues and late-onset effects in slow-dividing tissues<sup>7</sup>.

Many chronic symptoms only present months to years following radiation damage and are not related to stem cell loss or tissue proliferation rate. The processes involved in this type of injury include fibrosis, necrosis, inflammation, atrophy, and vascular damage<sup>7,29</sup>. These mechanisms all interact in creating long-term damage. Fibrosis is excessive scarring due to overactive wound healing and is probably the most common type of injury following radiation damage<sup>30</sup>, appearing often among stromal cells of many tissues. Tissue necrosis and atrophy result in degeneration of the affected tissue. Necrosis is most damaging to the cerebral white matter of the brain while atrophy is characterized by sequential destruction of epithelial tissue. Endothelial cell damage and immunological inflammation lead to reduced vascular integrity, causing further broad tissue

damage through ischemia. Inflammatory responses can promote many of the above mechanisms as well as tissue-specific forms of radiation injury such as pneumonitis in lung<sup>7,31,32</sup>.

#### **1.1.4.1 Radiation Dose Fractionation**

The requirement to balance tumor elimination while minimizing side effects limits the overall effectiveness of radiation therapy, so identifying methods for improved radioprotection of normal tissue is indispensable for improving the efficacy of cancer treatment<sup>7</sup>. One treatment method that has been developed to maximize efficiency of cell killing on cancer cells while sparing normal tissue is dose fractionation. Dose fractionation attempts to take advantage of the differences in cell cycle kinetics and tissue microenvironment between tumor and normal tissue in order to bias cell killing toward cancer cells while sparing normal tissue. The effect of fractionation is based on the four “R” factors of radiobiology: repair of sublethal damage, cell cycle reassortment, reoxygenation, and repopulation. Fractionation increases the effectiveness of radiation on destroying tumors because it allows reoxygenation of previously hypoxic cancer cells and promotes reassortment of cycling cells into more radiosensitive phases of the cell cycle. Hypoxic cells are resistant to ROS-mediated DNA damage, so repeated irradiation of tumors sensitizes previously hypoxic cancer cells once the aerated surrounding cells have died<sup>33</sup>. At the same time, fractionation spares normal tissue by allowing time for DNA repair and progenitor repopulation of damaged regions. The dose, number and time delay of fractions must be calculated to maximize these benefits for each tissue type based on relative proliferation rate. These factors must all be carefully determined when attempting to balance the sparing of fast-dividing normal tissues with effective killing of an entire tumor cell population<sup>34</sup>.

#### **1.1.5 Radiosensitivity and Proliferation**

Radiosensitivity differs greatly among tissues and cell types, and the cellular variables underlying differences in radiosensitivity have been studied for over a century. Two major determinants of

radiosensitivity include proliferation rate and cell cycle status. Bergonié and Tribondeau in 1906 compared the radiosensitivity of various tissues and concluded that there was a direct correlation between proliferation rate and radiosensitivity for both normal and cancerous tissue<sup>35</sup>. This has since become a central tenet of radiobiology and continues to influence the interpretation of clinical outcomes from radiotherapy. As might be expected however, the “Law of Bergonié and Tribondeau” is an oversimplification that has numerous counterexamples<sup>36</sup>. Most notably, this tenet predicts that cancer cells should be inherently more radiosensitive than normal tissue due to their enhanced proliferation rate, however cancer is often relatively radioresistant<sup>2,3</sup>. More accurately, highly proliferative cells appear to exhibit merely a faster response to radiation<sup>36,37</sup>, meaning that cell death will be observed earlier than in slower-dividing cells although not necessarily more extensively.

#### **1.1.6 Radiosensitivity and Cell Cycle Kinetics**

Radiosensitivity also varies across the cell cycle. While there is certainly variability among cell types<sup>37</sup>, cells are typically most radiosensitive during G2/M phase, and especially during mitosis<sup>38-40</sup>. Radiosensitivity is decreased during G1 phase and is minimal during the end of S phase. Differential radiosensitivity throughout the cell cycle has historically been performed by irradiating cells following synchronization by various cell cycle inhibitors, and some variability is also inherent based on the particular method used to achieve synchronization. Live-sorting cells by flow cytometry to avoid the use of inhibitors has also demonstrated similar hypersensitivity of G2/M cells to low-dose IR<sup>41</sup>.

## **1.2 MECHANISMS OF CELL DEATH**

There are many forms of cell death, each activated in response to particular conditions and stimuli within either the internal or external cellular environment. Major mechanisms of cell death likely to result from radiation exposure are apoptosis, necrosis, mitotic catastrophe and autophagy. There are also additional specialized forms of cell death unrelated to radiation damage such as anoikis (due to the loss of adhesive interactions with the extracellular matrix), entosis (non-phagocytic engulfment of one cell by another) and

cornification (formation of the outer epidermal layer of dead keratinocytes as part of normal skin development)<sup>42</sup>. In addition to cell death, DNA damage and other stressors can also lead to replicative arrest or senescence<sup>43</sup>.

### **1.2.1 Necrosis**

Necrosis has historically been believed to be a passive cell death mechanism in response to tremendous external stress, resulting from conditions such as microbial toxins, immune activation, certain types of DNA damage, inadequate signaling ligand availability and insufficient nutrient access. However, more recently it has been established that necrosis can also be a form of programmed cell death that is molecularly regulated as part of development and other normal physiological processes, often sharing signaling pathways with apoptosis. Unlike apoptosis however, the completion of necrosis results in cellular lysis, releasing cellular contents. If necrosis occurs in response to infection, necrosis can thereby amplify infection by releasing microbes and toxins into the environment. The release of cellular contents also induces an immune response which can potentially accentuate tissue damage<sup>42,44</sup>.

### **1.2.2 Autophagy**

Autophagy is a cytoprotective response whereby stressed or dying cells isolate and degrade internal organelles in an attempt to preserve and recycle limited remaining resources. Inducers of autophagy include starvation, absence of necessary growth factors and toxic agents. While autophagy is considered a mechanism of cell death, except in the case of recycling cellular resources or stimulating immune activation in dying cells, it is typically an emergency protective mechanism. Autophagy attempts to maintain cellular homeostasis and energy reserves in order to prevent cell death. Autophagy therefore primarily accompanies cell death as opposed to regulating it, and inhibition of autophagy is often ineffective at preventing cell death induction<sup>42,45</sup>.

### **1.2.3 Mitotic Catastrophe**

Mitotic catastrophe is cell death stimulated by major errors during mitosis, inducing destruction of the cell either during mitosis or the subsequent G1 phase in order to prevent the propagation of damaging chromosomal aberrations to future generations. Mitotic catastrophe can be identified by the presence of small micronuclei or multiple nuclei. Mitotic catastrophe activates mitotic cell cycle arrest through the DNA Damage Response and results in either cell death through apoptosis/ necrosis or cell cycle exit as senescence. Mitotic catastrophe is not a true independent mechanism of cell death but instead merely a checkpoint response that leads to cell death through one of the previously described mechanisms<sup>42</sup>.

### **1.2.4 Senescence**

Senescence is sometimes considered to be a form of cell death, however despite not being able to further proliferate, senescent cells are otherwise functional and metabolically active.

Senescence is most commonly enacted as “replicative senescence” due to the repeated shrinking of telomeres below a certain threshold over several generations of cell division.

Shortening of telomeres activates the DNA Damage Response along with the cell cycle inhibitor tumor suppressors p53, retinoblastoma protein (Rb) and p16, leading to permanent inactivation of replicative capacity. Senescence can also be prematurely induced by multiple kinds of stress, including exogenous DNA damage. It is considered to be a mechanism of tumor suppression because in addition to maintaining genomic integrity in future generations, senescence is actually induced in primary cells by the activation of oncogenes<sup>43</sup>. Due to the inactivation of apoptosis in many cancers<sup>3,13</sup>, senescence is often the dominant mechanism for tumor suppression by DNA damaging agents. Senescent cells can be easily identified by their large, flat multinucleated morphology along with expression of senescence-associated  $\beta$ -galactosidase<sup>43</sup>.

### **1.2.5 Apoptosis**

Apoptosis describes programmed cell death or “cellular suicide” through defined molecular signaling pathways. Apoptosis can be enacted through either extrinsic or intrinsic mechanisms.

Extrinsic apoptosis induced programmed cell death through TNF family receptor-mediated signaling based on either the presence of toxic ligands or reduced concentration of necessary ligands. Signal transduction leads to activation of the initiator caspases 8,9, or 10, which then activate the “executioner” caspases 3, 6 and 7. Extrinsic apoptosis is caspase-dependent but does not always require mitochondrial permeabilization, which is an essential feature of the intrinsic pathway. Multiple internal cellular stresses are capable of activating the intrinsic pathway, including oxidative stress, DNA damage, accumulation of unfolded proteins, absence of growth factors, and others. The intrinsic apoptosis pathway is regulated by a homeostatic balance of pro and anti-apoptotic proteins. The Bcl-2 family of proteins include anti-apoptotic proteins such as Bcl-2, Bcl-x and Bcl-xL, along with pro-apoptotic proteins such as Bax, Bad, Bid and Bim. Apoptotic stimuli upregulate the relative amount of pro-apoptotic Bcl-2 family proteins, overcoming their inhibition by anti-apoptotic family members and leading to mitochondrial permeabilization. Cytochrome c release from the permeabilized mitochondria induces formation of the apoptosome complex, activating caspase-9 which subsequently activates caspases 3, 6 and 7. Caspase-3 is the primary executioner caspase and activates several downstream substrates through cleavage, including caspase-activated DNase (CAD), which degrades nuclear DNA and promotes chromosomal condensation. Caspase-3 also induces cytoskeletal changes and disintegration of the cell as a whole. Caspase-independent apoptosis also occurs through proteins such as apoptosis inducing factor (AIF)<sup>46</sup>, which can directly induce DNA fragmentation and chromatin condensation<sup>42,47</sup>. Unlike necrosis, degraded cellular contents remain packaged within membranes during apoptosis, avoiding widespread immune activation and allowing phagocytic disposal of dead cells by macrophages<sup>44,47</sup>.

#### **1.2.5.1 p53 in Apoptosis**

p53 is the major transcriptional regulator of apoptosis, upregulating the expression of pro-apoptotic Bcl-2 family members leading to mitochondrial permeabilization. p53 also transcriptionally activates several other genes that promote apoptosis, including phosphatase and tensin homolog (PTEN), an inhibitor of the pro-survival PI3 kinase

signaling pathway<sup>48</sup>. The action of p53 is controlled by numerous DNA damage-induced post-translational modifications which regulate its interaction with various substrates. p53 protein is maintained at low levels under basal conditions due to constitutive ubiquitination by Mouse double minute 2 homolog (MDM2). The DNA Damage Response factors Ataxia telangiectasia mutated (ATM) and checkpoint kinase (Chk)1/2 phosphorylate p53 on serine 15 and 20, stabilizing the protein by blocking MDM2-mediated ubiquitination. Serine 46 is also phosphorylated, leading to induction of specific apoptotic genes, although the responsible kinase is not known. p53 acetylation at multiple residues also promotes DNA binding and subsequent transcriptional activation of apoptotic genes<sup>49</sup>.

#### **1.2.5.2 MST1-JNK-H2AX Pathway**

Several overlapping pathways are involved in DNA fragmentation and chromatin condensation at the end stages of apoptosis downstream of caspase-3 activation. One important downstream target of caspase-3 is mammalian Ste20-like kinase (MST1), an important kinase within the Hippo signaling pathway that controls organ size by promoting apoptosis during development<sup>50</sup>. Caspase-3 cleaves MST1, causing its translocation into the nucleus<sup>51</sup>. DNA damage also induces autophosphorylation of MST1 on threonine 183, which combines with caspase cleavage to fully activate MST1<sup>52,53</sup>. Upon activation and nuclear translocation, MST1 phosphorylates histone H2AX on serine 139 (S139). Phosphorylation of H2AX on S139 is required for DNA fragmentation and degradation at the end of apoptosis, as it appears to be responsible for recruiting caspase-activated DNase (CAD) to DNA<sup>51,54</sup>. Histone H2B is also phosphorylated by MST1 in parallel with H2AX S139 phosphorylation and is responsible for apoptotic chromatin condensation<sup>55,56</sup>. MST1 can additionally phosphorylate c-Jun N-terminal kinase (JNK)<sup>57,58</sup>, which can in turn also pan-phosphorylate H2AX-S139<sup>54</sup> to induce DNA fragmentation and chromatin condensation.

### 1.3 DNA DAMAGE RESPONSE

DNA DSBs activate an intricate network of molecular signaling cascades known as the DNA damage response (DDR) (Fig. 1.1), which is an intricate network of molecular signaling that enables proper damage sensing, recruitment of repair factors and DNA repair<sup>22-24</sup>. In mammals, the Mre11–Rad50–Nbs1 (MRN) complex is involved in the initial sensing of DNA breaks<sup>25,26</sup>. The MRN complex binds broken DNA ends, holding them together and initiating the prerequisite end processing necessary for repair. Activation of ATM involves recruitment by MRN to DSBs<sup>25,27,28</sup> together with autophosphorylation at serine 1981 and subsequent cleavage of the ATM dimer<sup>26,28,29</sup>. While the absolute requirements and specific order of ATM activation steps are unclear due to varying results across different cell types and assay conditions, the presence of broken DNA ends, the end resection activity of MRN, ATM autophosphorylation, and ATM monomerization all contribute to the maximal activation of ATM kinase following DNA damage<sup>62,66</sup>. Activated ATM then phosphorylates histone H2AX on serine 139 to create  $\gamma$ H2AX<sup>67,68</sup>, which serves as a docking site for downstream repair factors<sup>69</sup>. ATM is one member of the phosphatidylinositol 3-kinase-related kinases (PIKKs) along with ATM and Rad3-related (ATR) and DNA-dependent protein kinase catalytic subunit (DNA-PKcs). All three PIKKs can compensate for loss of the others in  $\gamma$ H2AX phosphorylation, however ATM is the primary PIKK for DSBs, while ATR is predominantly involved in signaling and repair of single-strand replication errors<sup>70</sup> and DNA-PKcs primarily acts through non-homologous end joining DNA repair<sup>71,72</sup>.  $\gamma$ H2AX has various important roles in the DDR, including recruitment of DDR factors, maintaining close proximity of broken DNA ends, signal amplification of the overall DDR response, and directly promoting DNA repair<sup>73</sup>. Mediator of DNA damage checkpoint protein 1 (MDC1) directly binds  $\gamma$ H2AX, recruiting additional MRN and ATM which induces a positive feedback loop that promotes expansion of  $\gamma$ H2AX for megabases around the DNA break and amplifies the DDR signal<sup>73-75</sup>. Additional DDR factors are also recruited, including several ubiquitin ligases and p53 binding protein 1 (53BP1) among others<sup>60</sup>, leading to activation of biological pathways such as cell cycle checkpoints and DNA repair. If DNA damage cannot be sufficiently repaired, the DDR can also induce apoptosis by the activation of p53 through PIKKs and checkpoint proteins<sup>12,76</sup>. Following completion of DNA repair, various phosphatases act to reverse DDR activation and return the chromatin to a baseline state<sup>77-83</sup>.

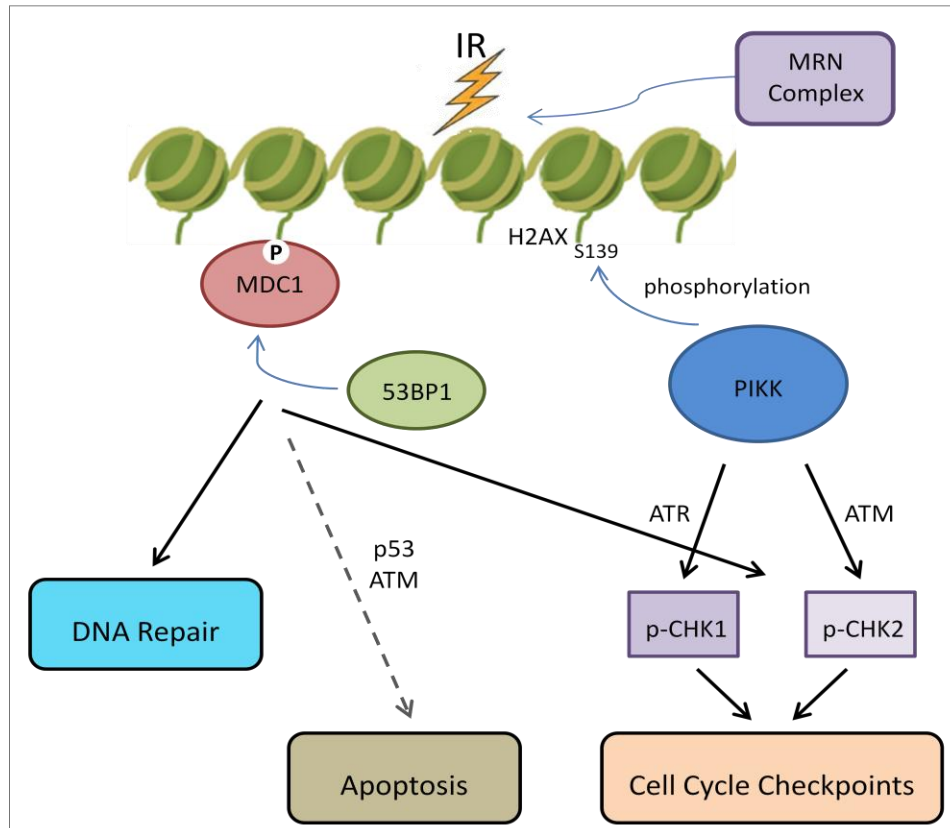


**Figure 1.1. An overview of the DNA Damage Response.** This diagram focuses on some of the important early molecular signaling and downstream biological outcomes investigated in this project.

### 1.3.1 Cell Cycle Checkpoints

In addition to phosphorylating H2AX, ATM phosphorylates Chk2 kinase and p53 among other proteins. Activated Chk2 and ATM stabilize p53 in response to DSBs, leading to transcriptional activation of the protein p21. p21 blocks cell cycle progression at the G1/S transition by inhibiting the action of cyclin/cdk complexes, while S-phase entry is further blocked through the degradation of cell division cycle 25A (Cdc25A) and other cyclins by ATM/Chk2. Chk1 is activated by ATR, which is most active during S phase, and both Chk1 and Chk2 can phosphorylate Wee1 to block further cell cycle progression during S phase. Wee1 is also involved in G2 arrest, together with ATR and Chk1. G1 checkpoint arrest factors also play a role in initiating G2 arrest, but ATR and Chk1 are responsible for its maintenance<sup>84,85</sup>, while Cdc25A inhibition is also

involved. Multiple cell cycle and other factors combine to mute the DDR response during mitosis<sup>38,86</sup>. In general cell cycle checkpoint proteins have primary roles during particular cell cycle phases, however they function together to promote arrest throughout the cell cycle.

### **1.3.2 DSB Repair**

DNA DSBs are typically repaired through one of two pathways, non-homologous end joining (NHEJ) or homologous recombination (HR). NHEJ is a rapid process occurring primarily during G1 phase of the cell cycle. NHEJ is typically completed within 30min of DSB induction, however it is error-prone and can lead to mutations. HR in contrast is error free due to its utilization of a template DNA strand, however it can therefore only occur efficiently during S/G2 when sister DNA strands are available and usually requires several hours to complete<sup>1,87</sup>. NHEJ begins with the Ku70/80 heterodimer binding the broken DNA ends and subsequently recruiting DNA-PKcs. The MRN complex aids with recruiting repair factors and processing broken DNA ends together with the protein Artemis<sup>88,89</sup>, while a complex of proteins involving DNA ligase IV and X-ray repair cross-complementing protein 4 (XRCC4) ligates the broken DNA ends together<sup>1,59</sup>. HR is a relatively more complex process, beginning with the processing of DNA to create single-stranded overhangs by MRN and various nucleases<sup>59</sup>. This single-stranded DNA is bound by replication protein A (RPA) and Rad51 as strand invasion occurs through the homologous template aided by other proteins such as breast cancer (BRCA)1/2 and Rad54, followed by DNA synthesis and resolution of the DNA junctions<sup>1,59</sup>.

## **1.4 STEM CELLS**

Stem cells are non-specialized cell types that have the capacity to undergo asymmetric cell division, producing both a differentiated daughter cell and an identical daughter stem cell. Daughter cells are capable of differentiating into any cell type within their defined lineage and tissue type<sup>90</sup>. Pluripotent stem cells such as embryonic stem (ES) cells are theoretically capable of producing progeny that differentiate into any cell type<sup>91</sup>, while tissue-specific or adult stem cells are multipotent and are restricted to differentiate only into cell types of that tissue. Tissue-specific stem cells exist within well-defined niches,

a microenvironment consisting of surrounding support cells and differentiated progenitors. Stem cell function and regulation is controlled by signals from the surrounding niche as well as its internal signaling. These niches also regulate the proliferation of stem cells<sup>90,92</sup>.

#### **1.4.1 Stem Cell Epigenetics**

Stem cell pluripotency and overall gene expression is dictated by their epigenetic profile. Stem cells exhibit unique epigenetic regulation, including DNA hypomethylation, large areas of euchromatin and enhanced levels of specific histone modifications. DNA is wrapped and compacted around proteins known as histones within the nucleus to create a DNA-protein complex known as chromatin. There are four core histones: H2A, H2B, H3, and H4, in addition to several histone variants. Post-translational modifications on these histones can regulate gene transcription, and stem cells exhibit distinctive modulation of histone modifications that can control their pluripotency. Pluripotency is associated with enrichment of both the activating mark histone 3 lysine 4 methylation as well as the repressive mark histone 3 lysine 27 methylation. This dual signature known as the “bivalent” chromatin structure maintains ES cells in a poised state for rapid transcription upon differentiation stimuli. Histone 3 lysine 4 methylation in particular gene regions is associated with reduced DNA methylation, which is repressive for transcription, further demonstrating the bivalent regulation of gene expression in stem cells. Histone 3 lysine 56 acetylation is also greatly elevated in embryonic stem cells and promotes expression of pluripotency genes<sup>93,94</sup>.

#### **1.4.2 Proliferation and Cell Cycle in Stem Cells**

Many stem cell compartments contain both non-dividing quiescent stem cell populations as well as an additional pool of actively dividing stem cells. These populations may be differentially involved in tissue regeneration following injury versus normal tissue turnover and homeostasis<sup>92</sup>. Embryonic stem cells are rapidly proliferating, and this rapid proliferation appears to be an important characteristic of pluripotency. Additionally, embryonic stem cells exhibit a shortened G1 cell cycle phase that may also be involved in maintaining their undifferentiated state<sup>95-97</sup>.

Following DNA damage, both embryonic and neural stem cells both uniquely fail to activate G1 checkpoint arrest<sup>95,96,98-101</sup>. The lack of G1 arrest in ES cells is associated with cytoplasmic sequestration of p53<sup>102</sup> and Chk2<sup>99</sup>. p21 protein is also absent in ES and neural stem cells, despite the expression of p21 mRNA<sup>96,98,100,103</sup>.

### **1.4.3 Maintaining Genomic Stability in Stem Cells**

Since stem cells are responsible for regenerating all of the differentiated cell types of a tissue, maintaining their genomic integrity is imperative. Stem cells therefore exhibit multiple mechanisms for promoting genomic stability. One method for preventing genomic instability in stem cells is elevated antioxidant defenses. ES cells are resistant to high levels of damaging reactive oxygen species (ROS) due to higher expression of ROS-inactivating enzymes and maintain lower endogenous ROS levels than differentiated cells<sup>104,105</sup>. They also show high expression of transporter and efflux pumps that can remove potentially damaging chemicals from the cell<sup>104</sup>. ES cells additionally express higher levels of heat shock proteins, which protect against the misfolding of proteins following cellular stress. As another mechanism of genome protection, ES cells exhibit a low mutation rate, with baseline mutation frequencies up to 1000 fold less than murine embryonic fibroblasts, at least at certain loci<sup>105,106</sup>.

#### **1.4.3.1 DNA Damage Sensitivity**

While embryonic stem cells demonstrate robust mechanisms for maintaining genomic stability under baseline conditions, ES and neural stem cells in culture are extremely sensitive to elevated levels of DNA damage and readily undergo DNA damage-induced apoptosis<sup>102,105,107-112</sup>. It is often argued that the removal of damaged stem cells from a population has evolved in order to prevent the perpetuation of genomic instability within a tissue, which can lead to organ dysfunction or cancer, however this proposal is only theoretical. ES cells are primed to apoptose by constitutively active Bax<sup>105,113</sup> but do not require the upstream apoptotic regulator p53<sup>102</sup>, which is insufficiently translocated to the nucleus in ES cells<sup>99,102</sup>. The absence of a G1 checkpoint may contribute to the

sensitivity of ES cells to DNA damage, as restoration of the G1 checkpoint through Chk2 overexpression was able to reduce IR-induced apoptosis in ES cells<sup>99,106</sup>. While p53 may not be directly related to ES cell apoptosis, p53 can alternatively induce differentiation following DNA damage by blocking expression of the pluripotency gene Nanog<sup>114</sup>. Neural stem cells have also been shown to cease dividing and differentiate following DNA damage<sup>110</sup>.

Tissue-specific stem cells vary in their radiation responses both across different tissues and among different populations within a particular niche. While the radiosensitivity of individually labeled neural stem cells *in vivo* has not been investigated, numerous reports have observed cell death and reduced proliferation of neural precursors within hippocampal regions of neurogenesis<sup>115–120</sup>. Intestinal crypt stem cells also readily undergo IR-induced apoptosis<sup>121,122</sup>, in contrast with stem cells of the colon<sup>123</sup>. The intestine is now believed to contain multiple stem cell populations and lineages however<sup>124–126</sup>, each with varying radiosensitivities<sup>127,128</sup>. While testicular stem cell loss has long been associated with infertility after radiation exposure<sup>129</sup>, labeled spermatogonial stem cells have in fact been shown to be radioresistant while adjacent non-stem spermatogonia undergo IR-induced apoptosis<sup>130</sup>. Stem cells within multiple tissue niches of skin have demonstrated radioresistance<sup>131,132</sup>, although the hair follicle niche may contain differentially regulated stem cell populations<sup>133</sup> similar to intestinal crypts. Mesenchymal stem cells from bone marrow represent another radioresistant stem cell population<sup>134</sup>, while the relative radiosensitivity of hematopoietic stem cells appears to be species-dependent<sup>135–137</sup>. While certain characteristics are clearly conserved among all stem cell populations, it is apparent that stem cell radiation responses are highly context-dependent.

### 1.4.3.2 DNA Damage Response and DNA Repair

Despite the apoptotic responses of many stem cell populations in response to DNA damage, most studies report rapid and efficient DNA repair capabilities in stem cells. ES cells are very efficient at mismatch repair, which is important for fixing base misincorporation and other nucleotide base errors during DNA replication and may account for their low mutation rate. Limited studies suggest enhanced base excision repair in ES cells due to elevated expression of repair proteins, which reverses chemical modifications to DNA as well as single-strand breaks<sup>105</sup>. ES cells are however sensitive to UV-induced damage, with disagreement among the literature concerning their capacity for nucleotide excision repair of UV-induced lesions<sup>105,112,138</sup>. There is a great deal of conflicting information concerning repair of DSBs in ES cells. The majority of studies observed that both ES and neural stem cells show efficient repair of DSBs<sup>104,109,139-142</sup>. These stem cells predominantly repair DNA damage through homologous recombination due to their short G1 and elevated expression of repair factors<sup>143-147</sup>, however efficient NHEJ<sup>139,148,149</sup> also contributes to their DNA repair efficiency. In agreement with these studies, robust DDR induction has also been shown in cultured embryonic and neural stem cells<sup>101,109,111,144,150,151</sup>. Despite strong evidence for efficient DDR signaling and DNA repair in stem cells, multiple studies also report that stem cells exhibit reduced DNA repair capacity. Differences appear to exist between mouse and human stem cells<sup>107</sup>; in fact one study found murine but not human ES cells to be deficient in repairing DNA breaks<sup>152</sup>. Murine induced pluripotent stem cells have also been found to exhibit inadequate H2AX phosphorylation and DNA repair<sup>153</sup>, and one of the few studies to actually compare stem cells with isogenic progeny observed that ES cells were less efficient at both induction and resolution of  $\gamma$ H2AX foci<sup>154</sup>. Unirradiated ES cell lines exhibit high basal  $\gamma$ H2AX which is believed to be important for regulating self-renewal<sup>155,156</sup>, but this basal  $\gamma$ H2AX appears to be independent of DDR signaling<sup>157</sup>.

The molecular signaling occurring within tissue stem cells in response to DNA damage is sometimes contradictory with their overall radiosensitivity. DDR foci have been observed in intestinal crypt stem cells<sup>158,159</sup> despite the presence of IR-induced apoptosis in those same cells. Similarly, while spermatogonial stem cells of testis were shown to be radioresistant, they fail to display  $\gamma$ H2AX or MDC1 foci correlating with reduced DNA repair based on 53BP1 foci resolution<sup>130</sup>. The DDR has not been well-detailed in neural stem cells *in vivo*, as previous studies have investigated the DDR principally within developmental contexts<sup>103,160</sup> without the use of stem cell markers. Limited evidence from existing studies actually shows enhanced DDR foci and anti-apoptotic protein expression<sup>103</sup>, in contrast with radiosensitivity data from other publications. Both mesenchymal<sup>134,161</sup> and hair follicle<sup>132</sup> stem cells show elevated DDR and DNA repair capacity in agreement with their radiosensitivity data, and HSC molecular radiation responses were again species-dependent<sup>135-137</sup>.

## **1.5 DNA DAMAGE-RESPONSIVE HISTONE MODIFICATIONS**

DNA damage induces substantial changes in chromatin, both globally and around DNA break sites. Specific histone modifications may play a role in all aspects of DNA repair, including controlling access of repair factors to DNA, signaling through the DNA Damage Response, transcriptional repression and reassembly of chromatin following repair<sup>162-164</sup>. Numerous histone modifications have been identified that are either beneficial or detrimental toward DNA repair signaling, and I will focus on a few relevant for this study.

### **1.5.1 H2AX S139**

Histone H2AX is phosphorylated by ATM at serine 139 (S139) to create  $\gamma$ H2AX as part of the DNA Damage Response<sup>67</sup>, serving as a docking site for downstream DDR signaling and promoting DNA repair. While  $\gamma$ H2AX foci around DSBs is the primary function of H2AX S139 phosphorylation, pan-nuclear H2AX S139 phosphorylation (H2AX-pS139) has been observed in response to both DNA damaging agents and other stimuli<sup>165,166</sup>. This pan-nuclear H2AX-pS139

has been attributed to diffusion of DDR factors, creation of small DNA fragments, global chromatin changes, viral infection and apoptosis in various contexts. Apoptotic H2AX-S139 forms a ring or pan-nuclear stain around the nucleus following induction of apoptosis. Reports vary in reporting whether the PIKK proteins ATM and DNA-PKcs<sup>55</sup> or the apoptotic factors MST1<sup>51,57</sup> and JNK<sup>54</sup> are responsible for apoptotic H2AX-S139 phosphorylation. H2AX-pS139 is required for DNA fragmentation and degradation at the end of apoptosis, likely acting through the recruitment of caspase-associated DNases<sup>51,54</sup>. H2AX-pS139 also interacts with AIF in order to degrade DNA as part of a programmed necrosis cell death pathway<sup>167</sup>. This apoptotic H2AX-S139 does not include MDC1 or 53BP1 and is associated with inhibition of DDR amplification due to inactivating caspase-mediated cleavage of MDC1<sup>165,168</sup>.

### **1.5.2 H2AX Y142**

The tyrosine 142 (Y142) residue on histone H2AX is also an important regulator of molecular responses to DNA damage. H2AX-Y142 phosphorylation (H2AX-pY142) is mediated by WSTF kinase<sup>169</sup> and EYA phosphatase<sup>170</sup>. H2AX-pY142 is inversely regulated with H2AX-pS139, as Y142 is phosphorylated under basal conditions and is dephosphorylated following DNA damage, paralleling  $\gamma$ H2AX induction<sup>169,170</sup>. Basal H2AX-pY142 is necessary for maintenance of normal DDR signaling in response to DNA damage<sup>169</sup>, whereas removal of Y142 phosphorylation is required for MDC1 binding to  $\gamma$ H2AX and subsequent DDR amplification. In addition to blocking DNA repair signaling, the presence of H2AX-pY142 following induction of DSBs instead recruits apoptotic factors, leading to induction of apoptosis through JNK<sup>170</sup>. The structure of the Y142 residue itself also appears to be important for normal DDR signaling and radiosensitivity<sup>171,172</sup>. Additionally, both IR and drug-induced apoptosis may involve co-regulation of the H2AX S139 and Y142 residues<sup>172,173</sup>.

### **1.5.3 H3K56ac**

Histone 3 lysine 56 acetylation (H3K56ac) has been identified as an important DNA damage-responsive histone modification that may play a substantial role in DDR signaling and chromatin

structure around DNA breaks. Several studies have assessed global changes in H3K56ac levels in response to genotoxic stress, with contradictory results concerning whether levels increase<sup>174–176</sup> or decrease<sup>177–179</sup>. In yeast, H3K56ac promotes deposition of H3 histones on to chromatin during DNA replication and following repair<sup>180–183</sup>, promoting genomic stability. H3K56ac has also been shown to be enhanced during S phase and beneficial for genomic stability in mammals<sup>184</sup>. In contrast, H3K56ac is reduced at DSB sites and constitutively enhanced H3K56ac may impair NHEJ and break-induced replication by blocking resolution of repair factor foci<sup>177,185</sup>. Temporal evidence suggests that these contrasting results are due to a biphasic response of H3K56ac exhibits a biphasic response following DNA damage<sup>177,186</sup>. Proper initiation of DDR signaling and DNA repair factor recruitment may therefore require initial reduction of H3K56ac levels followed by rapid restoration of H3K56ac to restore the basal chromatin configuration state and complete DNA repair<sup>177,186</sup>.

#### **1.5.3.1 Regulators of H3K56ac**

Several acetyltransferases and deacetylases have been associated with H3K56ac. In yeast, H3K56ac is acetylated by Rtt109 and deacetylated by the sirtuin family homologs hybrid sterility (Hst)3 and Hst4<sup>181,183,187</sup>. H3K56ac regulation appears to be more complex in mammalian cells, as both GCN5<sup>178</sup> and CREB-binding protein (CBP)/p300<sup>174,175</sup> have been identified as relevant acetyltransferases. Conserved in both yeast and mammalian cells is the requirement of the histone chaperone Anti-silencing function protein 1 (Asf1) (ASF1A in mammals)<sup>174,181,183,186,188</sup>, which directs CBP/p300 to chromatin and promotes their interaction with H3K56ac. Several deacetylases for H3K56 have been identified as well in human cells. In addition to histone deacetylase (HDAC)1 and HDAC2<sup>177</sup> multiple sirtuin family members have been associated with H3K56 deacetylation, namely sirtuin (SIRT)1 and SIRT2<sup>174,184</sup> as well as SIRT6<sup>189</sup>.

#### **1.5.3.1.1 p300/CBP**

p300 and CBP are closely related nuclear proteins. In addition to their role as histone acetyltransferases, p300 and CBP also act as transcriptional coactivators by directing assembly of transcriptional machinery at promoter regions<sup>190,191</sup>. Genomic localization of p300 binding elucidated that p300 is predominantly recruited to pluripotency genes in ES cells<sup>192</sup>, mirroring the enrichment of H3K56ac at pluripotency gene promoters<sup>93,94</sup>. p300 is also necessary for proper regulation of ES differentiation<sup>193</sup>. p300 and CBP also play a role in the induction of apoptosis, primarily through their regulation of p53. p300 binding to p53 may promote its degradation under basal conditions, but upon cellular stress p300/CBP acetylation of p53 promotes p53 transcriptional activation of target genes<sup>190,194–196</sup>. Additionally, p300 and CBP are also mutated in many cancers<sup>197</sup> and p300 (but not CBP) loss has been shown to impair apoptosis in culture cells<sup>198</sup>.

## **1.6 PROJECT SUMMARY**

The goals of my thesis research were to identify the molecular basis for stem cell radiation responses. Unintended sequelae resulting from radiation therapy have been attributed to the loss of tissue regenerative potential. While there are many mechanisms of radiation-induced normal tissue injury, my project exclusively investigated stem cell dropout, which affects all actively proliferating and regenerative tissues. Destruction of stem cell compartments leads to progressive loss of tissue function and integrity due to dysregulation of normal tissue turnover as differentiated functional tissue compartments are unable to be replenished over time. The clinical motivation underlying this dissertation is to understand the cellular targets of radiation damage and the molecular mechanisms underlying this radiosensitivity. My thesis work began by confirming that only stem cells undergo programmed cell death following exposure to therapeutic IR doses, while surrounding differentiated cells within the niche are radioresistant. The primary focus of my project was then to elucidate the molecular mechanisms responsible for this differential radiosensitivity among stem and differentiated cells. My studies focus on differences in DNA

Damage Response signaling and regulation of histone modifications that contribute to stem cell IR hypersensitivity.

Since stem cells are responsible for generating all differentiated cell types of a tissue, maintaining genomic integrity is of utmost importance to ensure that mutations are not passed on to future progeny. Identifying the details of stem cell responses to DNA damage has therefore been a popular research topic. However, the vast majority of studies previously performed only focused on a particular stem cell model, either in culture or within a specific tissue niche. This precludes identifying broadly applicable mechanisms concerning stem cell radiation responses that are conserved across multiple tissue types. We therefore utilized multiple clinically relevant stem cell niches in order to identify molecular mechanisms responsible for IR-induced normal tissue injury. We assessed cell death and DDR signaling in the dentate gyrus of brain, seminiferous tubules in testis, intestinal crypts and hair follicles. There has also been a stark lack of emphasis in the literature on the use of primary, early passage culture cells. Stem cells can rapidly evolve genomic and epigenomic changes upon culturing<sup>199,200</sup> that may result in modified stem cell molecular responses to DNA damage, so avoiding extended passage of cells is essential. The majority of published studies also do not compare cultured stem cells with directly differentiated, isogenic progeny. This introduces additional complications such as strain variation, cell type-specific differences and additional culture artifacts from the use of established cell lines. We wanted to study stem cell radioresponses together both *in vivo* and in culture, so we took great efforts to establish primary culture models that recapitulate observed *in vivo* phenomena. We established two culture models, murine embryonic stem cells (ES) and neural stem cells (NS). ES cells were primarily purchased from American Type Culture Collection (ATCC) or the Washington University Murine Embryonic Stem Cell Core for convenience, but are originally isolated from the inner cell mass of 4.5 day old blastocysts, while we isolate neural stem cells ourselves from the hippocampus of P0-P2 neonatal mice. ES and NS cells are non-specifically differentiated by removal of LIF or EGF/FGF, respectively, from media conditions (Fig. 1.2). Differentiated ES cells (ED) take on a fibroblast-like appearance while differentiated NS cells (ND) are mixed but biased towards astrocytic differentiation due to supplementation with serum to promote proliferation<sup>201</sup>. We utilized non-targeted differentiation because we are interested in the effect

of merely losing stemness as opposed to any lineage-specific phenotypes. Through establishing this culture system, we have been able to more accurately assess the role of differentiation state in dictating radiation responses.

The first chapter of my thesis analyzes the relative radiosensitivity of stem cells as compared to their differentiated progeny. The remaining two chapters examine the molecular mechanisms underlying the observed differential radiosensitivity between stem and differentiated cells. We first compared induction of the DDR and DNA repair between stem and differentiated cells in order to determine whether inhibited signaling responses to DNA damage could contribute to increased radiosensitivity. Since the purpose of our experimental design was to discover conserved IR-phenotypes linked specifically to differentiation status, we wished to examine molecular regulators of stemness that could also potentially influence radiosensitivity or the DDR. Cell type and differentiation status are determined by unique transcriptional programs that are controlled by specific combinations of histone modifications<sup>202</sup>. In addition to controlling binding of transcription factors to DNA, histone modifications can also regulate access of repair factors. Differentiation status, epigenetic profiles and DNA repair signaling are thus all related (Fig. 1.3). My thesis attempts to define the connections between these features and how they can characterize cellular radiosensitivity. A better understanding of the molecular mechanisms underlying radiation responses of stem and differentiated cells will promote future targeted therapies for reducing detrimental sequelae in patients.

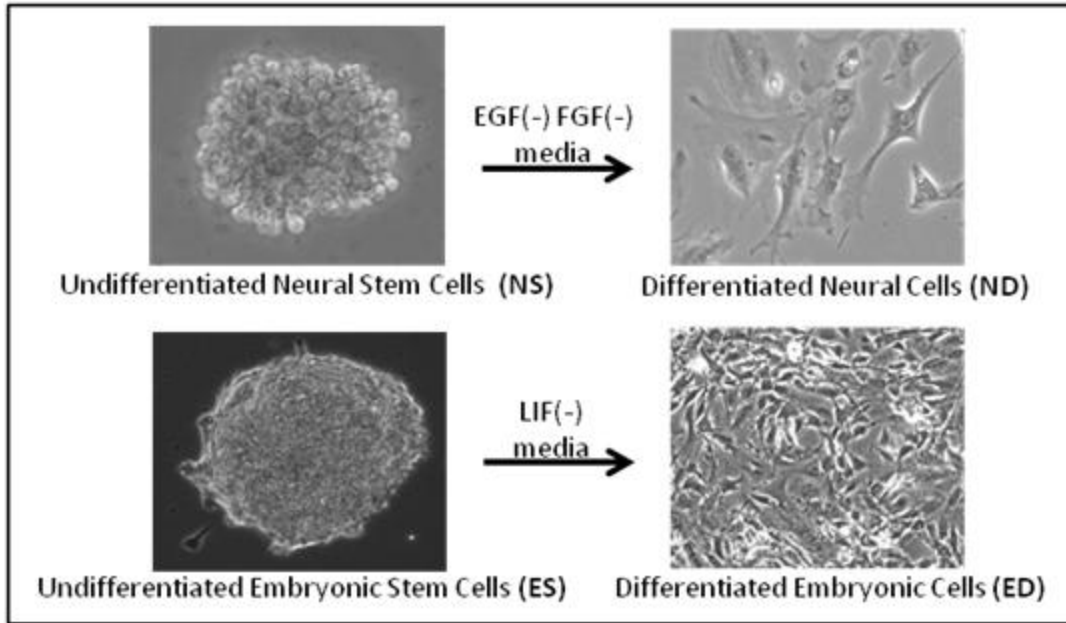


Figure 1.2. Primary stem cell culture models utilized in this study.

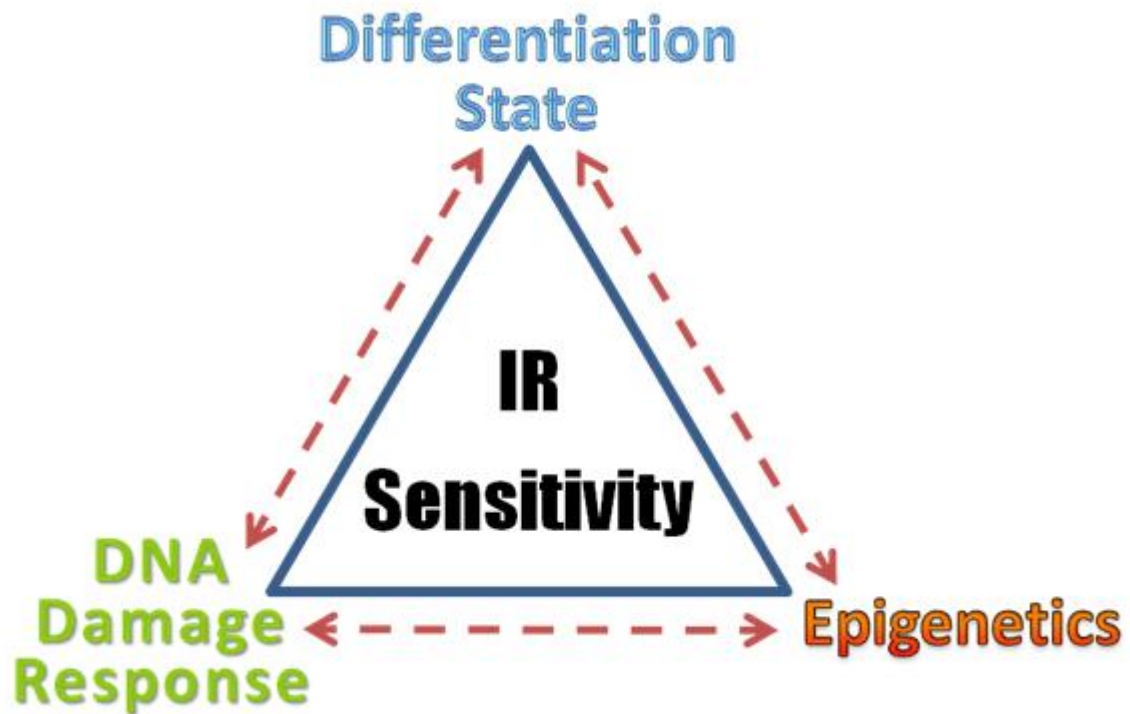


Figure 1.3. The interrelatedness of the DDR, differentiation state and epigenetics in controlling cellular radiosensitivity.

## 1.7 REFERENCES

1. Van Gent, D. C., Hoeijmakers, J. H. & Kanaar, R. Chromosomal stability and the DNA double-stranded break connection. *Nat Rev Genet* **2**, 196–206 (2001).
2. Kastan, M. B., Canman, C. E. & Leonard, C. J. P53, cell cycle control and apoptosis: implications for cancer. *Cancer Metastasis Rev.* **14**, 3–15 (1995).
3. Brown, J. M. & Attardi, L. D. The role of apoptosis in cancer development and treatment response. *Nat. Rev. Cancer* **5**, 231–7 (2005).
4. Abdullah, L. N. & Chow, E. K.-H. Mechanisms of chemoresistance in cancer stem cells. *Clin. Transl. Med.* **2**, 3 (2013).
5. Alison, M. R., Lin, W.-R., Lim, S. M. L. & Nicholson, L. J. Cancer stem cells: In the line of fire. *Cancer Treat. Rev.* (2012). doi:10.1016/j.ctrv.2012.03.003
6. Cojoc, M., Mäbert, K., Muders, M. H. & Dubrovskaya, A. A role for cancer stem cells in therapy resistance: cellular and molecular mechanisms. *Semin. Cancer Biol.* (2014). doi:10.1016/j.semcancer.2014.06.004
7. Stone, H., Coleman, C., Anscher, M. & McBride, W. Effects of radiation on normal tissue: consequences and mechanisms. *Lancet Oncol.* **4**, 529–536 (2003).
8. Hall, E. J. in *Radiobiol. Radiol.* 5–16 (2000).
9. Ward, J. F. The complexity of DNA damage: relevance to biological consequences. *Int J Radiat Biol* **66**, 427–432 (1994).
10. Donnelly, E. H. *et al.* Acute radiation syndrome: assessment and management. *South. Med. J.* **103**, 541–6 (2010).
11. Mettler Jr, F. A. & Voelz, G. L. Major Radiation Exposure: What To Expect and How to Respond. *New Engl J Med* **346**, 1554–1561 (2002).
12. Jackson, S. P. & Bartek, J. The DNA-damage response in human biology and disease. *Nature* **461**, 1071–1078 (2009).
13. Roninson, I. B., Broude, E. V & Chang, B. D. If not apoptosis, then what? Treatment-induced senescence and mitotic catastrophe in tumor cells. *Drug Resist. Updat.* **4**, 303–13 (2001).
14. Baumann, M., Krause, M. & Hill, R. Exploring the role of cancer stem cells in radioresistance. *Nat. Rev. Cancer* **8**, 545–54 (2008).
15. Hittelman, W. N., Liao, Y., Wang, L. & Milas, L. Are cancer stem cells radioresistant? *Future Oncol.* **6**, 1563–76 (2010).
16. Vlashi, E., McBride, W. H. & Pajonk, F. Radiation responses of cancer stem cells. *J. Cell. Biochem.* **108**, 339–42 (2009).
17. Feinendegen, L. E. Evidence for beneficial low level radiation effects and radiation hormesis. *Br. J. Radiol.* **78**, 3–7 (2005).

18. Tubiana, M., Feinendegen, L., Yang, C. & Kaminski, J. The linear no-threshold relationship is inconsistent with radiation biologic and experimental data. *Radiology* **251**, (2009).
19. Morgan, W. F. & Bair, W. J. Issues in low dose radiation biology: the controversy continues. A perspective. *Radiat. Res.* **179**, 501–10 (2013).
20. Mauch, P. *et al.* Hematopoietic stem cell compartment: acute and late effects of radiation therapy and chemotherapy. *Int. J. Radiat. Oncol. Biol. Phys.* **31**, 1319–39 (1995).
21. Duffner, P. K. Long-term effects of radiation therapy on cognitive and endocrine function in children with leukemia and brain tumors. *Neurologist* **10**, 293–310 (2004).
22. Gibson, E. & Monje, M. Effect of cancer therapy on neural stem cells: implications for cognitive function. *Curr. Opin. Oncol.* **24**, 672–678 (2012).
23. Ash, P. The influence of radiation on fertility in man. *Br. J. Radiol.* **53**, 271–8 (1980).
24. Withers, H. R. Regeneration of intestinal mucosa after irradiation. *Cancer* **28**, 75–81 (1971).
25. Smith, D. H. & DeCosse, J. J. Radiation damage to the small intestine. *World J. Surg.* **10**, 189–94 (1986).
26. Ginot, A., Doyen, J., Hannoun-Levi, J. M. & Courdi, A. [Normal tissue tolerance to external beam radiation therapy: skin]. *Cancer Radiother* **14**, 379–385 (2010).
27. Rubin, P. The Franz Buschke lecture: late effects of chemotherapy and radiation therapy: a new hypothesis. *Int J Radiat Oncol Biol Phys* **10**, 5–34 (1984).
28. Hellman, S. & Botnick, L. E. Stem cell depletion: an explanation of the late effects of cytotoxins. *Int. J. Radiat. Oncol. Biol. Phys.* **2**, 181–4 (1977).
29. Zhao, W. & Robbins, M. E. C. Inflammation and chronic oxidative stress in radiation-induced late normal tissue injury: therapeutic implications. *Curr. Med. Chem.* **16**, 130–43 (2009).
30. Bentzen, S. M. Preventing or reducing late side effects of radiation therapy: radiobiology meets molecular pathology. *Nat. Rev. Cancer* **6**, 702–13 (2006).
31. Shrieve, D. C. & Loeffler, J. S. in *Hum. Radiat. Inj.* 14–20 (2010).
32. Zhao, W. & Robbins, M. E. C. Inflammation and chronic oxidative stress in radiation-induced late normal tissue injury: therapeutic implications. *Curr. Med. Chem.* **16**, 130–43 (2009).
33. Hall, E. J. in *Radiobiol. Radiol.* 91–111 (2000).
34. Hall, E. J. in *Radiobiol. Radiol.* 397–418 (2000).
35. Bergonié, J. & Tribondeau, L. Interpretation of Some Results from Radiotherapy and an Attempt to Determine a Rational Treatment Technique. 1906. *Yale J. Biol. Med.* **76**, 181–2 (2003).
36. Vogin, G. & Foray, N. The law of Bergonié and Tribondeau: a nice formula for a first approximation. *Int. J. Radiat. Biol.* **89**, 2–8 (2013).

37. Denekamp, J. Cell kinetics and radiation biology. *Int. J. Radiat. Biol. Relat. Stud. Phys. Chem. Med.* **49**, 357–80 (1986).
38. Giunta, S., Belotserkovskaya, R. & Jackson, S. P. DNA damage signaling in response to double-strand breaks during mitosis. *J Cell Biol* **190**, 197–207 (2010).
39. Pawlik, T. M. & Keyomarsi, K. Role of cell cycle in mediating sensitivity to radiotherapy. *Int. J. Radiat. Oncol. Biol. Phys.* **59**, 928–42 (2004).
40. Hsu, T. C., Dewey, W. C. & Humphrey, R. M. Radiosensitivity of cells of Chinese hamster in vitro in relation to the cell cycle. *Exp. Cell Res.* **27**, 441–452 (1962).
41. Short, S. C., Woodcock, M., Marples, B. & Joiner, M. C. Effects of cell cycle phase on low-dose hyper-radiosensitivity. *Int. J. Radiat. Biol.* **79**, 99–105 (2009).
42. Galluzzi, L. *et al.* Molecular definitions of cell death subroutines: recommendations of the Nomenclature Committee on Cell Death 2012. *Cell Death Differ.* **19**, 107–20 (2012).
43. Kuilman, T., Michaloglou, C., Mooi, W. J. & Peeper, D. S. The essence of senescence. *Genes Dev.* **24**, 2463–79 (2010).
44. Proskuryakov, S. Y. ., Konoplyannikov, A. G. & Gabai, V. L. Necrosis: a specific form of programmed cell death? *Exp. Cell Res.* **283**, 1–16 (2003).
45. Kroemer, G. & Levine, B. Autophagic cell death: the story of a misnomer. *Nat. Rev. Mol. Cell Biol.* **9**, 1004–10 (2008).
46. Candé, C. *et al.* Apoptosis-inducing factor (AIF): a novel caspase-independent death effector released from mitochondria. *Biochimie* **84**, 215–22
47. Elmore, S. Apoptosis: a review of programmed cell death. *Toxicol. Pathol.* **35**, 495–516 (2007).
48. Fridman, J. S. & Lowe, S. W. Control of apoptosis by p53. *Oncogene* **22**, 9030–40 (2003).
49. Taira, N. & Yoshida, K. Post-translational modifications of p53 tumor suppressor: determinants of its functional targets. *Histol. Histopathol.* **27**, 437–43 (2012).
50. Song, H. *et al.* Mammalian Mst1 and Mst2 kinases play essential roles in organ size control and tumor suppression. *Proc. Natl. Acad. Sci. U. S. A.* **107**, 1431–6 (2010).
51. Wen, W. *et al.* MST1 promotes apoptosis through phosphorylation of histone H2AX. *J Biol Chem* **285**, 39108–39116 (2010).
52. Graves, J. D., Draves, K. E., Gotoh, Y., Krebs, E. G. & Clark, E. A. Both phosphorylation and caspase-mediated cleavage contribute to regulation of the Ste20-like protein kinase Mst1 during CD95/Fas-induced apoptosis. *J. Biol. Chem.* **276**, 14909–15 (2001).
53. Praskova, M., Khoklatchev, A., Ortiz-Vega, S. & Avruch, J. Regulation of the MST1 kinase by autophosphorylation, by the growth inhibitory proteins, RASSF1 and NORE1, and by Ras. *Biochem. J.* **381**, 453–62 (2004).

54. Lu, C. *et al.* Cell apoptosis: requirement of H2AX in DNA ladder formation, but not for the activation of caspase-3. *Mol. Cell* **23**, 121–32 (2006).
55. Solier, S. & Pommier, Y. The apoptotic ring: a novel entity with phosphorylated histones H2AX and H2B and activated DNA damage response kinases. *Cell Cycle* **8**, 1853–9 (2009).
56. Cheung, W. L. *et al.* Apoptotic Phosphorylation of Histone H2B Is Mediated by Mammalian Sterile Twenty Kinase. *Cell* **113**, 507–517 (2003).
57. Ura, S., Nishina, H., Gotoh, Y. & Katada, T. Activation of the c-Jun N-terminal kinase pathway by MST1 is essential and sufficient for the induction of chromatin condensation during apoptosis. *Mol. Cell. Biol.* **27**, 5514–22 (2007).
58. Ura, S., Masuyama, N., Graves, J. D. & Gotoh, Y. MST1-JNK promotes apoptosis via caspase-dependent and independent pathways. *Genes Cells* **6**, 519–30 (2001).
59. Warmerdam, D. O. & Kanaar, R. Dealing with DNA damage: relationships between checkpoint and repair pathways. *Mutat. Res.* **704**, 2–11 (2010).
60. Polo, S. E. & Jackson, S. P. Dynamics of DNA damage response proteins at DNA breaks: a focus on protein modifications. *Genes Dev.* **25**, 409–33 (2011).
61. Lee, J.-H. & Paull, T. T. ATM activation by DNA double-strand breaks through the Mre11-Rad50-Nbs1 complex. *Science* **308**, 551–4 (2005).
62. Lavin, M. F. ATM and the Mre11 complex combine to recognize and signal DNA double-strand breaks. *Oncogene* **26**, 7749–58 (2007).
63. Uziel, T. *et al.* Requirement of the MRN complex for ATM activation by DNA damage. *EMBO J.* **22**, 5612–21 (2003).
64. Lee, J.-H. & Paull, T. T. Activation and regulation of ATM kinase activity in response to DNA double-strand breaks. *Oncogene* **26**, 7741–8 (2007).
65. Bakkenist, C. J. & Kastan, M. B. DNA damage activates ATM through intermolecular autophosphorylation and dimer dissociation. *Nature* **421**, 499–506 (2003).
66. Shiloh, Y. & Ziv, Y. The ATM protein kinase: regulating the cellular response to genotoxic stress, and more. *Nat. Rev. Mol. Cell Biol.* **14**, 197–210 (2013).
67. Burma, S., Chen, B. P., Murphy, M., Kurimasa, A. & Chen, D. J. ATM phosphorylates histone H2AX in response to DNA double-strand breaks. *J. Biol. Chem.* **276**, 42462–7 (2001).
68. Stiff, T. *et al.* ATM and DNA-PK function redundantly to phosphorylate H2AX after exposure to ionizing radiation. *Cancer Res.* **64**, 2390–6 (2004).
69. Paull, T. T. *et al.* A critical role for histone H2AX in recruitment of repair factors to nuclear foci after DNA damage. *Curr. Biol.* **10**, 886–95 (2000).
70. Cimprich, K. A. & Cortez, D. ATR : an essential regulator of genome integrity. **9**, (2008).

71. Chen, B. P. C. *et al.* Cell cycle dependence of DNA-dependent protein kinase phosphorylation in response to DNA double strand breaks. *J. Biol. Chem.* **280**, 14709–15 (2005).
72. Chan, D. & Chen, B. Autophosphorylation of the DNA-dependent protein kinase catalytic subunit is required for rejoining of DNA double-strand breaks. *Genes ...* **16**, 2333–2338 (2002).
73. Podhorecka, M., Skladanowski, A. & *et al.* H2AX Phosphorylation: Its Role in DNA Damage Response and Cancer Therapy. *J. Nucleic Acids* **2010**, (2010).
74. Lou, Z. *et al.* MDC1 maintains genomic stability by participating in the amplification of ATM-dependent DNA damage signals. *Mol. Cell* **21**, 187–200 (2006).
75. Soutoglou, E. & Misteli, T. Activation of the cellular DNA damage response in the absence of DNA lesions. *Science* **320**, 1507–10 (2008).
76. Norbury, C. J. & Zivhotovsky, B. DNA damage-induced apoptosis. *Oncogene* **23**, 2797–808 (2004).
77. Shaltiel, I. a, Krenning, L., Bruinsma, W. & Medema, R. H. The same, only different - DNA damage checkpoints and their reversal throughout the cell cycle. *J. Cell Sci.* **2**, 607–620 (2015).
78. Cha, H. *et al.* Wip1 directly dephosphorylates gamma-H2AX and attenuates the DNA damage response. *Cancer Res* **70**, 4112–4122 (2010).
79. Shreeram, S. *et al.* Wip1 phosphatase modulates ATM-dependent signaling pathways. *Mol. Cell* **23**, 757–64 (2006).
80. Fiscella, M. *et al.* Wip1, a novel human protein phosphatase that is induced in response to ionizing radiation in a p53-dependent manner. *Proc. Natl. Acad. Sci. U. S. A.* **94**, 6048–53 (1997).
81. Demidov, O. N. *et al.* Wip1 phosphatase regulates p53-dependent apoptosis of stem cells and tumorigenesis in the mouse intestine. *Cell Stem Cell* **1**, 180–90 (2007).
82. Chowdhury, D. *et al.* gamma-H2AX dephosphorylation by protein phosphatase 2A facilitates DNA double-strand break repair. *Mol. Cell* **20**, 801–9 (2005).
83. Petersen, P. *et al.* Protein phosphatase 2A antagonizes ATM and ATR in a Cdk2- and Cdc7-independent DNA damage checkpoint. *Mol. Cell. Biol.* **26**, 1997–2011 (2006).
84. Lossaint, G., Besnard, E., Fisher, D., Piette, J. & Dulić, V. Chk1 is dispensable for G2 arrest in response to sustained DNA damage when the ATM/p53/p21 pathway is functional. *Oncogene* **30**, 4261–74 (2011).
85. Liu, Q. *et al.* Chk1 is an essential kinase that is regulated by Atr and required for the G2/M DNA damage checkpoint. *Genes & Dev.* **14**, 1448–1459 (2000).
86. Shaltiel, I. a, Krenning, L., Bruinsma, W. & Medema, R. H. The same, only different - DNA damage checkpoints and their reversal throughout the cell cycle. *J. Cell Sci.* **2**, 607–620 (2015).
87. Mao, Z., Bozzella, M., Seluanov, A. & Gorbunova, V. Comparison of nonhomologous end joining and homologous recombination in human cells. *DNA Repair (Amst)*. **7**, 1765–71 (2008).

88. Xie, A., Kwok, A. & Scully, R. Role of mammalian Mre11 in classical and alternative nonhomologous end joining. *Nat. Struct. Mol. Biol.* **16**, 814–8 (2009).
89. Yuan, J. & Chen, J. MRE11-RAD50-NBS1 complex dictates DNA repair independent of H2AX. *J. Biol. Chem.* **285**, 1097–104 (2010).
90. Morrison, S. J., Shah, N. M. & Anderson, D. J. Regulatory Mechanisms in Stem Cell Biology. *Cell* **88**, 287–298 (1997).
91. Armstrong, L. Epigenetic control of embryonic stem cell differentiation. *Stem Cell Rev.* **8**, 67–77 (2012).
92. Li, L. & Xie, T. Stem cell niche: structure and function. *Annu. Rev. Cell Dev. Biol.* **21**, 605–31 (2005).
93. Tan, Y., Xue, Y., Song, C. & Grunstein, M. Acetylated histone H3K56 interacts with Oct4 to promote mouse embryonic stem cell pluripotency. *Proc. Natl. Acad. Sci. U. S. A.* **110**, 11493–8 (2013).
94. Xie, W. *et al.* Histone h3 lysine 56 acetylation is linked to the core transcriptional network in human embryonic stem cells. *Mol. Cell* **33**, 417–27 (2009).
95. Fluckiger, A.-C. *et al.* Cell cycle features of primate embryonic stem cells. *Stem Cells* **24**, 547–56 (2006).
96. Suvorova, I. I., Katolikova, N. V & Pospelov, V. a. New insights into cell cycle regulation and DNA damage response in embryonic stem cells. *Int. Rev. Cell Mol. Biol.* **299**, 161–98 (2012).
97. Ruiz, S. *et al.* A high proliferation rate is required for cell reprogramming and maintenance of human embryonic stem cell identity. *Curr. Biol.* **21**, 45–52 (2011).
98. Dasa, D. *et al.* MicroRNAs Regulate p21Waf1/cip1 Protein Expression and the DNA Damage Response in Human Embryonic Stem Cells. *Stem Cells N/A–N/A* (2012). doi:10.1002/stem.1108
99. Hong, Y. & Stambrook, P. J. Restoration of an absent G 1 arrest and protection from apoptosis in embryonic stem cells after ionizing radiation. *Proc Natl Acad Sci U S A* **101**, 14443–14448 (2004).
100. Roque, T. *et al.* Lack of a p21(waf1/cip) -Dependent G1/S Checkpoint in Neural Stem and Progenitor Cells After DNA Damage in vivo. *Stem Cells* **30**, 537-547 (2011).
101. Momcilović, O. *et al.* Ionizing radiation induces ataxia telangiectasia mutated-dependent checkpoint signaling and G(2) but not G(1) cell cycle arrest in pluripotent human embryonic stem cells. *Stem Cells* **27**, 1822–35 (2009).
102. Aladjem, M. I. *et al.* ES cells do not activate p53-dependent stress responses and undergo p53-independent apoptosis in response to DNA damage. *Curr Biol* **8**, 145–155 (1998).
103. Tanori, M. *et al.* Developmental and oncogenic radiation effects on neural stem cells and their differentiating progeny in mouse cerebellum. *Stem Cells* **31**, 2506–16 (2013).
104. Saretzki, G., Armstrong, L. & Leake, A. Stress defense in murine embryonic stem cells is superior to that of various differentiated murine cells. *Stem Cells* **22**, 962–971 (2004).

105. Giachino, C., Orlando, L. & Turinetti, V. Maintenance of genomic stability in mouse embryonic stem cells: relevance in aging and disease. *Int. J. Mol. Sci.* **14**, 2617–36 (2013).
106. Hong, Y., Cervantes, R. B., Tichy, E., Tischfield, J. A. & Stambrook, P. J. Protecting genomic integrity in somatic cells and embryonic stem cells. *Mutat Res* **614**, 48–55 (2007).
107. Wyles, S. P., Brandt, E. B. & Nelson, T. J. Stem Cells: The Pursuit of Genomic Stability. *Int. J. Mol. Sci.* **15**, 20948–20967 (2014).
108. Liu, S. *et al.* ATR autophosphorylation as a molecular switch for checkpoint activation. *Mol. Cell* **43**, 192–202 (2011).
109. Acharya, M. M. *et al.* Consequences of ionizing radiation-induced damage in human neural stem cells. *Free Radic. Biol. Med.* **49**, 1846–1855 (2010).
110. Zou, Y. *et al.* Responses of human embryonic stem cells and their differentiated progeny to ionizing radiation. *Biochem. Biophys. Res. Commun.* **426**, 100–5 (2012).
111. Schneider, L., Fumagalli, M. & d'Adda di Fagagna, F. Terminally differentiated astrocytes lack DNA damage response signaling and are radioresistant but retain DNA repair proficiency. *Cell Death Differ.* **19**, 582–591 (2011).
112. De Waard, H. *et al.* Cell-type-specific consequences of nucleotide excision repair deficiencies: Embryonic stem cells versus fibroblasts. *DNA Repair (Amst)*. **7**, 1659–69 (2008).
113. Dumitru, R. *et al.* Human Embryonic Stem Cells Have Constitutively Active Bax at the Golgi and Are Primed to Undergo Rapid Apoptosis. *Mol. Cell* (2012). doi:10.1016/j.molcel.2012.04.002
114. Lin, T. *et al.* p53 induces differentiation of mouse embryonic stem cells by suppressing Nanog expression. *Nat. Cell Biol.* **7**, 165–71 (2005).
115. Saha, S. *et al.* Increased apoptosis and DNA double-strand breaks in the embryonic mouse brain in response to very low-dose X-rays but not 50 Hz magnetic fields. *J. R. Soc. Interface* **11**, (2014).
116. Tada, E., Parent, J. M., Lowenstein, D. H. & Fike, J. R. X-irradiation causes a prolonged reduction in cell proliferation in the dentate gyrus of adult rats. *Neuroscience* **99**, 33–41 (2000).
117. Limoli, C. & Ward, J. A new method for introducing double-strand breaks into cellular DNA. *Radiat. Res.* **134**, 160–169 (1993).
118. Monje, M. L., Mizumatsu, S., Fike, J. R. & Palmer, T. D. Irradiation induces neural precursor-cell dysfunction. *Nat. Med.* **8**, 955–62 (2002).
119. Mizumatsu, S. *et al.* Extreme sensitivity of adult neurogenesis to low doses of X-irradiation. *Cancer Res.* **63**, 4021–7 (2003).
120. Peissner, W., Kocher, M., Treuer, H. & Gillardon, F. Ionizing radiation-induced apoptosis of proliferating stem cells in the dentate gyrus of the adult rat hippocampus. *Brain Res. Mol. Brain Res.* **71**, 61–8 (1999).

121. Potten, C. S., Merritt, A., Hickman, J., Hall, P. & Faranda, A. Characterization of Radiation-induced Apoptosis in the Small Intestine and Its Biological Implications. *Int. J. Radiat. Biol.* **65**, 71–78 (1994).
122. Potten, C. S., Al-Barwari, S. E. & Searle, J. Differential radiation response amongst proliferating epithelial cells. *Cell Tissue Kinet* **11**, 149–160 (1978).
123. Merritt, a J. *et al.* Differential expression of bcl-2 in intestinal epithelia. Correlation with attenuation of apoptosis in colonic crypts and the incidence of colonic neoplasia. *J. Cell Sci.* **108 ( Pt 6)**, 2261–71 (1995).
124. Barker, N. *et al.* Identification of stem cells in small intestine and colon by marker gene Lgr5. *Nature* **449**, 1003–7 (2007).
125. Sangiorgi, E. & Capecchi, M. R. Bmi1 is expressed in vivo in intestinal stem cells. *Nat. Genet.* **40**, 915–20 (2008).
126. Potten, C. S., Owen, G. & Booth, D. Intestinal stem cells protect their genome by selective segregation of template DNA strands. *J. Cell Sci.* **115**, 2381–2388 (2002).
127. Yan, K. S. *et al.* The intestinal stem cell markers Bmi1 and Lgr5 identify two functionally distinct populations. *Proc. Natl. Acad. Sci. U. S. A.* **109**, 466–71 (2012).
128. Zhu, Y., Huang, Y.-F., Kek, C. & Bulavin, D. V. Apoptosis differently affects lineage tracing of Lgr5 and Bmi1 intestinal stem cell populations. *Cell Stem Cell* **12**, 298–303 (2013).
129. Withers, H. R., Hunter, N., Barkley Jr., H. T. & Reid, B. O. Radiation survival and regeneration characteristics of spermatogenic stem cells of mouse testis. *Radiat Res* **57**, 88–103 (1974).
130. Rube, C. E., Zhang, S., Miebach, N., Fricke, A. & Rube, C. Protecting the heritable genome: DNA damage response mechanisms in spermatogonial stem cells. *DNA Repair (Amst)*. **10**, 159–68 (2011).
131. Rachidi, W. *et al.* Sensing radiosensitivity of human epidermal stem cells. *Radiother. Oncol.* **83**, 267–76 (2007).
132. Sotiropoulou, P. A. *et al.* Bcl-2 and accelerated DNA repair mediates resistance of hair follicle bulge stem cells to DNA-damage-induced cell death. *Nat Cell Biol* **12**, 572–582 (2010).
133. Li, L. & Clevers, H. Coexistence of quiescent and active adult stem cells in mammals. *Science* **327**, 542–5 (2010).
134. Sugrue, T., Brown, J. a L., Lowndes, N. F. & Ceredig, R. Multiple facets of the DNA damage response contribute to the radioresistance of mouse mesenchymal stromal cell lines. *Stem Cells* **31**, 137–45 (2013).
135. Mohrin, M. *et al.* Hematopoietic Stem Cell Quiescence Promotes Error-Prone DNA Repair and Mutagenesis. *Cell Stem Cell* **7**, 174–185 (2010).
136. Milyavsky, M. *et al.* A Distinctive DNA Damage Response in Human Hematopoietic Stem Cells Reveals an Apoptosis-Independent Role for p53 in Self-Renewal. *Cell Stem Cell* **7**, 186–197 (2010).

137. Seita, J., Rossi, D. J. & Weissman, I. L. Differential DNA damage response in stem and progenitor cells. *Cell Stem Cell* **7**, 145–147 (2010).
138. Luo, L. Z. *et al.* DNA repair in human pluripotent stem cells is distinct from that in non-pluripotent human cells. *PLoS One* **7**, e30541 (2012).
139. Fan, J. *et al.* Human induced pluripotent cells resemble embryonic stem cells demonstrating enhanced levels of DNA repair and efficacy of nonhomologous end-joining. *Mutat. Res.* **713**, 8–17 (2011).
140. Fung, H. & Weinstock, D. M. Repair at single targeted DNA double-strand breaks in pluripotent and differentiated human cells. *PLoS One* **6**, e20514 (2011).
141. Maynard, S. *et al.* Human embryonic stem cells have enhanced repair of multiple forms of DNA damage. *Stem Cells* **26**, 2266–74 (2008).
142. Lan, M. L. *et al.* Characterizing the Radioresponse of Pluripotent and Multipotent Human Stem Cells. *PLoS One* **7**, e50048 (2012).
143. Tichy, E. D. *et al.* Mouse embryonic stem cells, but not somatic cells, predominantly use homologous recombination to repair double-strand DNA breaks. *Stem Cells Dev.* **19**, 1699–711 (2010).
144. Adams, B. R., Golding, S. E., Rao, R. R. & Valerie, K. Dynamic dependence on ATR and ATM for double-strand break repair in human embryonic stem cells and neural descendants. *PLoS One* **5**, e10001 (2010).
145. Rousseau, L. *et al.* In vivo importance of homologous recombination DNA repair for mouse neural stem and progenitor cells. *PLoS One* **7**, e37194 (2012).
146. Serrano, L. *et al.* Homologous recombination conserves DNA sequence integrity throughout the cell cycle in embryonic stem cells. *Stem Cells Dev.* **20**, 363–74 (2011).
147. Tichy, E. D. *et al.* The abundance of Rad51 protein in mouse embryonic stem cells is regulated at multiple levels. *Stem Cell Res.* **9**, 124–34 (2012).
148. Adams, B. R., Hawkins, A. J., Povirk, L. F. & Valerie, K. ATM-independent, high-fidelity nonhomologous end joining predominates in human embryonic stem cells. *Aging (Albany NY)* **2**, 582–596 (2010).
149. Bogomazova, A. N., Lagarkova, M. a, Tskhovrebova, L. V, Shutova, M. V & Kiselev, S. L. Error-prone nonhomologous end joining repair operates in human pluripotent stem cells during late G2. *Aging (Albany. NY)*. **3**, 584–96 (2011).
150. Carlessi, L., De Filippis, L., Lecis, D., Vescovi, A. & Delia, D. DNA-damage response, survival and differentiation in vitro of a human neural stem cell line in relation to ATM expression. *Cell Death Differ.* **16**, 795–806 (2009).
151. Chuykin, I. A., Lianguzova, M. S., Pospelova, T. V & Pospelov, V. A. Activation of DNA damage response signaling in mouse embryonic stem cells. *Cell Cycle* **7**, 2922–2928 (2008).
152. Bañuelos, C. a *et al.* Mouse but not human embryonic stem cells are deficient in rejoining of ionizing radiation-induced DNA double-strand breaks. *DNA Repair (Amst)*. **7**, 1471–83 (2008).

153. Zhang, M., Yang, C., Liu, H. & Sun, Y. Induced Pluripotent Stem Cells Are Sensitive to DNA Damage. *Genomics Proteomics Bioinforma.* **11**, 320–326 (2013).
154. Hennicke, T. *et al.* mESC-based in vitro differentiation models to study vascular response and functionality following genotoxic insults. *Toxicol Sci.* **144**, 138–150 (2014).
155. Turinetto, V. *et al.* High basal  $\gamma$ H2AX levels sustain self-renewal of mouse embryonic and induced pluripotent stem cells. *Stem Cells* **30**, 1414–23 (2012).
156. Fernando, R. N. *et al.* Cell cycle restriction by histone H2AX limits proliferation of adult neural stem cells. *Proc. Natl. Acad. Sci.* **108**, 1–6 (2011).
157. Banáth, J. P. *et al.* Explanation for excessive DNA single-strand breaks and endogenous repair foci in pluripotent mouse embryonic stem cells. *Exp. Cell Res.* **315**, 1505–20 (2009).
158. Hua, G. *et al.* Crypt Base Columnar Stem Cells in Small Intestines of Mice are Radioresistant. *Gastroenterology* **143**, 1266–1276 (2012).
159. Wang, F. *et al.* P53-participated cellular and molecular responses to irradiation are cell differentiation-determined in murine intestinal epithelium. *Arch. Biochem. Biophys.* **542**, 21–7 (2014).
160. Gatz, S. A. *et al.* Requirement for DNA ligase IV during embryonic neuronal development. *J. Neurosci.* **31**, 10088–10100 (2011).
161. Oliver, L. *et al.* Differentiation Related Response to DNA Breaks in Human Mesenchymal Stem Cells. *Stem Cells* (2013). doi:10.1002/stem.1336
162. Friedl, A. a, Mazurek, B. & Seiler, D. M. Radiation-induced alterations in histone modification patterns and their potential impact on short-term radiation effects. *Front. Oncol.* **2**, 117 (2012).
163. Greenberg, R. a. Histone tails: Directing the chromatin response to DNA damage. *FEBS Lett.* **585**, 2883–90 (2011).
164. Lukas, J., Lukas, C. & Bartek, J. More than just a focus: The chromatin response to DNA damage and its role in genome integrity maintenance. *Nat. Cell Biol.* **13**, 1161–9 (2011).
165. Solier, S. & Pommier, Y. The nuclear  $\gamma$ -H2AX apoptotic ring: implications for cancers and autoimmune diseases. *Cell. Mol. Life Sci.* **139**, (2014).
166. Meyer, B. *et al.* Clustered DNA damage induces pan-nuclear H2AX phosphorylation mediated by ATM and DNA-PK. *Nucleic Acids Res.* **41**, 6109–18 (2013).
167. Baritaud, M., Boujrad, H., Lorenzo, H. K., Krantic, S. & Susin, S. a. Histone H2AX: The missing link in AIF-mediated caspase-independent programmed necrosis. *Cell Cycle* **9**, 3166–3173 (2010).
168. Solier, S. & Pommier, Y. MDC1 cleavage by caspase-3: a novel mechanism for inactivating the DNA damage response during apoptosis. *Cancer Res.* **71**, 906–13 (2011).
169. Xiao, A. *et al.* WSTF regulates the H2A.X DNA damage response via a novel tyrosine kinase activity. *Nature* **457**, 57–62 (2009).

170. Cook, P. J. *et al.* Tyrosine dephosphorylation of H2AX modulates apoptosis and survival decisions. *Nature* **458**, 591–6 (2009).
171. Xie, A., Odate, S., Chandramouly, G. & Scully, R. H2AX post-translational modifications in the ionizing radiation response and homologous recombination. *Cell Cycle* **9**, 3602–10 (2010).
172. Brown, J. a L., Eykelenboom, J. K. & Lowndes, N. F. Co-mutation of histone H2AX S139A with Y142A rescues Y142A-induced ionising radiation sensitivity. *FEBS Open Bio* **2**, 313–7 (2012).
173. Zhang, Y. *et al.* Imatinib induces H2AX phosphorylation and apoptosis in chronic myelogenous leukemia cells in vitro via caspase-3/Mst1 pathway. *Acta Pharmacol. Sin.* **33**, 551–7 (2012).
174. Das, C., Lucia, M. S., Hansen, K. C. & Tyler, J. K. CBP/p300-mediated acetylation of histone H3 on lysine 56. *Nature* **459**, 113–7 (2009).
175. Vempati, R. K. *et al.* p300-mediated acetylation of histone H3 lysine 56 functions in DNA damage response in mammals. *J. Biol. Chem.* **285**, 28553–64 (2010).
176. Vempati, R. K. DNA damage in the presence of chemical genotoxic agents induce acetylation of H3K56 and H4K16 but not H3K9 in mammalian cells. *Mol. Biol. Rep.* **39**, 303–8 (2012).
177. Miller, K. M. *et al.* Human HDAC1 and HDAC2 function in the DNA-damage response to promote DNA nonhomologous end-joining. *Nat Struct Mol Biol* **17**, 1144–1151 (2010).
178. Tjeertes, J. V, Miller, K. M. & Jackson, S. P. Screen for DNA-damage-responsive histone modifications identifies H3K9Ac and H3K56Ac in human cells. *EMBO J* **28**, 1878–1889 (2009).
179. Maroschik, B. *et al.* Radiation-induced alterations of histone post-translational modification levels in lymphoblastoid cell lines. *Radiat. Oncol.* **9**, 15 (2014).
180. Drogaris, P. *et al.* Histone deacetylase inhibitors globally enhance h3/h4 tail acetylation without affecting h3 lysine 56 acetylation. *Sci. Rep.* **2**, 220 (2012).
181. Costelloe, T. & Lowndes, N. F. Chromatin assembly and signalling the end of DNA repair requires acetylation of histone H3 on lysine 56. *Subcell Biochem* **50**, 43–54 (2010).
182. Wurtele, H. *et al.* Histone H3 lysine 56 acetylation and the response to DNA replication fork damage. *Mol. Cell. Biol.* **32**, 154–72 (2012).
183. Chen, C.-C. *et al.* Acetylated lysine 56 on histone H3 drives chromatin assembly after repair and signals for the completion of repair. *Cell* **134**, 231–43 (2008).
184. Yuan, J., Pu, M., Zhang, Z. & Lou, Z. Histone H3-K56 acetylation is important for genomic stability in mammals. *Cell Cycle* **8**, 1747–1753 (2009).
185. Che, J. *et al.* Hyper-Acetylation of Histone H3K56 Limits Break-Induced Replication by Inhibiting Extensive Repair Synthesis. *PLoS Genet.* **11**, e1004990 (2015).
186. Battu, A., Ray, A. & Wani, A. a. ASF1A and ATM regulate H3K56-mediated cell-cycle checkpoint recovery in response to UV irradiation. *Nucleic Acids Res.* **39**, 7931–7945 (2011).

187. Minard, L. V, Williams, J. S., Walker, A. C. & Schultz, M. C. Transcriptional regulation by Asf1: new mechanistic insights from studies of the DNA damage response to replication stress. *J. Biol. Chem.* **286**, 7082–92 (2011).
188. Das, C. *et al.* Binding of the histone chaperone ASF1 to the CBP bromodomain promotes histone acetylation. *Proc. Natl. Acad. Sci. U. S. A.* **111**, E1072–81 (2014).
189. Yang, B., Zwaans, B. M. M., Eckersdorff, M. & Lombard, D. B. The sirtuin SIRT6 deacetylates H3 K56Ac in vivo to promote genomic stability. *Cell Cycle* **8**, 2662–3 (2009).
190. Giordano, A. & Avantaggiati, M. L. p300 and CBP: partners for life and death. *J. Cell. Physiol.* **181**, 218–30 (1999).
191. Kalkhoven, E. CBP and p300: HATs for different occasions. *Biochem. Pharmacol.* **68**, 1145–55 (2004).
192. Chen, X. *et al.* Integration of external signaling pathways with the core transcriptional network in embryonic stem cells. *Cell* **133**, 1106–17 (2008).
193. Zhong, X. & Jin, Y. Critical roles of coactivator p300 in mouse embryonic stem cell differentiation and Nanog expression. *J. Biol. Chem.* **284**, 9168–75 (2009).
194. Avantaggiati, M. L. *et al.* Recruitment of p300/CBP in p53-dependent signal pathways. *Cell* **89**, 1175–84 (1997).
195. Grossman, S. R. p300/CBP/p53 interaction and regulation of the p53 response. *Eur. J. Biochem.* **268**, 2773–8 (2001).
196. Brooks, C. L. & Gu, W. The impact of acetylation and deacetylation on the p53 pathway. *Protein Cell* **2**, 456–62 (2011).
197. Iyer, N. G., Ozdag, H. & Caldas, C. p300/CBP and cancer. *Oncogene* **23**, 4225–31 (2004).
198. Yuan, Z. M. *et al.* Function for p300 and not CBP in the apoptotic response to DNA damage. *Oncogene* **18**, 5714–7 (1999).
199. Diaz Perez, S. V *et al.* Derivation of new human embryonic stem cell lines reveals rapid epigenetic progression in vitro that can be prevented by chemical modification of chromatin. *Hum. Mol. Genet.* **21**, 751–64 (2012).
200. Silva, S. S., Rowntree, R. K., Mekhoubad, S. & Lee, J. T. X-chromosome inactivation and epigenetic fluidity in human embryonic stem cells. *Proc. Natl. Acad. Sci. U. S. A.* **105**, 4820–5 (2008).
201. Yin, X., Feng, Z. & Du, J. [Effects of neonatal calf serum on differentiation of human fetal neural stem cells in the hippocampus]. *Di Yi Jun Yi Da Xue Xue Bao* **24**, 1164–6, 1170 (2004).
202. Heintzman, N. D. *et al.* Histone modifications at human enhancers reflect global cell-type-specific gene expression. *Nature* **459**, 108–12 (2009).

## **CHAPTER 2**

---

# **Stem Cells are Radiosensitive in Contrast with their Differentiated Progeny**

## 2.1 ABSTRACT

The exposure of normal tissue to ionizing radiation (IR) during radiotherapy for cancer treatment leads to undesired sequelae. Normal tissue injury resulting from ionizing radiation (IR) during cancer radiotherapy has been in part attributed to reduced regenerative capacity of tissues. Utilizing multiple *in vivo* tissue niches and culture models, we demonstrate that normal stem cells are highly radiosensitive while their isogenic differentiated progeny are radioresistant. Stem cell apoptosis is associated with differential induction of pro- and anti-apoptotic proteins, occurs in all cell cycle phases and is independent of proliferation status. By determining that normal tissue injury involves loss of individual stem cells within their respective niches and not the entire stem cell compartment, this work has identified potential targets for future therapeutic intervention. By inhibiting these apoptotic pathways in stem cells specifically, strategies may be developed for minimizing side effects from radiation therapy.

## 2.2 METHODS

### 2.2.1 Cell Lines and Differentiation

Karyotypically normal early passage ES cells (EDJ22) were obtained from the Murine Embryonic Stem Cell Core of Siteman Cancer Center at Washington University. ES cells were grown on gelatin-coated plates, and maintained in stem cell culture media containing Knockout DMEM, 10 ng/ml leukemia inhibitory factor (LIF), 2 mM L-glutamine (Invitrogen), non-essential amino acids MEM (Corning), 15 % FBS, 0.2 %  $\beta$ -mercaptoethanol, 1 % penicillin/streptomycin and 40  $\mu$ g/ml gentamicin (Invitrogen) and not used for more than 5 passages. Cells were passaged every 2 days using 0.05% Trypsin/0.53mM EDTA (Corning). Differentiated cells (ED) were generated by culturing ES cells in media lacking LIF for 5-7 days. Neural stem (NS) cells were isolated from dentate gyri of late stage mouse embryos (E15-E18) or new born pups (P0-P1) and cultured in neural stem cell media containing Knockout DMEM/F-12 containing 15 mM Hepes (Stem Cell Technologies) with 1% N2 supplement, 2 % B27 supplement, 10ng/ml bFGF, 20ng /ml EGF, 1 % penicillin/streptomycin and 40  $\mu$ g/ml gentamicin (Invitrogen) and thereafter differentiated in the absence of EGF/FGF growth factors with addition of 10% FBS (Hyclone) for ~7 days.

### 2.2.2 Animal Models

Mouse strain C57BL/6 was used for all animal studies. Adult 6-8 week old males were utilized for harvest of brain, intestine, skin and testis for sectioning. For breeding, 1-6 month old male and female mice of similar age were allowed to mate continuously, with pregnant females isolated independently before giving birth. P0-P2 mouse pups were sacrificed by rapid decapitation prior to dissection for neural stem cell isolation. Procedures for all studies were been approved by the Animal Studies Committee at Washington University Medical Center.

### 2.2.3 Antibodies

Details of the antibodies used in this work are described in Table 2.1.

**Table 2.1. Antibody Information Table**

Protein Target	Species	Company	Catalog #	Assay	Conditions
Bax	mouse	Santa Cruz	sc-7480	WB	1:250 in milk
Bcl2	rabbit	Cell Signaling	#2870	WB	1:100 in milk
BrdU (AlexaFluor 488 conjugated)	mouse	Invitrogen	B35139	FACS	1:20
cleaved Caspase-3	rabbit	Cell Signaling	#9664	IHC-F, WB	1:500, 1:500 in milk
Cleaved PARP	mouse	BD Biosciences	51-9000017	IHC-F	1:100
Ki67	rabbit	NeoMarkers	RB-1510-P0	IHC-F	1:100
Lin28	rabbit	Abcam	ab46020	WB	1:1000 in milk
Nanog	rabbit	Abcam	ab80892	WB	1:1000 in milk
Oct4	rabbit	Abcam	ab19857	IF, IHC-F	1:200, 1:200
PARP	rabbit	Cell Signaling	#9542	WB	1:2000 in milk
PCNA	mouse	Millipore	NA-03	IHC-F	1:100
Pro Caspase-3	rabbit	Cell Signaling	#9665	WB	1:1000
Sox2	rabbit	Abcam	ab7959	IHC-F	1:100
Sox2	mouse	Abcam	ab79351	IF, IHC-F	1:200, 1:100
SSEA1	mouse	Abcam	ab16285	IHC-F	1:100
GAPDH	mouse	Sigma Aldrich	G8795	WB	1:100,000 in milk
FITC-conjugated anti-rabbit	donkey	Vector	FI-1000	IF, IHC-F	1:100
FITC-conjugated anti-mouse	horse	Vector	FI-2000	IF, IHC-F	1:100
Texas Red-conjugated anti-mouse	horse	Vector	TI-2000	IF, IHC-F	1:100
Texas Red-conjugated anti-rabbit	donkey	Vector	TI-1000	IF, IHC-F	1:100

HRP-conjugated anti-mouse	rabbit	Sigma Aldrich	A9044	WB	1:5000 in milk
HRP-conjugated anti-rabbit	goat	Sigma Aldrich	A0545	WB	1:5000 in milk

#### **2.2.4 X-Ray Irradiation and Tissue Sectioning**

Cells and animals were irradiated in the RS-2000 Biological Research Irradiator (Rad-Source) at room temperature, with mock/control irradiated samples brought into the room to simulate the reduction in ambient temperature and account for any stress imparted by the travel. Cells were always placed within the central circle directly under the x-ray source to maintain consistency in dose between samples. Animals were anesthetized with isoflurane and placed on their back in the machine for whole-body irradiation to properly expose all tissues of interest to the x-ray source. Accuracy of all doses was confirmed by dosimeter probe. Both cells and animals were randomly assigned to individual timepoints or sham-irradiation controls.

Following irradiation, mice were sacrificed at specific timepoints by CO<sub>2</sub> asphyxiation and cervical dislocation. Organs were harvested, placed in OCT media and frozen in liquid nitrogen. Frozen tissues were sectioned on a cryostat machine at a thickness of 10 µm, placed onto adhesive slides and stored at -80°C.

#### **2.2.5 Apoptosis Assays (TUNEL, Annexin V, Annexin XII/ pSIVA)**

Apoptosis in tissue sections (staining and microscopy) and cultured cells (flowcytometry), were analyzed using various assays such as TUNEL, Annexin V, and Annexin XII following manufacturer's protocol. In cultured cells, APO-BrdU TUNEL Assay kit with Alexa Fluor 488 Anti-BrdU (Invitrogen) was used for TUNEL assay, Annexin- V FITC detection kit (BD Pharmingen) was used for Annexin V staining, and GLO pSIVA-IANBD Apoptosis / Viability Flow Kit (Imgenex) for Annexin XII staining. 10,000 cells were counted for flow cytometry analysis. TUNEL staining on tissue sections was performed with the DeadEND fluorescent TUNEL system (Promega).

### **2.2.6 Western blotting**

Cellular protein lysates were collected in RIPA buffer, electrophoresed on 4-15 % Tris-Glycine polyacrylamide gels (BioRad), transferred onto PVDF membranes and after blocking with 5 % BSA or milk in TBS-T incubated overnight at 4 °C with various primary antibodies followed by secondary antibody incubation. Super ECL (GE/Pierce) was used as substrate for detection on autoradiography film or ChemiDoc MP digital system (BioRad).

### **2.2.7 Immunofluorescent Staining**

Cryosections were fixed in 4 % formaldehyde, permeabilized with 0.2 % Triton-X 100 (Sigma), blocked in 2 % BSA in PBS, probed using primary antibodies and detected using 5 µg/ml secondary antibodies labeled with FITC or TexasRed (Vector Labs). After mounting in Vectashield mounting media containing DAPI (Vector Labs), microscopic observations, scoring and quantifications were done and fluorescent images were taken.

Cells were similarly fixed in 4% formaldehyde and permeabilized with 0.2% Triton-X 100 before blocking in 2 % BSA and antibody incubation. For double-color staining, primary antibodies were incubated together for 1h at 37°C followed by wash and incubation with fluorescently-tagged secondary antibodies for 30 min at 37°C.

### **2.2.8 Clonogenic Survival Assay**

Cells were used in a colony formation assay to measure cell survival after IR treatment using standard protocols. Cells were plated, irradiated at various doses and allowed to grow for 7 to 14 days. Any colonies formed were fixed and stained with crystal violet (Sigma). The number of colonies (with >50 cells) per dish was counted, and the surviving fractions were calculated as the ratio of the plating efficiencies of treated cells to untreated cells.

### **2.2.9 Neutral Comet Assay**

To assess and quantify DNA breaks and apoptotic fragmentation of DNA, neutral comet assays were performed using CometSlide assay kits (Trevigen). Cells were irradiated with 6 Gy, lysed, electrophoresed in agarose in TAE buffer and stained with SYBR Green (Trevigen). Olive moment of the comets was calculated by multiplying the percentage of DNA in the tail by the displacement between the means of the head and tail distributions. CometScore™ Version 1.5 (TriTek) was used to calculate Olive Moment. A total of 50–75 comets were scored and analyzed per sample in each experiment with each series of timepoints repeated at least three independent times as both biological and technical replicates. Individual comets were randomly selected for scoring from similar regions of the slide in all samples. Outliers were eliminated that fell greater than 1.5 standard deviations from the mean. Data from all samples was approximately normally distributed, and the standard deviation between samples within the same experiment was similar. Samples were excluded from analysis only due to technical errors from the assay or cells being visibly unhealthy.

### **2.2.10 Cell Cycle Analysis**

For phase-specificity of apoptosis, live cells were incubated for 1h at 37°C with Vibrant FAM Caspase-3 and 7 FLICA reagent (Invitrogen). Cells were subsequently fixed for 15min with 4% formaldehyde at 4°C prior to overnight ethanol fixation at -20°C in order to preserve cytoplasmic contents during ethanol permabolization. Fixed cells were subsequently incubated with RNase and propidium iodide followed by flow cytometric analysis. Total and apoptotic populations were gated for each cell cycle phase, and the ratio of apoptotic to total cells within each phase was obtained.

ES and ED cells were incubated with 20µM BrdU (Sigma) for 30min, washed 2 times and chased for various timepoints to allow cell cycle progression. Cells were then fixed overnight in ethanol at -20°C, incubated with RNase and propidium iodide, and analyzed by flow cytometry. For *in vivo* BrdU incorporation, 100ul of 10mg/ml BrdU was injected intraperitoneally. Mice were sacrificed

after 72h, and skin sections were isolated for frozen sectioning. BrdU incorporation into skin was detected by immunofluorescence.

#### **2.2.11 Viability Assay**

Cells were plated in equal numbers onto dishes and were either allowed to grow for 24-48hr (ES) or differentiated for 3-4 days. Cells were then irradiated with 6Gy and incubated for the specified period of time. Cells were harvested by trypsinization into single-cell suspensions and counted on the Vi-Cell Viability Analyzer (Beckman Coulter) by trypan blue incorporation. At least 100,000 cells were counted per sample.

#### **2.2.12 Microscopy and Image Processing**

Micrographs were captured utilizing MetaSystems ISIS imaging software on Zeiss Axioplan2 microscope or ZEN software on Zeiss LSM510 confocal microscope with the 20x, 63x or 100x objective lenses. Minimal threshold and contrast manipulation was performed equally across entire images. Controls were processed equally with treated samples. Adobe Photoshop CS3 software was utilized for composing the collages of multiple pictures and labeling micrographs and Immunoblots in individual layers.

#### **2.2.13 Statistical Analysis**

A 'two-tailed' Student's *t*-test was used to calculate the statistical significance of the observed differences. In all cases, differences were considered statistically significant when  $p < 0.05$ .

Unless otherwise indicated, values represent mean  $\pm$  SEM.

### **2.3 INTRODUCTION**

Radiation therapy utilizes ionizing radiation (IR) to produce lethal DNA double-strand breaks (DSBs) in cancer cells; however detrimental side effects often result from unintended damage to normal tissue<sup>1</sup>.

Patients undergoing radiotherapy experience acute and chronic sequelae such as hair loss, skin

regeneration defects, erosion of intestinal epithelium, malabsorption, hematopoietic anomalies, infertility, and neurocognitive impairments<sup>1-5</sup>. Normal tissue injury following radiotherapy has been attributed to the loss of regenerative capacity in stem cell compartments<sup>6,7</sup>, however the molecular details of normal stem cell radiosensitivity remain unclear.

Ionizing radiation (IR)-induced cell death is caused by DNA damage, especially complex DNA double strand breaks<sup>8</sup>. Under tolerable ranges, damaged DNA is efficiently repaired, but if beyond the repairable state or in the event that the DNA repair process is hampered, cells either stop dividing or undergo programmed cell death<sup>9</sup>. Cells vary in their response to DNA damage depending on the cell type, differentiation status, proliferation state and cell cycle stage<sup>10</sup>. An improved understanding of cellular radiation responses is essential for the development of strategies to protect normal tissue during radiotherapy. However, despite indications for stem cells playing a role in normal tissue injury resulting from radiotherapy<sup>11-13</sup> studies on the relative radiosensitivity of stem cells remain debatable at experimental and molecular mechanistic levels. While many investigators acknowledge high radiosensitivity in stem cells<sup>14-19</sup> other reports show relative radioresistance<sup>20-22</sup>. There is, however, a lack of direct comparison of differential radiation responses in stem and differentiated cells *in vivo* and of stem cells with their isogenic progeny in cell culture models. Moreover, the usage of primary, early passage cells could avoid possible culture artifacts. Further, the molecular mechanisms of differential radiosensitivities must be elucidated to develop therapeutics that minimize stem cell drop-out and resulting radiation damage to the normal tissue.

We demonstrate that stem cells are hypersensitive to relatively low dose IR both *in vivo* in normal stem niches of various tissues as well as in karyotypically normal, early passage primary mouse embryonic and neural stem cells as compared to their isogenic differentiated progeny. IR-induced apoptosis in stem cells occurs within few hours after irradiation and involves the action of various apoptotic factors. This apoptosis is broadly distributed across the cell cycle in stem cells, while differentiated cells apoptose primarily during G2/M phase. The observed differential radiosensitivity between stem and differentiated

cells is not due to enhanced proliferation in stem cells, suggesting that enhanced radiosensitivity is inherent to an undifferentiated cell state.

## **2.4 RESULTS**

### **2.4.1 Normal stem cells *in vivo* are radiation hypersensitive while surrounding non-stem cells are relatively radioresistant**

To analyze the radiosensitivity of stem cells compared to differentiated non-stem cells *in vivo*, C57BL/6 male mice were whole-body irradiated and observed for apoptosis in the stem cell niches of the subgranular (SGZ) and subventricular zones (SVZ) in brain, hair follicle bulge in skin, intestinal crypt and seminiferous tubules of testis. The selected stem cell compartments are located within four clinically relevant tissues that each exhibit deleterious consequences from radiation therapy. A dose curve was performed from 0-10Gy and apoptosis was observed in each niche relative to labeled stem cells at 6h, 12, 24h and 48h following irradiation. Apoptosis was exclusive to individually stem cells within all niches at lower doses as indicated by various markers, and almost every stem cell present was undergoing cell death at 6Gy (Fig. 2.1, 2.2). Apoptosis was not observed in any unirradiated samples (Fig. 2.2, 2.3). While apoptosis was observed in stem cells following exposures to as low as 2Gy IR, only minimal apoptosis was seen in differentiated cells at doses 8Gy and above. These data establish that stem and differentiated cells exhibit varying thresholds for responding to DNA damage.

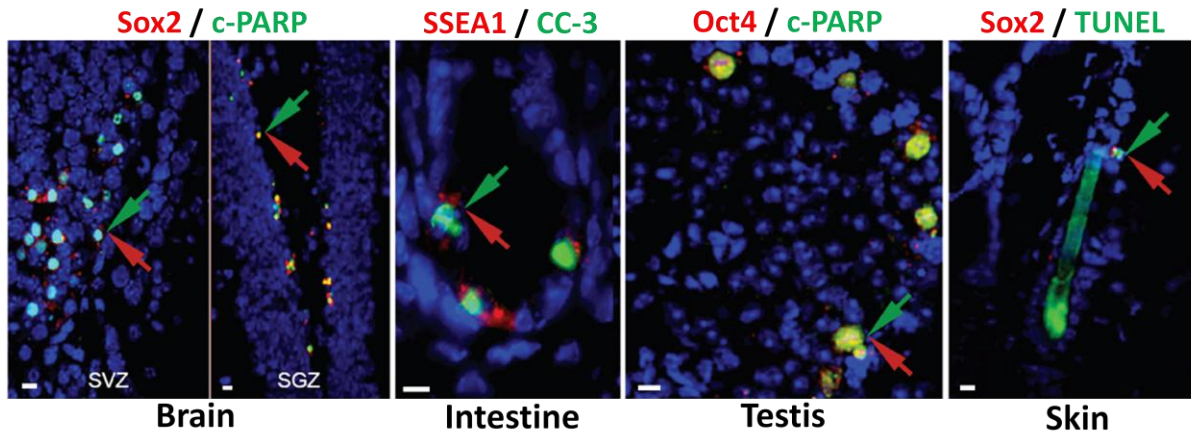


**Figure 2.1. IR-induced apoptosis is exclusive to stem cells *in vivo*.** Immunofluorescence co-staining of stem cell markers (red; Sox2, Stage-specific embryonic antigen 1 [SSEA1], Oct4) and apoptosis markers (green; c-PARP, CC-3,) in tissue niches 12h following 6Gy whole body irradiation. Green and red arrows indicate cells positive for both stem cell marker and apoptosis marker. DAPI=DNA. SVZ=subventricular zone; SGZ=subgranular zone. CC-3=cleaved caspase-3; c-PARP=cleaved Poly ADP-ribose polymerase (PARP). White scale bars, 10 $\mu$ m.

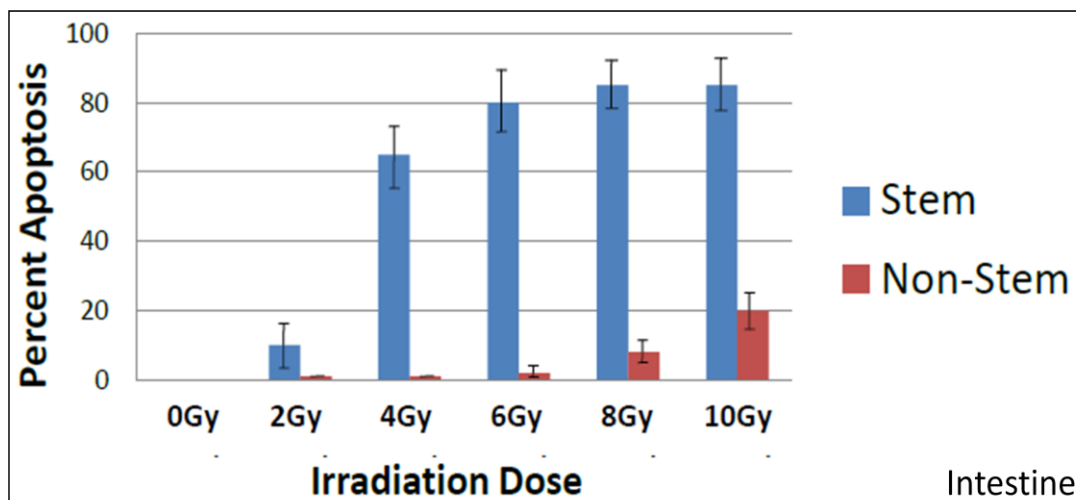


**Figure 2.2. Dose curve of IR-induced apoptosis among stem and non-stem cells *in vivo*.** The percentage of apoptotic stem and non-stem cells was measured at 12h after incremental irradiation doses. Stem and non-stem cells were scored within the entire intestinal crypt and proliferative zone of the villus. No apoptosis was observed in the terminally differentiated upper villus. N=3 (combined counting of 3 sections each from 3 independent mice). Error bars indicate SEM.

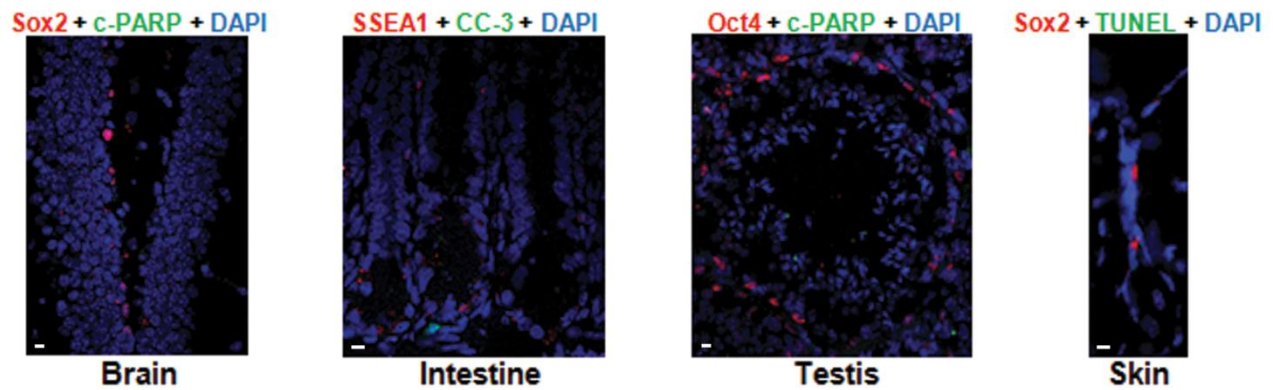


**Figure 2.3. *In vivo* sham irradiation apoptosis negative controls.** Immunofluorescence co-staining of stem cell markers (red; Sox2, SSEA1, Oct4) and apoptosis markers (green; c-PARP, CC-3, TUNEL) in tissue niches 12h following 0Gy sham whole body irradiation. DAPI=DNA. CC-3=cleaved caspase-3; c-PARP=cleaved PARP. White scale bars, 10 $\mu$ m.

#### **2.4.2 Radiation hypersensitivity is recapitulated by primary embryonic and neuronal stem cells in culture**

We also established two sets of karyotypically normal, early passage, primary cell culture models in mouse embryonic stem cells (ES) and neural stem cells (NS) along with their isogenic differentiated non-stem counterparts (ED and ND, respectively). Both stem cell models were directly differentiated by passage in the absence of specific growth factors (Fig. 2.4 A-B).

Radiation responses of stem cells could thus be assessed in parallel with their isogenic, recently differentiated progeny in order to compare outcomes. ES cells demonstrated a progressive linear decrease in viable cell number across multiple timepoints following 6Gy irradiation (Fig. 2.5).

Significantly higher levels of apoptosis were detected in both cell culture models compared to their differentiated progeny following 6Gy IR (Fig. 2.6 A-C). Clonogenic survival curves confirmed logarithmic higher rates of cell killing in stem cells compared to non-stem cells at all doses, accounting for both cell death and senescence in measuring cellular replicative capacity following irradiation (Fig. 2.7). DNA fragmentation is among the final steps of apoptosis as the nucleus is degraded by caspases and DNases. As a further indicator of apoptosis, we utilized comet assays

to assess late-stage apoptotic DNA fragmentation. Comet assays employed single-cell gel electrophoresis following irradiation and nuclear lysis. Differentiated cells displayed progressive reduction of DNA breaks over time following irradiation, whereas DNA breaks in stem cells starkly increased beginning at 8h post-IR consistent with apoptotic DNA fragmentation (Fig. 2.8 A-B). The apoptotic effectors of cleaved poly ADP-ribose polymerase (PARP) and caspase-3 were also detected exclusively in stem cells beginning 4h post-irradiation. Additionally, differential levels of pro- and anti-apoptotic Bcl-2 family member proteins were observed in stem and non-stem cells. Pro-apoptotic Bax was higher in ES cells and increased upon irradiation, while the anti-apoptotic Bcl-2 showed higher expression in ED cells (Fig. 3.9 A-B). These results demonstrate that stem cells are substantially more radiosensitive than non-stem differentiated cells and readily undergo IR-induced cell death.

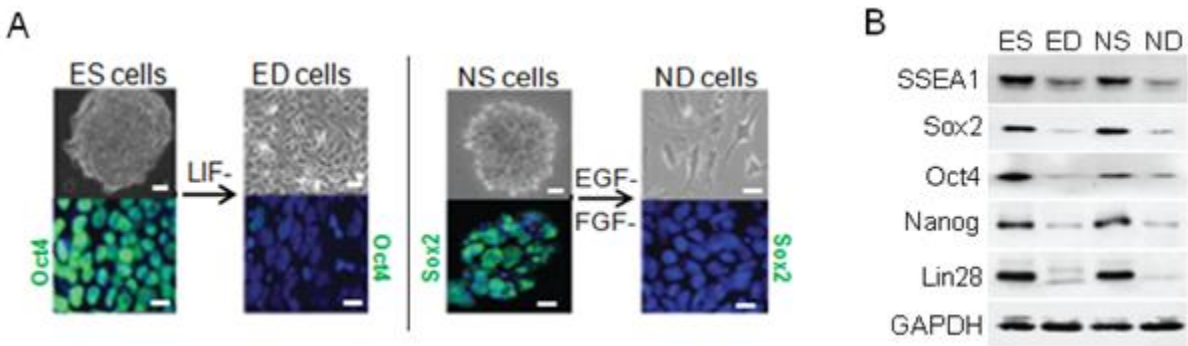


**Figure 2.4. Differentiation of stem cell culture models.** (A) Bright field images and immunofluorescence staining for stem cell markers (green; Oct4, Sox2) demonstrating differentiation of ES cells into ED cells and NS cells into ND cells. DAPI=DNA. White scale bars, 10µm. (B) Western blots for stem cell markers on unirradiated ES, ED, NS and ND. GAPDH served as a loading control.

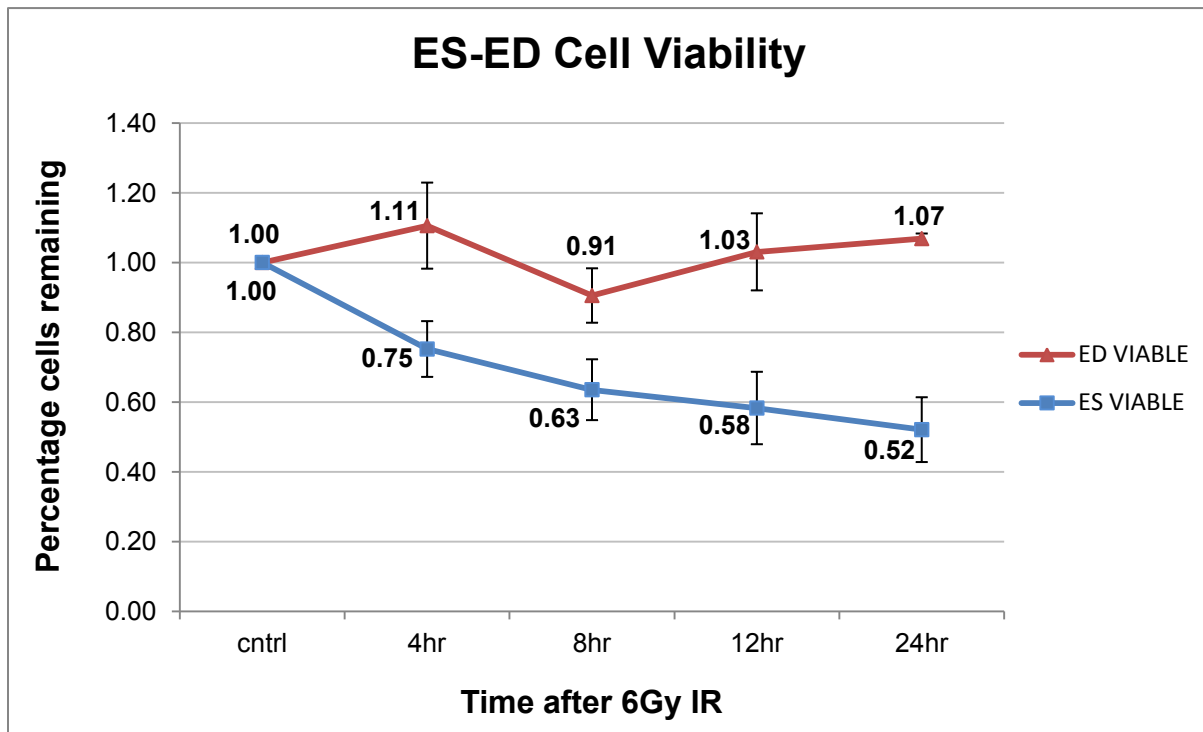


**Figure 2.5. Differential viability of ES and ED cells following irradiation.** ES and ED cells were irradiated with 6Gy during exponential growth and incubated for the indicated times prior to viability counting by trypan blue incorporation. N=3. Error bars indicate SEM.

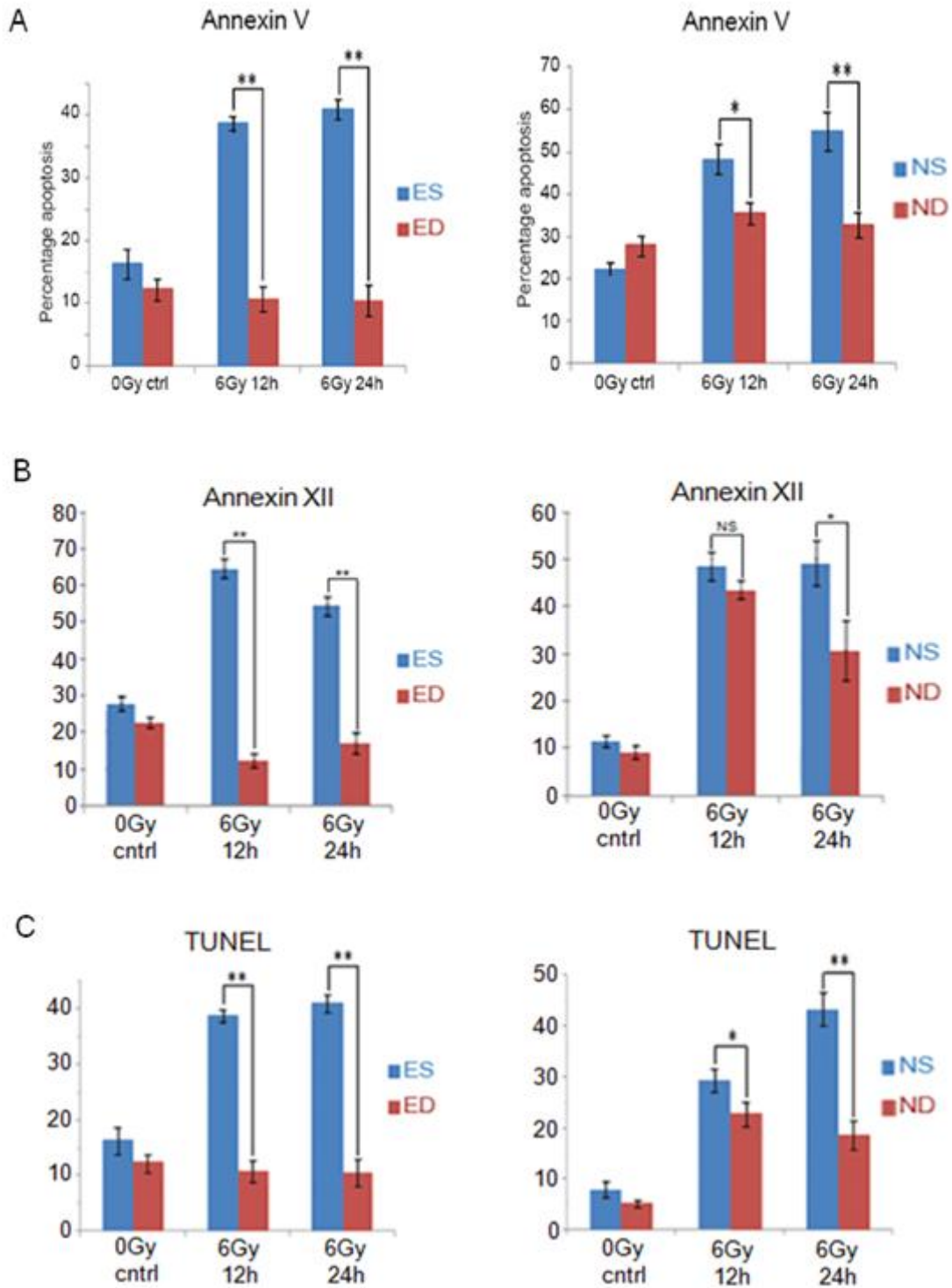


**Figure 2.6. Stem cells but not directly differentiated progeny undergo IR-induced apoptosis in culture.** Flow cytometric analysis of apoptosis comparing ES and ED or NS and ND cells by (A) Annexin-V, (B) Annexin-XII, and (C) TUNEL labeling following sham or 6Gy IR at indicated timepoints. N=3; \* =  $p < 0.05$ ; \*\* =  $p < 0.01$ ; otherwise not significant.

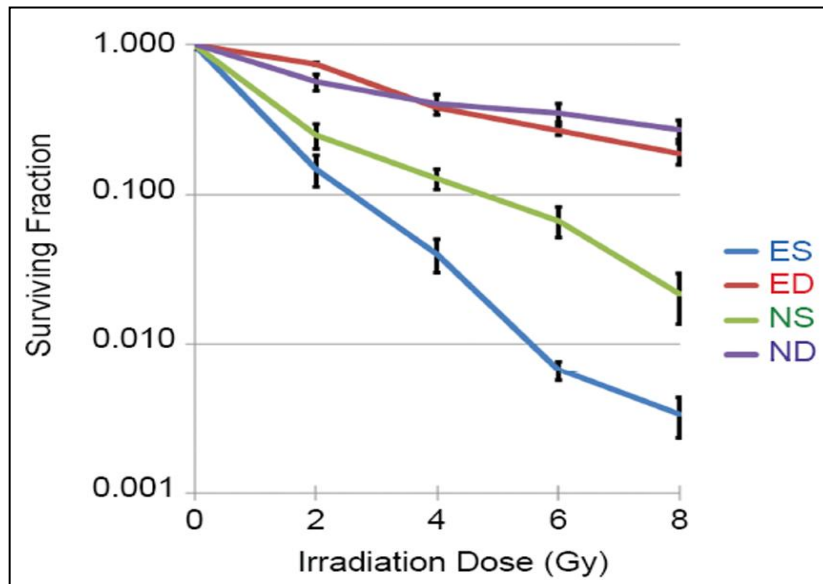


**Figure 2.7. Clonogenic survival of cell culture models after various IR doses.** ES, ED, NS and ND cells were irradiated 6h after plating. N =3. Error bars indicate SEM.

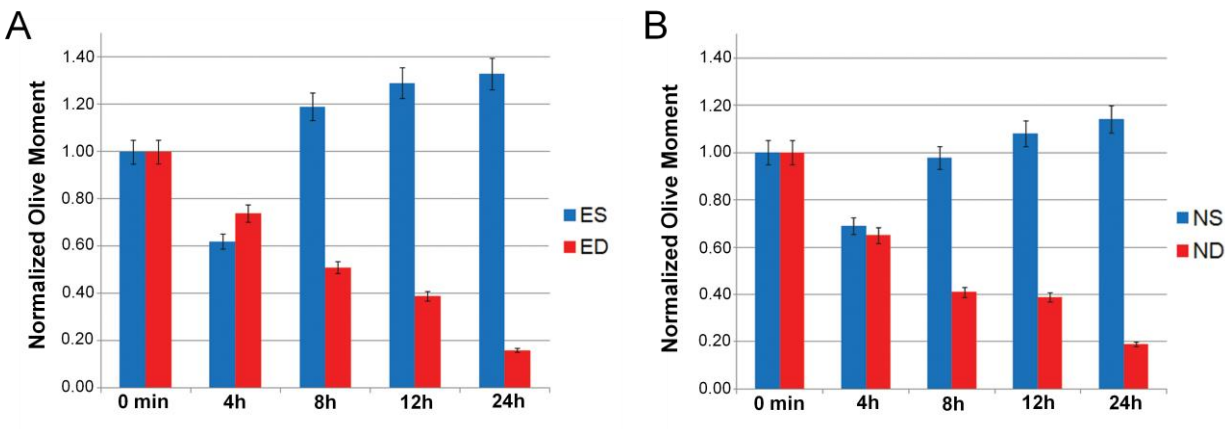


**Figure 2.8. Neutral comet assay on cell culture models at late timepoints.** Olive moments of (A) ES and ED or (B) NS and ND cell comet assay tails were quantified at different timepoints following sham or 6Gy IR and normalized to the irradiated 0min timepoint to demonstrate apoptotic nuclear fragmentation in stem cells at late timepoints. N=3. Error bars indicate SEM.

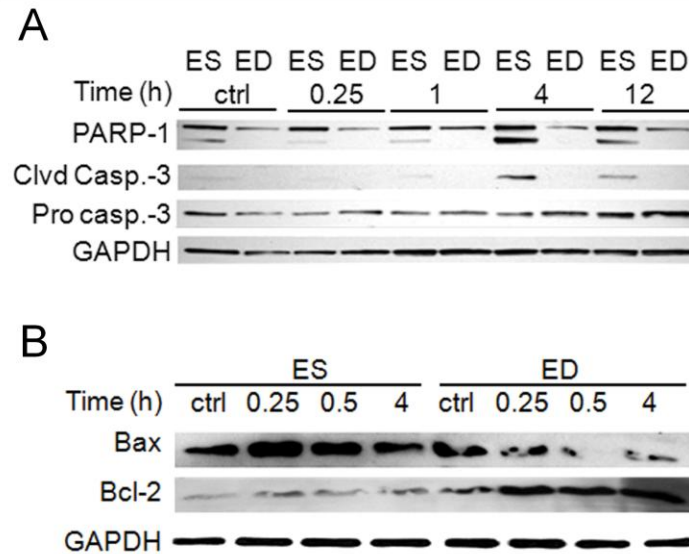


**Figure 2.9. Western blots for apoptotic effectors.** ES and ED cells were collected at various time points following mock or 6Gy irradiation. GAPDH served as a loading control. Cleaved caspase-3=cleaved caspase-3; Pro caspase-3=Pro caspase-3.

### 2.4.3 Radiation hypersensitivity in stem cells is independent of proliferation status

Since the Law of Bergonié and Tribondeau states that radiosensitivity is strongly correlated with proliferation rate<sup>23</sup>, we examined whether the observed differential radiosensitivity between stem and non-stem cells was due to differences in proliferation status. ES and ED cells in culture were found to proliferate at similar rates as measured by BrdU pulse-chase (Fig 2.10), and Ki67 staining identified both resting and proliferative cells among both the stem and non-stem cell populations in vivo (Fig. 2.11). Additionally, replicating cells within S phase were detected broadly throughout and surrounding unirradiated hair follicles by proliferating cell nuclear antigen (PCNA) staining (Fig. 2.12 A) and BrdU incorporation (Fig. 2.12 B). The relative ratio of proliferative vs. apoptotic stem cells was then quantified in the SGZ. While only about 30% of stem cells were proliferative, 75% of stem cells underwent apoptosis (Fig. 2.13 A). Stem cells in vivo were radiosensitive at low doses, while IR-induced apoptosis was only observed at 8Gy or higher among non-stem cells of the “proliferative zone” above the intestinal crypt (Fig. 2.2, 2.13 B).

Terminally differentiated cells were highly radioresistant at all tested doses (Fig. 2.14). These data indicate that while proliferation status may affect radiosensitivity in non-stem cells, the hypersensitivity of stem cells to IR is an inherent property of their undifferentiated state.

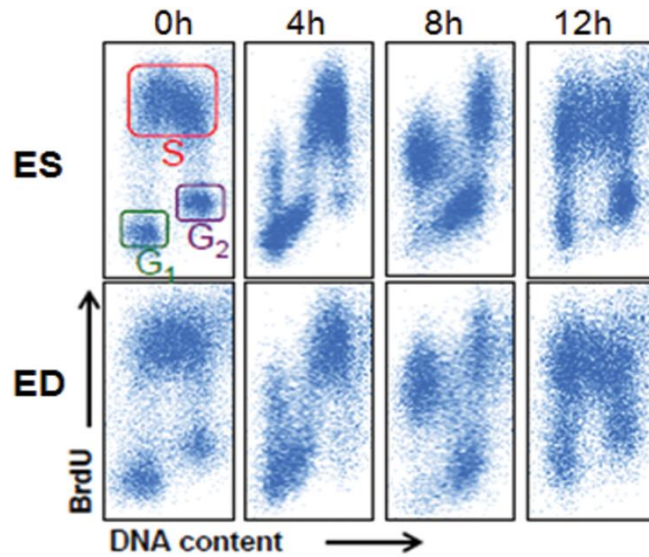


**Figure 2.10. BrdU pulse-chase profiles labeling cell cycle progression of unirradiated stem and non-stem cells.** Timepoints indicate incubation time following removal of BrdU. Rectangles indicate the presence of G1, S, and G2 populations. 20,000 gated cells were counted for analysis.

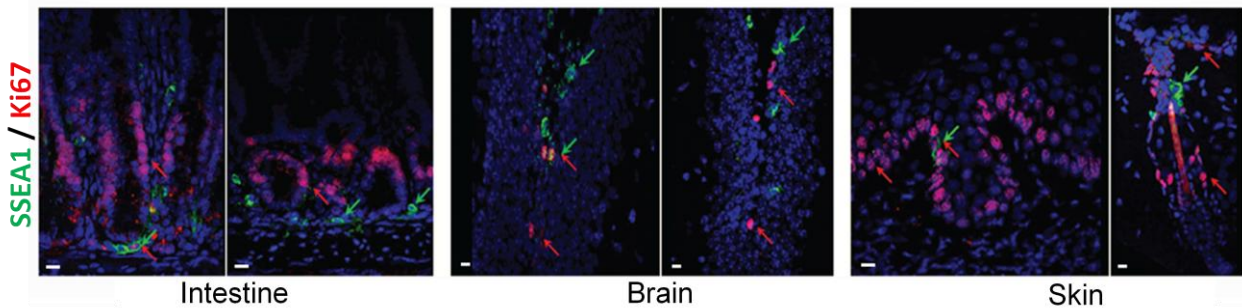


**Figure 2.11. Proliferation status of stem and non-stem cells *in vivo*.** Immunofluorescence co-staining of proliferation marker Ki-67 (red) and stem cell marker SSEA1 (green) in unirradiated tissue niches. DAPI=DNA. Green arrows indicate stem cells, red arrows indicate proliferative cells. White scale bar, 10 $\mu$ m.

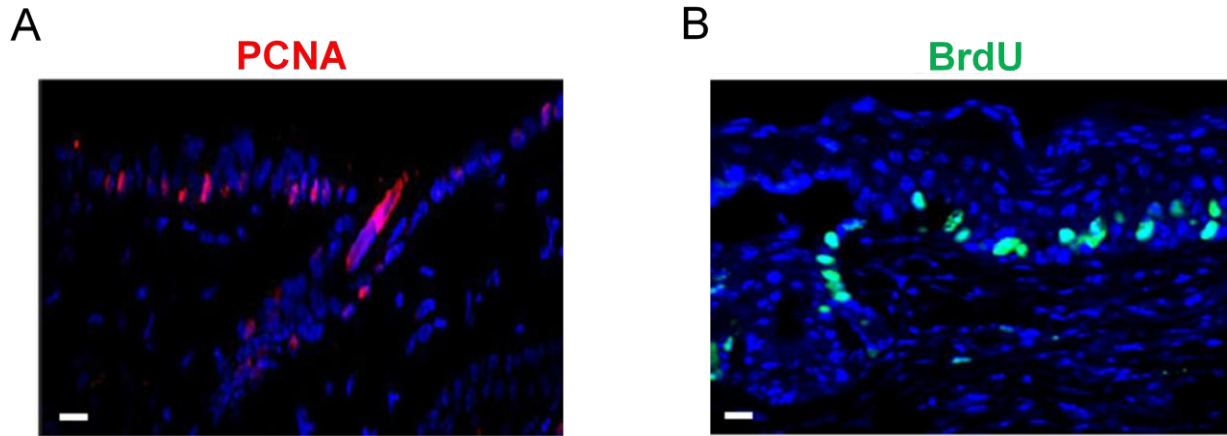


**Figure 2.12. Proliferating cells exist both within and outside of the hair follicle bulge stem cell region.** Immunofluorescence staining of (A) S-phase marker PCNA (red) and (B) BrdU (green) in unirradiated skin. DAPI=DNA. White scale bars, 10µm.

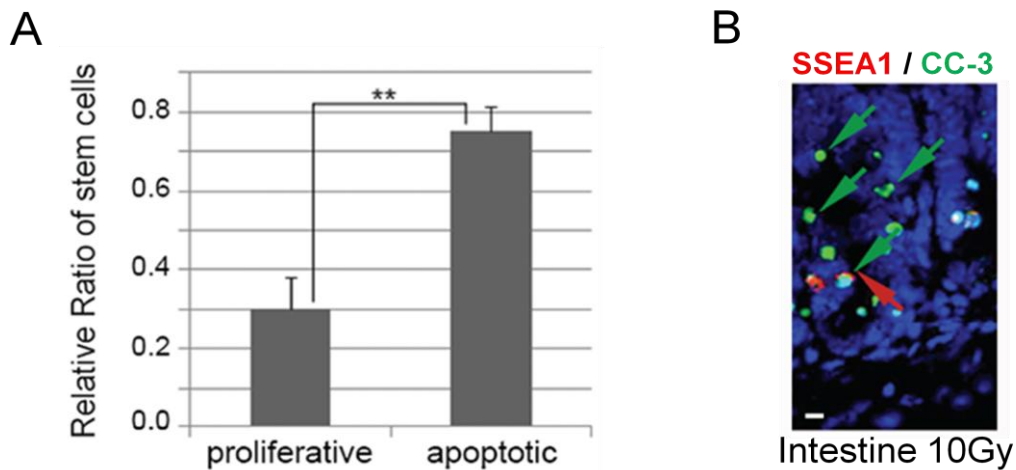


**Figure 2.13. Apoptosis relative to proliferation status of stem and non-stem cells *in vivo*.** (A) The fraction of Ki-67 positive (proliferative) or TUNEL positive (apoptotic) cells among Sox2+ stem cells was quantified across the dentate gyrus at 6h following 6Gy irradiation. N=3 (combined counting from 7 gyri sections each from 3 separate mice). \*\* =  $p < 0.01$ . (B) Immunofluorescence co-staining of SSEA1 (red) and CC-3, (red) in intestinal crypt and the proliferative lower villus 12h following 10Gy whole body irradiation. Green and red arrows indicate cells positive for both stem cell marker and apoptosis marker. DAPI=DNA. CC-3 = cleaved caspase-3. White scale bar, 10µm.

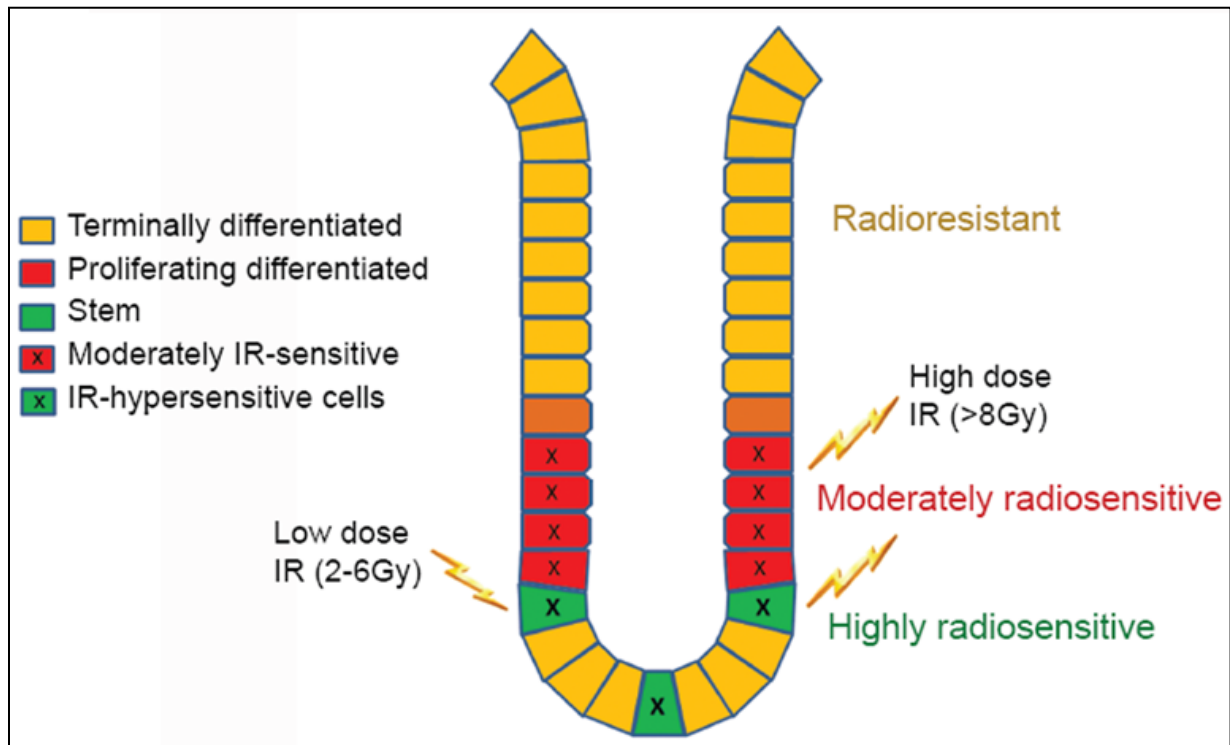


**Figure 2.14. Model of radiosensitivity relative to proliferation status within the intestinal crypt and villus.** All intestinal crypt stem cells are radiosensitive at low doses, while only proliferative progenitors of the lower villus display any apoptosis among differentiated cell population.

#### 2.4.4 IR-induced apoptosis of stem cells is more widely distributed throughout the cell cycle

We also investigated potential differences between stem and non-stem cells in radiosensitivity across the cell cycle phases. As expected, substantially higher IR-induced apoptosis was detected in stem cells overall compared to their differentiated progeny (Fig. 2.15). The “apoptotic ratio” was then quantified throughout each cell cycle phase (Fig. 2.15 inserts) by comparing the relative percentage of apoptotic cells present in each phase relative to the overall proportion of the total cell population within that phase. Apoptotic ratios were thus normalized to the overall cell cycle distribution. Ratios above or below 1.0 indicated increased or reduced propensity to undergo apoptosis in that phase, respectively. ED cells displayed a strongly increasing apoptotic

ratio within the G2/M population over time post-irradiation, while in G1 the ratio remained low. In contrast, ES cells apoptosed across all phases of the cell cycle, displaying a 2-3 times higher apoptotic ratio in G1 as compared to the ED cells.

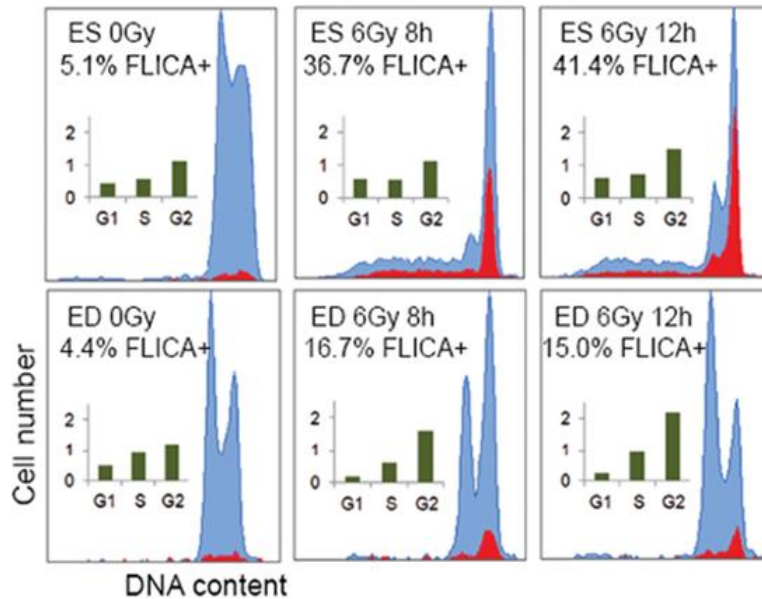


**Figure 2.15. Differentially distributed radiosensitivity across the cell cycle in stem and non-stem cells.** ES and ED cells were co-stained with FLICA apoptosis marker and propidium iodide at 8h and 12h after sham or 6Gy IR. The ratio of apoptotic cells (red) relative to total cells (blue) in each cell cycle phase was calculated to obtain the apoptotic ratio (inserted graphs). Ratios above or below 1.0 indicate increased or decreased apoptosis, respectively, within that phase when normalized to the phase distribution of the total cell population.

## 2.5 DISCUSSION

During radiation therapy patients often suffer from normal tissue injury, limiting the dose that can be used on the tumor. Normal tissue injury as a result of radiation therapy<sup>1</sup> has long been associated with the loss of regenerative stem cell compartments in the affected tissues<sup>6</sup>, resulting in clinical consequences such as cognitive impairment<sup>24</sup>, infertility<sup>25</sup>, intestinal epithelial erosion<sup>4,26</sup> and hair loss<sup>5</sup>. Unfortunately, our

understanding of stem cell radiation responses remains incomplete. While several reports suggest high radiosensitivity of stem cells compared to differentiated cells in the intestine<sup>27-29</sup> and brain<sup>17,30</sup> as well as in ES cells<sup>19,31</sup>, others have reported relative resistance of stem cells within testis<sup>22</sup> and skin<sup>21</sup>. Such ambiguity may be due to the presence of different stem cell populations within these tissue compartments<sup>32,33</sup>, heterogeneity among tissue types, uncertainty about the true detection/ location of stem cells within these niches<sup>34</sup>, or potentially even from developmental variation within stem cell compartments. Moreover, the use of different cell lines as well as prolonged culturing of cells, which possibly influences the cells' radiation response, might contribute to the heterogeneity between studies<sup>35</sup>. Thus in this study we chose to analyze early passages of primary stem cells along with multiple *in vivo* adult stem cell tissue niches as compared to their isogenic, directly differentiated progeny. We observed stem cell-specific radiosensitivity in all four analyzed tissue niches and both culture models, suggesting that IR hypersensitivity is a common phenomenon among different types of stem cells.

Stem cell-specific IR-induced apoptosis is detected in stem cell niches *in vivo* at 2Gy and above, while adjacent differentiated cells are radioresistant below 8-10Gy. These observations suggest the likely existence of a threshold of DNA damage above which cells are unable to repair, as has been previously suggested<sup>36</sup>. This threshold probably exists for various cell types *in vivo* and is likely defined by the specifics of a cell's molecular response to DNA damage. The IR-induced apoptosis-prone phenotype of stem cells and loss of function of apoptosis upon differentiation was confirmed by clonogenic survival assay and comet assay. Further, ES cells showed higher expression and activation of pro-apoptotic Bax, in agreement with studies showing constitutively higher levels of Bax in human embryonic stem cells<sup>37</sup>. ES cells displayed lower expression of anti-apoptotic Bcl-2, which correlates with priming of stem cells to apoptose in response to DNA damage as has been previously published for human embryonic stem cells<sup>31</sup>.

It has long been established that cellular proliferation rate directly correlates with radiosensitivity<sup>23</sup>. However, highly proliferative tissues may merely elicit the fastest response to radiation and not necessarily the greater overall radiosensitivity<sup>38</sup>. When combined with the predominant use of rapidly dividing culture models for studying stem cell biology, there remains uncertainty as to whether stem cell

hypersensitivity is an inherent property of an undifferentiated state or merely a result of rapid proliferation. Additionally, stem cells vary in their proliferation rates *in vivo*, as some stem cells are quiescent within their niche while others are proliferating<sup>34</sup>. We studied multiple tissue niches representing varying proliferation rates and observed that low dose IR-induced apoptosis was exclusive to stem cells independent of their proliferation status. The highly proliferative non-stem progenitors of the intestinal crypt underwent low levels of IR-induced apoptosis at higher doses, at which dose terminally differentiated non-dividing cells stay highly radioresistant. This demonstrates the stark contrast in radiation responses of cells at varying differentiation states *in vivo*, in which proliferation state appears only to affect the radiosensitivity of differentiated cells while stem cells are ubiquitously radiosensitive. Our findings provide compelling evidence against this established assumption about the true factors affecting cellular radiosensitivity and should lead to improved understanding of the true basis of stem cell hypersensitivity.

According to the surviving fraction of cells irradiated in each phase following synchronization, G2/M is typically considered the most radiosensitive phase of the cell cycle followed by G1 and then S phase<sup>39</sup>, although large variability exists between cell lines<sup>38</sup>. In order to focus on the cell cycle responses to radiation that contribute to differential IR-induced apoptosis among ES and ED cells, we chose to assess cell cycle phase radiosensitivity through a unique approach. We investigated whether differences in the cell cycle arrest of ES and ED cells were associated with a bias in the induction of apoptosis across different cell cycle phases post-irradiation. By measuring the prevalence of FLICA -positive apoptotic cells across the cell cycle relative to the total cell cycle distribution, we were able to determine whether there exists any cell cycle phase bias among the apoptotic population in ES and ED cells. We found that ES cells maintained apoptotic sensitivity fairly evenly throughout the cell cycle, which could explain stem cells radiation hypersensitivity, while apoptosis in ED cells was clearly higher towards G2. The hypersensitivity of stem cells to radiation may be aided by the fact that they remain relatively radiosensitive at all phases of the cell cycle, while radioresistant differentiated cells in contrast are only radiosensitive during a portion of the cell cycle. It is known that stem cells fail to activate G1 checkpoint arrest following DNA damage<sup>40-</sup>

<sup>42</sup> cells, suggesting a potential connection between the absence of a G1 checkpoint and a more broad distribution of apoptosis throughout the cell cycle.

This work demonstrates stem cells are hypersensitive to IR both in culture and within multiple tissue niches. We have shown that at therapeutic doses typically used in radiation therapy (2-10Gy)<sup>43</sup>, only stem cells undergo IR-induced cell death. The clinical side effects from radiation therapy are therefore not due to loss of the stem cell compartment as a whole, but instead to the individual stem cells within the niche. By targeting radioprotective therapies and drugs toward radiosensitive stem cells substantial progress can be made towards minimizing damaging sequelae of radiation therapy, therefore improving the efficiency and effectiveness of radiation therapy overall.

## 2.6 REFERENCES

1. Stone, H., Coleman, C., Anscher, M. & McBride, W. Effects of radiation on normal tissue: consequences and mechanisms. *Lancet Oncol.* **4**, 529–536 (2003).
2. Kinsella, T. J. Effects of radiation therapy and chemotherapy on testicular function. *Prog. Clin. Biol. Res.* **302**, 157–171; discussion 172–177 (1989).
3. al-Mefty, O., Kersh, J. E., Routh, A. & Smith, R. R. The long-term side effects of radiation therapy for benign brain tumors in adults. *J Neurosurg* **73**, 502–512 (1990).
4. Withers, H. R. Regeneration of intestinal mucosa after irradiation. *Cancer* **28**, 75–81 (1971).
5. Ginot, A., Doyen, J., Hannoun-Levi, J. M. & Courdi, A. [Normal tissue tolerance to external beam radiation therapy: skin]. *Cancer Radiother* **14**, 379–385 (2010).
6. Hellman, S. & Botnick, L. E. Stem cell depletion: an explanation of the late effects of cytotoxins. *Inf. J. Radiat. Oncol. Biol. Phys.* **2**, 181–184 (1977).
7. Rubin, P. The Franz Buschke lecture: late effects of chemotherapy and radiation therapy: a new hypothesis. *Int J Radiat Oncol Biol Phys* **10**, 5–34 (1984).
8. Lomax, M. E., Folkes, L. K. & O'Neill, P. Biological consequences of radiation-induced DNA damage: Relevance to radiotherapy. *Clin. Oncol.* **25**, 578–585 (2013).
9. Jonathan, E. C., Bernhard, E. J. & McKenna, W. G. How does radiation kill cells? *Curr. Opin. Chem. Biol.* **3**, 77–83 (1999).
10. Iyama, T. & Wilson, D. M. DNA repair mechanisms in dividing and non-dividing cells. *DNA Repair (Amst)*. **12**, 620–36 (2013).

11. Withers, H. R. & Elkind, M. M. Radiosensitivity and fractionation response of crypt cells of mouse jejunum. *Radiat. Res.* **38**, 598–613 (1969).
12. Mizumatsu, S. et al. Extreme sensitivity of adult neurogenesis to low doses of X-irradiation. *Cancer Res.* **63**, 4021–7 (2003).
13. Vissink, A., van Luijk, P., Langendijk, J. & Coppes, R. Current ideas to reduce or salvage radiation damage to salivary glands. *Oral Dis.* (2014). doi:10.1111/odi.12222
14. Fan, J. et al. Human induced pluripotent cells resemble embryonic stem cells demonstrating enhanced levels of DNA repair and efficacy of nonhomologous end-joining. *Mutat. Res.* **713**, 8–17 (2011).
15. De Waard, H. et al. Cell-type-specific consequences of nucleotide excision repair deficiencies: Embryonic stem cells versus fibroblasts. *DNA Repair (Amst)*. **7**, 1659–69 (2008).
16. Merritt, a J. et al. Differential expression of bcl-2 in intestinal epithelia. Correlation with attenuation of apoptosis in colonic crypts and the incidence of colonic neoplasia. *J. Cell Sci.* **108 ( Pt 6)**, 2261–71 (1995).
17. Peissner, W., Kocher, M., Treuer, H. & Gillardon, F. Ionizing radiation-induced apoptosis of proliferating stem cells in the dentate gyrus of the adult rat hippocampus. *Brain Res. Mol. Brain Res.* **71**, 61–8 (1999).
18. Acharya, M. M. et al. Consequences of ionizing radiation-induced damage in human neural stem cells. *Free Radic. Biol. Med.* **49**, 1846–1855 (2010).
19. Zou, Y. et al. Responses of human embryonic stem cells and their differentiated progeny to ionizing radiation. *Biochem. Biophys. Res. Commun.* **426**, 100–5 (2012).
20. Rachidi, W. et al. Sensing radiosensitivity of human epidermal stem cells. *Radiother. Oncol.* **83**, 267–76 (2007).
21. Sotiropoulou, P. A. et al. Bcl-2 and accelerated DNA repair mediates resistance of hair follicle bulge stem cells to DNA-damage-induced cell death. *Nat Cell Biol* **12**, 572–582 (2010).
22. Rube, C. E., Zhang, S., Miebach, N., Fricke, A. & Rube, C. Protecting the heritable genome: DNA damage response mechanisms in spermatogonial stem cells. *DNA Repair (Amst)*. **10**, 159–68 (2011).
23. Bergonié, J. & Tribondeau, L. Interpretation of Some Results from Radiotherapy and an Attempt to Determine a Rational Treatment Technique. 1906. *Yale J. Biol. Med.* **76**, 181–2 (2003).
24. Duffner, P. K. Long-term effects of radiation therapy on cognitive and endocrine function in children with leukemia and brain tumors. *Neurologist* **10**, 293–310 (2004).
25. Ash, P. The influence of radiation on fertility in man. *Br. J. Radiol.* **53**, 271–8 (1980).
26. Smith, D. H. & DeCosse, J. J. Radiation damage to the small intestine. *World J. Surg.* **10**, 189–94 (1986).

27. Thotala, D. et al. Pyridoxamine protects intestinal epithelium from ionizing radiation-induced apoptosis. *Free Radic. Biol. Med.* **47**, 779–85 (2009).
28. Potten, C. S., Merritt, A., Hickman, J., Hall, P. & Faranda, A. Characterization of Radiation-induced Apoptosis in the Small Intestine and Its Biological Implications. *Int. J. Radiat. Biol.* **65**, 71–78 (1994).
29. Potten, C. S., Al-Barwari, S. E. & Searle, J. Differential radiation response amongst proliferating epithelial cells. *Cell Tissue Kinet* **11**, 149–160 (1978).
30. Monje, M. L., Mizumatsu, S., Fike, J. R. & Palmer, T. D. Irradiation induces neural precursor-cell dysfunction. *Nat. Med.* **8**, 955–62 (2002).
31. Liu, J. C. et al. High Mitochondrial Priming Sensitizes hESCs to DNA-Damage-Induced Apoptosis. *Cell Stem Cell* **13**, 483–491 (2013).
32. Zhu, Y., Huang, Y.-F., Kek, C. & Bulavin, D. V. Apoptosis differently affects lineage tracing of Lgr5 and Bmi1 intestinal stem cell populations. *Cell Stem Cell* **12**, 298–303 (2013).
33. Yan, K. S. et al. The intestinal stem cell markers Bmi1 and Lgr5 identify two functionally distinct populations. *Proc. Natl. Acad. Sci. U. S. A.* **109**, 466–71 (2012).
34. Li, L. & Clevers, H. Coexistence of quiescent and active adult stem cells in mammals. *Science* **327**, 542–5 (2010).
35. Diaz Perez, S. V et al. Derivation of new human embryonic stem cell lines reveals rapid epigenetic progression in vitro that can be prevented by chemical modification of chromatin. *Hum. Mol. Genet.* **21**, 751–64 (2012).
36. Bañuelos, C. a et al. Mouse but not human embryonic stem cells are deficient in rejoining of ionizing radiation-induced DNA double-strand breaks. *DNA Repair (Amst)*. **7**, 1471–83 (2008).
37. Dumitru, R. et al. Human Embryonic Stem Cells Have Constitutively Active Bax at the Golgi and Are Primed to Undergo Rapid Apoptosis. *Mol. Cell* (2012). doi:10.1016/j.molcel.2012.04.002
38. Denekamp, J. Cell kinetics and radiation biology. *Int. J. Radiat. Biol. Relat. Stud. Phys. Chem. Med.* **49**, 357–80 (1986).
39. Pawlik, T. M. & Keyomarsi, K. Role of cell cycle in mediating sensitivity to radiotherapy. *Int. J. Radiat. Oncol. Biol. Phys.* **59**, 928–42 (2004).
40. Aladjem, M. I. et al. ES cells do not activate p53-dependent stress responses and undergo p53-independent apoptosis in response to DNA damage. *Curr Biol* **8**, 145–155 (1998).
41. Momcilović, O. et al. Ionizing radiation induces ataxia telangiectasia mutated-dependent checkpoint signaling and G(2) but not G(1) cell cycle arrest in pluripotent human embryonic stem cells. *Stem Cells* **27**, 1822–35 (2009).
42. Tanori, M. et al. Developmental and oncogenic radiation effects on neural stem cells and their differentiating progeny in mouse cerebellum. *Stem Cells* **31**, 2506–16 (2013).

43. Murray, D., McBride, W. H. & Schwartz, J. L. Radiation biology in the context of changing patterns of radiotherapy. *Radiat. Res.* **182**, 259–72 (2014).

## **CHAPTER 3**

---

# **Stem Cells Exhibit an Attenuated DNA Damage Response**

### **3.1 ABSTRACT**

We have previously demonstrated that stem cells are hypersensitive to ionizing radiation (IR) and readily undergo IR-induced apoptosis while differentiated progeny are quite radioresistant. Here we investigate whether a uniquely aberrant DNA Damage Response (DDR) in stem cells contributes to this IR hypersensitivity. Our study determines that stem cells fail to sufficiently activate and maintain DDR signaling. Despite normal sensing of DNA breaks, recruitment/ retention of repair factors at DNA break sites is attenuated in stem cells. This attenuated DDR results in diminished DNA repair efficacy and improper cell cycle checkpoint arrest. Interestingly, while these stem cells are unable to induce  $\gamma$ H2AX foci, during apoptosis they induce pan-nuclear H2AX S139 phosphorylation through the activation of MST1 and JNK. By investigating this pathway for the first time in stem cells, we provide a potential mechanism for IR-induced apoptosis independent of DDR signaling. We thus establish that molecular radiation responses can vary greatly from canonical signaling in specialized cell types such as stem cells, suggesting that DDR signaling is less ubiquitous than currently believed.

### **3.2 METHODS**

#### **3.2.1 Stem Cell Culture and Differentiation:**

Normal embryonic stem (ES) cells were freshly isolated directly from the inner cell mass of blastocyst stage mouse embryos (E4.5), and later procured from the Washington University Embryonic Stem Cell Core Facility or ATCC as karyotypically normal early passage ES cells (EDJ22, RW4). Cells were grown feeder-free on gelatin-coated plates and maintained in high glucose DMEM with HEPES (Invitrogen) containing 10% Fetal Bovine Serum (Invitrogen), 10% Newborn Calf Serum (Invitrogen), 0.2% beta-mercaptoethanol (Invitrogen), a nucleoside mix containing final concentrations of 80 $\mu$ g/ml adenosine, 85 $\mu$ g/ml guanosine, 73 $\mu$ g/ml cytidine, 73 $\mu$ g/ml uridine and 24 $\mu$ g/ml thymidine (Sigma Aldrich) and 10ng/ml LIF (Invitrogen). ES cells were passaged with 0.05% trypsin containing 0.53mM EDTA (Invitrogen) and selective isolation of independent colonies from any differentiated cells present. They were differentiated by culture in the absence of LIF for several days. ES cells were tested bi-monthly for mycoplasma contamination.

Neural stem cells were freshly isolated by dissecting the hippocampal region of brains from P0-P2 mouse pups and were cultured in suspension after dissociation and trituration in AB2 Basal Neural Medium (Aruna Biomedical) containing 20ng/ml EGF, 10ng/ml bFGF, 1% N2-Supplement and 2% B27 (Invitrogen). Neural stem cells were differentiated by addition of 10% FBS (Hyclone) and removal of EGF/FGF from culture medium upon plating into tissue culture-treated dishes for attachment.

### 3.2.2 Animal Models:

Wild-type mouse strain C57BL/6 was used for all *in vivo* assays unless otherwise noted. Adult 6-8 week old males were utilized for harvest of brain, intestine, skin and testis for sectioning. For breeding, 1-6 month old male and female mice of similar age were allowed to mate continuously, with pregnant females isolated independently before giving birth. P0-P2 mouse pups were sacrificed by rapid decapitation prior to dissection for neural stem cell isolation. Procedures for all studies were been approved by the Animal Studies Committee at Washington University Medical Center.

### 3.2.3 Antibodies

Details of the antibodies used in this work are described in Table 3.1.

**Table 3.1. Antibody Information Table**

Protein Target	Species	Company	Catalog #	Assay	Conditions
BrdU (AlexaFluor 488 conjugated)	mouse	Invitrogen	B35139	FACS	1:20
Histone H2AX	rabbit	Cell Signaling	#7631	IF, WB	1:150, 1:2000 in BSA
Ku80	rabbit	Cell Signaling	#2753	IF	1:200
MDC1	mouse	Millipore	05-1572	IF	1:150
MST1	rabbit	Cell Signaling	#3682	IHC-F	1:50
NBS1	rabbit	Abcam	ab32074	IF	1:200
Oct4	rabbit	Abcam	ab19857	IF, IHC-F	1:200, 1:200
PCNA	mouse	Millipore	NA-03	IHC-F	1:100
phospho-ATM (S1981)	mouse	Rockland	200-301-400	IF	1:200

phospho-ATM (S1981)	mouse	Cell Signaling	#4526	WB, IHC-F	1:500 in milk, 1:50
phospho-ATR (S1989)	rabbit	GeneTex	GTX128145	WB	1:1000 in BSA
phospho-Chk1 (S345)	rabbit	Cell Signaling	#2348	WB	1:1000 in BSA
phospho-DNA-PK (S2056)	rabbit	Abcam	ab18192	IF, IHC-F	1:200, 1:100
phospho-H3 (S10)	mouse	Pierce	MA5-15220	FACS	1:100
phospho-JNK (T183/Y185)	mouse	Santa Cruz	sc-6254	IHC-F, WB	1:50, 1:500
phospho-MST1 (T183)	rabbit	Cell Signaling	#3681	WB	1:1000 in BSA
PLZF	mouse	Santa Cruz	sc-28319	IHC-F	1:50
Rad51	rabbit	Santa Cruz	sc-8349	IHC-F	1:100
Sox2	rabbit	Abcam	ab7959	IHC-F	1:100
Sox2	mouse	Abcam	ab79351	IF, IHC-F	1:200, 1:100
SSEA1	mouse	Abcam	ab16285	IHC-F	1:100
Total ATM	rabbit	Cell Signaling	#2873	WB	1:1000 in BSA
Total ATR	rabbit	Cell Signaling	#2790	WB	1:500 in milk
Total Chk1	mouse	Cell Signaling	#2360	WB	1: 1000 in milk
$\gamma$ H2AX (S139)	mouse	Millipore	05-636	WB, IHC-F	1:4000 in BSA, 1:400
$\gamma$ H2AX (S139)	rabbit	Cell Signaling	#7631	IHC-F	1:150
GAPDH	mouse	Sigma Aldrich	G8795	WB	1:100,000 in milk
FITC-conjugated anti-rabbit	donkey	Vector	FI-1000	IF, IHC-F	1:100
FITC-conjugated anti-mouse	horse	Vector	FI-2000	IF, IHC-F	1:100
AMCA-conjugated anti-mouse	horse	Vector	CI-2000	IF	1:75
AMCA-conjugated anti-rabbit	donkey	Vector	CI-1000	IF	1:75
Texas Red-conjugated anti-mouse	horse	Vector	TI-2000	IF, IHC-F	1:100
Texas Red-conjugated anti-rabbit	donkey	Vector	TI-1000	IF, IHC-F	1:100
HRP-conjugated anti-mouse	rabbit	Sigma Aldrich	A9044	WB	1:5000 in milk
HRP-conjugated anti-rabbit	goat	Sigma Aldrich	A0545	WB	1:5000 in milk

### 3.2.4 X-Ray Irradiation and Tissue Sectioning:

Cells and animals were irradiated in the RS-2000 Biological Research Irradiator (Rad-Source) at room temperature, with mock/control irradiated samples brought into the room to simulate the reduction in ambient temperature and account for any stress imparted by the travel. Cells were always placed within the central circle directly under the x-ray source to maintain consistency in

dose between samples. Animals were anesthetized with isoflurane and placed on their back in the machine for whole-body irradiation to properly expose all tissues of interest to the x-ray source. Accuracy of all doses was confirmed by dosimeter probe. Both cells and animals were randomly assigned to individual timepoints or sham-irradiation controls.

Following irradiation, mice were sacrificed at specific timepoints by CO<sub>2</sub> asphyxiation and cervical dislocation. Organs were harvested, placed in OCT media and frozen in liquid nitrogen. Frozen tissues were sectioned on a cryostat machine at a thickness of 10µm, placed onto adhesive slides and stored at -80°C.

### **3.2.5 Western Blotting:**

Cellular protein lysates were collected in RIPA buffer, electrophoresed on 4-15% Tris-Glycine polyacrylamide gels (BioRad), transferred onto PVDF membranes and incubated overnight at 4°C with various primary antibodies followed by washing and secondary antibody incubation for 2hr at room temperature. Super ECL (GE/Pierce) was used as substrate for detection on autoradiography film or ChemiDoc MP digital system (BioRad).

### **3.2.6 Immunofluorescence:**

Freshly frozen tissues were isolated from testis, brain, intestine and skin following 6Gy irradiation or 0Gy mock before embedding in OCT media and sectioning onto slides. Slides of tissue sections or coverslips of cells were fixed in 4% formaldehyde and permeabilized with 0.2% Triton-X followed by blocking with 2% BSA. Tissues were incubated with primary antibodies in 1% BSA at 37°C for 3hr, washed and then incubated with secondary fluorescently-tagged secondary antibodies for 45min at 37°C. Tissues were then mounted in place with coverslips containing mounting media with DAPI (Vector) for identification of nuclei.

Cells were similarly fixed in 4% formaldehyde and permeabilized with 0.2% Triton-X before blocking. For double-color staining, primary antibodies were incubated together for 1hr at 37°C

followed by wash and incubation with fluorescently-tagged secondary antibodies for 30min at 37°C. For triple-color staining, following the original staining procedure, cells were incubated with 1:1000  $\alpha$ - $\gamma$ H2AX antibody for 15min at 37°C followed by 12min incubation at 37°C with the appropriate secondary antibody. Anti  $\gamma$ H2AX antibody was chosen to match Sox2 to avoid cross-reaction with the other target antigen of interest.

### **3.2.7 Neutral Comet Assay:**

To assess repair of DNA double strand breaks, neutral comet assays were performed using CometSlide assay kits (Trevigen). Cells were collected at multiple timepoints following 6 Gy irradiation or 0 Gy mock and embedded in agarose on slides at equal concentrations. Slides were electrophoresed in TAE buffer, fluorescently stained with SYBR Green (Trevigen), and visualized by fluorescent microscopy. Olive comet moment was calculated using the CometScore software (TriTek) to analyze 50-100 comets per sample, with each series of timepoints repeated at least three independent times as both biological and technical replicates. Individual comets were randomly selected for scoring from similar regions of the slide in all samples. Outliers were eliminated that fell greater than 1.5 standard deviations from the mean. Standard error was calculated for each cell type and timepoint normalized to the value of the 0min samples, while the significance of the difference between cell types over time was analyzed by Analysis of Covariance (ANCOVA) using XLStat statistical software (Addinsoft), with two-sided significance set at  $p < 0.05$ . Data from all samples was approximately normally distributed, and the standard deviation between samples within the same experiment was similar. Samples were excluded from analysis only due to technical errors from the assay or cells being visibly unhealthy.

### **3.2.8 Laser Microirradiation**

Stem cells (ES, NS) were co-plated with non-stem cells (ED, MEF) on glass coverslips and incubated for 2 days with 30 $\mu$ M BrdU (Sigma Aldrich) to sensitize DNA for DSB induction. Prior to laser microirradiation, cells were incubated with Stem Cell cDy1 Dye (Active Motif) for 30min to fluorescently label live stem cells for identification. Coverslips were then placed in circular

magnetic chambers (Quorum Technologies) with media to be properly aligned for microirradiation. Cells were microirradiated in a defined narrow region across adjacent stem and non-stem cells with 8000-12000 iterations of 405+633nm laser on the LSM 510 Confocal Microscope (Zeiss) at 45% power output. Care was taken to include stem (cDy1 positive) as well as non-stem cells in the DNA damage tracks. Cells were microirradiated for 20-30min per sample unless otherwise stated, with 6-12 regions of microirradiation per sample.

### **3.2.9 Cell Cycle Analysis**

For cell cycle profiling, cells were isolated at various timepoints following irradiation and ethanol-fixed overnight at -20°C. Ethanol-fixed cells were washed and incubated with RNase for 30min at 37°C for 30min before staining with propidium iodide and analyzing by flow cytometry.

ES and ED cells were incubated with 20µM BrdU (Sigma) for 30min, irradiated, washed 2 times and chased for various timepoints to allow cell cycle progression. Cells were then fixed overnight in ethanol at -20°C, incubated with RNase and propidium iodide, and analyzed by flow cytometry.

For G2/M checkpoint arrest, cells were first ethanol-fixed at various timepoints following sham or 6Gy irradiation. Cells were then washed, blocked in 2% BSA and incubated for 1h with phospho-histone H3 (S10) antibody at 37°C to label mitotic cells. Following washes, cells were incubated with 1:100 FITC-conjugated anti-mouse 2° antibody for 30min at room temperature. Following another wash cells were incubated with RNase and propidium iodide as before and analyzed by flow cytometry. G2/M arrest was indicated by decrease in the percentage of mitotic cells.

### **3.2.10 Cytogenetic Analysis**

Cells were incubated with 100ng/ml colcemid for 2-4hrs following 6Gy irradiation or 0Gy mock to arrest cells in metaphase. Mitotic cells were selectively isolated by mitotic shake-off, incubated in hypotonic buffer (0.56% KCl) for 8 min, fixed in acetate-methanol and dropped onto slides.

Fluorescent *in situ* hybridization was performed using oligonucleotide (TTAGGG)<sub>3</sub> PNA probes

using standard protocols and counterstained with DAPI. Chromosomes were then visualized by fluorescence microscopy and scored for chromosome aberrations. The number of chromosome aberrations was normally distributed for each sample, with similar standard deviations between samples from the same time point. Each sample was repeated three times. Chromosome aberrations were defined as chromosome or chromatid breaks, translocations, or radials. Standard error was calculated and statistical significance was determined by Student's *t*-test, with two-sided significance set at  $p < 0.05$ . Only full chromosome plates were scored, any partial plates were excluded from scoring.

### **3.2.11 Microscopy and Image Processing**

Micrographs were captured utilizing MetaSystems ISIS imaging software on Zeiss Axioplan2 microscope or ZEN software on Zeiss LSM510 confocal microscope with the 20x, 63x or 100x objective lenses. Minimal threshold and contrast manipulation was performed equally across entire images. Controls were processed equally with treated samples. Adobe Photoshop CS3 software was utilized for composing the collages of multiple pictures and labeling micrographs and Immunoblots in individual layers.

### **3.2.12 Statistical Analysis**

A 'two-tailed' Student's *t*-test was used to calculate the statistical significance of the observed differences. In all cases, differences were considered statistically significant when  $p < 0.05$ .

Unless otherwise indicated, values represent mean  $\pm$  SEM.

## **3.3 INTRODUCTION**

Radiation therapy utilizes ionizing radiation (IR) to produce lethal DNA double-strand breaks (DSBs) in cancer cells; however detrimental sequelae often result from unintended damage to normal tissue. Work from previous chapters elucidated that these consequences are likely due to the loss of stem cells from the affected tissue niche, as IR induces apoptosis only in stem cells while differentiated cells are radioresistant. Having established that stem cells are hypersensitive to IR both *in vivo* and in culture, we

examined the molecular mechanisms responsible for this differential radiosensitivity among stem and differentiated cells. An improved understanding of cellular radiation responses is essential for the development of strategies to protect normal tissue during radiotherapy.

Aberrant DNA damage response (DDR) signaling often leads to genomic instability and cell death <sup>1</sup>, suggesting that inadequate DDR signaling and DNA repair may contribute to radiation hypersensitivity. The DDR is an intricate network of molecular signaling following DSBs that enables proper damage sensing, recruitment of repair factors and subsequently DNA repair. In mammals, the Mre11–Rad50–Nbs1 (MRN) complex initially senses DNA breaks <sup>2,3</sup>. This is followed by activation of phosphatidylinositol 3-kinase-related kinases (PIKKs), which include ataxia telangiectasia mutated (ATM), ATM and Rad3-related (ATR), and DNA-dependent protein kinase catalytic subunit (DNA-PKcs). Activated ATM phosphorylates histone H2AX on serine 139, marking mega-bases of chromatin around the DSB with  $\gamma$ H2AX <sup>4,5</sup>, and serving as a docking site for downstream repair factors <sup>6</sup>. Following repair factor assembly and cell cycle checkpoint activation, the DDR initiates DNA DSB repair. In the absence of efficient repair, apoptosis may be induced to eliminate cells with compromised genomic integrity <sup>1</sup>.

Here we establish that stem cells across multiple tissue niches and culture models exhibit a severely attenuated DDR, demonstrating reduced activation and recruitment of various DDR and DNA repair factors following irradiation. We also show that stem cells demonstrate limited DNA repair and insufficient cell cycle checkpoint arrest, resulting in DDR-independent apoptosis through the MST1-JNK-H2AX pathway. By elucidating that stem cell radiosensitivity is associated with an abrogated DDR and inadequate DNA repair capacity, this work identifies potential molecular targets for radioprotecting stem cells to improve patient outcomes following radiation therapy.

## **3.4 RESULTS**

### **3.4.1 Stem cells exhibit an attenuated DDR**

We utilized tissue sections isolated from brain, testis, intestine and skin in order to delineate whether any differences in the DDR among stem and non-stem cells *in vivo* was associated with

their previously observed differential radiosensitivity. We observed a remarkable absence of  $\gamma$ H2AX foci from individually labeled stem cells in all tissues surveyed shortly following irradiation, while adjacent non-stem cells displayed robust IR-induced foci (IRIF) formation (Fig. 3.1) compared to unirradiated controls (Fig. 3.2). We then utilized subnuclear laser microirradiation in order to observe recruitment of DDR factors to defined regions of DNA damage in culture. Stem cells in culture also exhibited strongly attenuated IR-induction of  $\gamma$ H2AX both along microirradiation-induced DSBs (Fig. 3.3 A-B) and globally (Fig. 3.4 A) compared to equivalently-treated non-stem cells. Total H2AX levels were similar among the cell types and remained unchanged following irradiation (Fig. 3.4 A-B). H2AX S139 is phosphorylated primarily by activated ATM kinase<sup>4,5</sup>. We therefore investigated whether repressed ATM activation is responsible for the abrogation of  $\gamma$ H2AX formation in stem cells. Immunoblots showed markedly reduced activation of ATM by phosphorylation of serine 1981 (pATM) in stem cells without any reduction in total ATM levels (Fig. 3.5). ATM activation can also occur independently of its recruitment to DNA damage<sup>7</sup>, hence we assessed the recruitment of pATM to DSBs. Subnuclear microirradiation confirmed the inability of stem cells to adequately activate and recruit pATM to DNA breaks, while in contrast co-plated and co-treated non-stem cells displayed robust recruitment of pATM to the damaged region (Fig. 3.6). Complete abrogation of ATM activation and recruitment was also observed *in vivo* following irradiation (Fig. 3.7 A-B). Immunoblotting of stem cells in culture also demonstrated reduced ATR activation as indicated by both decreased phosphorylation of the DNA damage-responsive serine 1989 site<sup>8</sup> and diminished activation of the ATR substrate checkpoint kinase 1 (Chk1) (Fig. 3.8).

Stem cells failed to recruit activated non-homologous end joining (NHEJ) repair factor DNA-PKcs (pDNA-PKcs) phosphorylated at serine 2056<sup>9</sup> both in culture (Fig. 3.9 A) and *in vivo* within the SGZ (Fig. 3.9 B). Rad51 foci indicating homologous recombination (HR) repair were also not detected in stem cells *in vivo* within irradiated testis and intestine (Fig. 3.10 A-B). Despite the presence of actively proliferating stem cells *in vivo* (Fig. 2.11), only proliferating differentiated

cells displayed Rad51 foci. Together these data clearly demonstrate that stem cells exhibit severely abrogated induction and recruitment of DDR factors in response to IR.

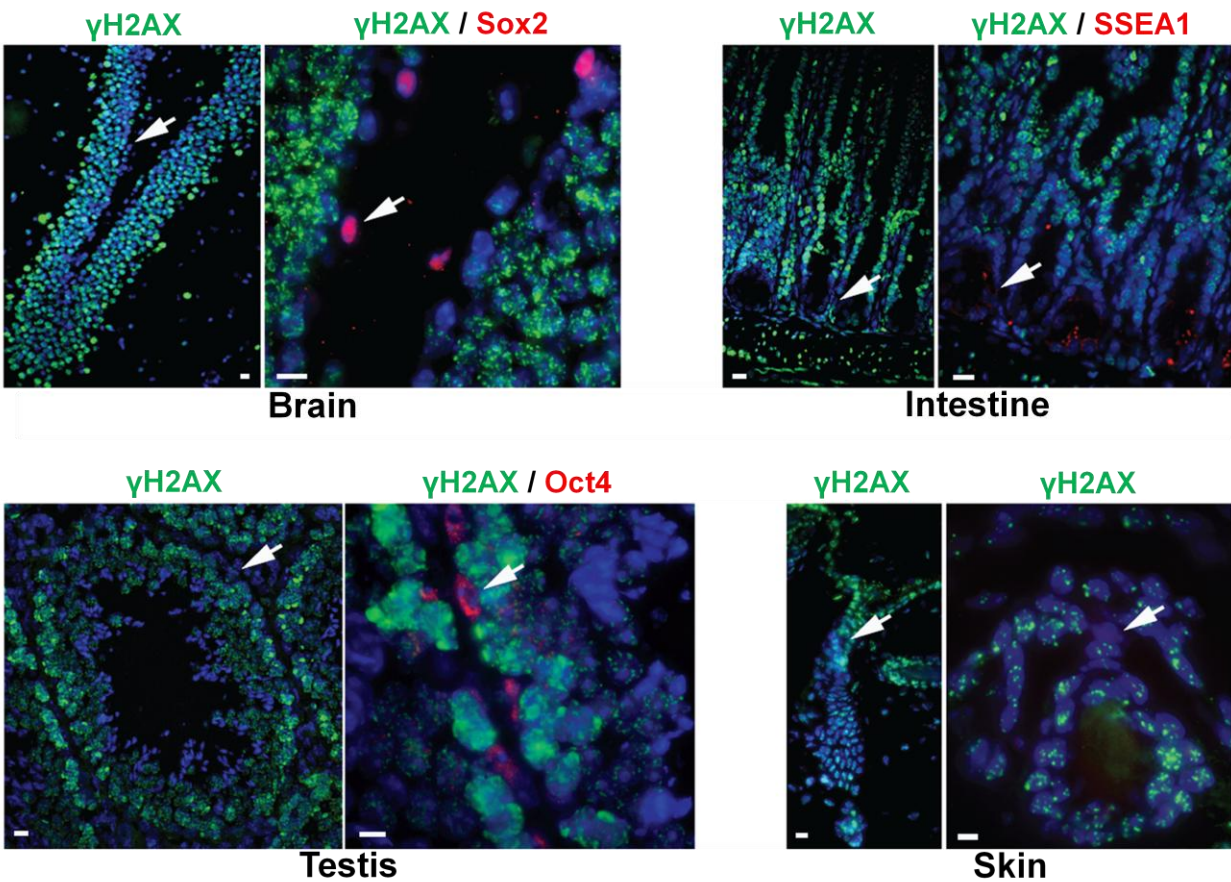


**Figure 3.1. Absence of  $\gamma$ H2AX IRIF in stem cells *in vivo*.** Immunofluorescence co-staining of stem cell markers (red; Sox2, SSEA1, Oct4) and  $\gamma$ H2AX (green) in tissue niches 15min following 6Gy IR. DAPI=DNA. Arrows indicate stem cells *in vivo* lacking  $\gamma$ H2AX IRIF.

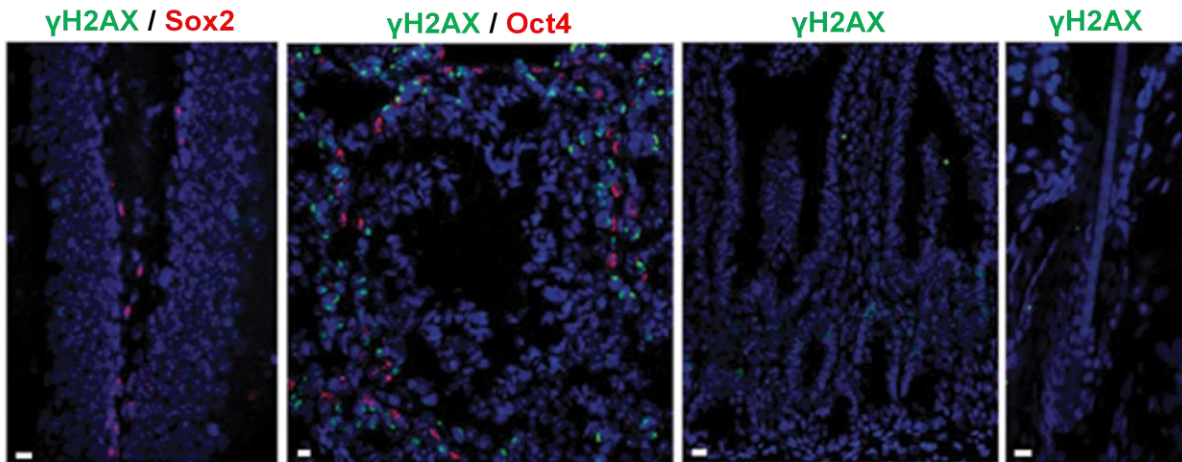


**Figure 3.2. Sham-irradiated negative controls for *in vivo*  $\gamma$ H2AX IRIF.** Immunofluorescence co-staining of stem cell markers (red, Sox2, Oct4) and  $\gamma$ H2AX (green) in tissue niches following sham irradiation.

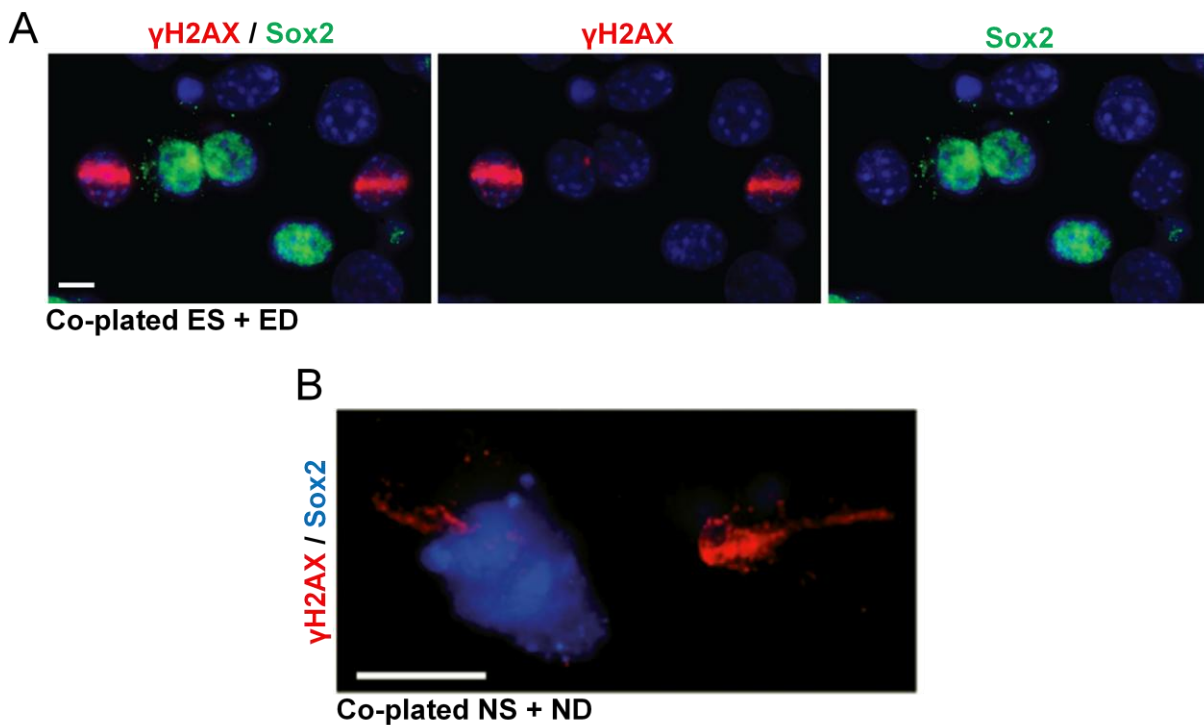


**Figure 3.3.  $\gamma$ H2AX induction is attenuated along DSBs in cultured stem cells.** Immunofluorescence co-staining of (A) Sox2 (green) and  $\gamma$ H2AX (red) on co-plated ES and ED cells, DAPI=DNA, or (B) Sox2 (blue) and  $\gamma$ H2AX (red) on co-plated NS and ND cells 30min following microirradiation. DAPI=DNA.  $\gamma$ H2AX was substantially attenuated in approximately 70% of laser tracks. White scale bars, 10 $\mu$ m.

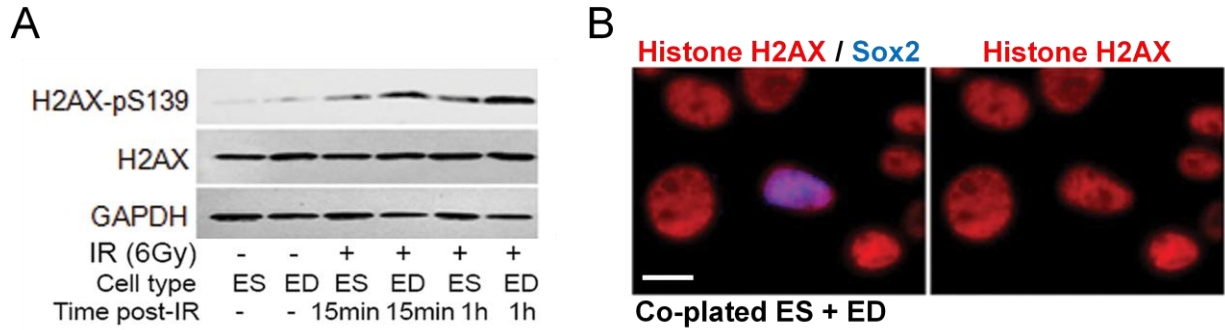


**Figure 3.4. Global attenuation of IR-induced  $\gamma$ H2AX in cultured stem cells is not due to reduced H2AX expression.** (A) Western blots for  $\gamma$ H2AX and histone H2AX at various time points following mock or 6Gy irradiation of ES and ED cells. GAPDH served as a loading control. (B) Immunofluorescence co-staining of Sox2 (blue) and histone H2AX (red) on co-plated unirradiated ES and ED cells. White scale bars, 10 $\mu$ m.

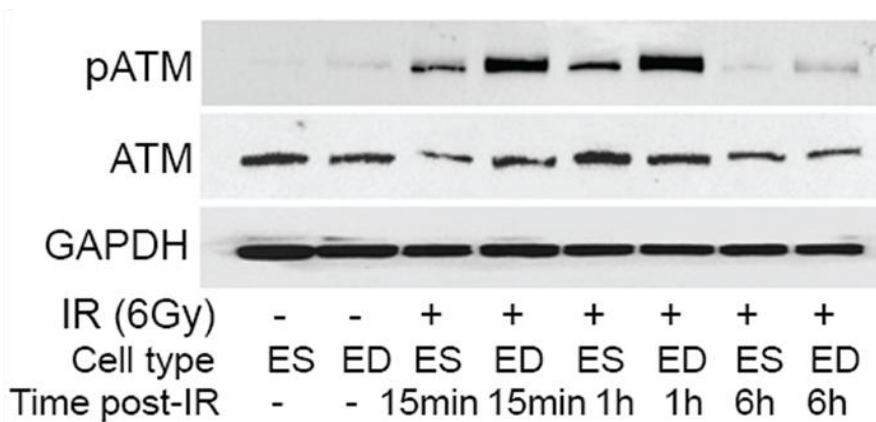


**Figure 3.5. IR-induced ATM activation is attenuated in cultured stem cells.** Western blots for pATM and total ATM at various time points following mock or 6Gy irradiation of ES and ED cells. GAPDH served as a loading control.

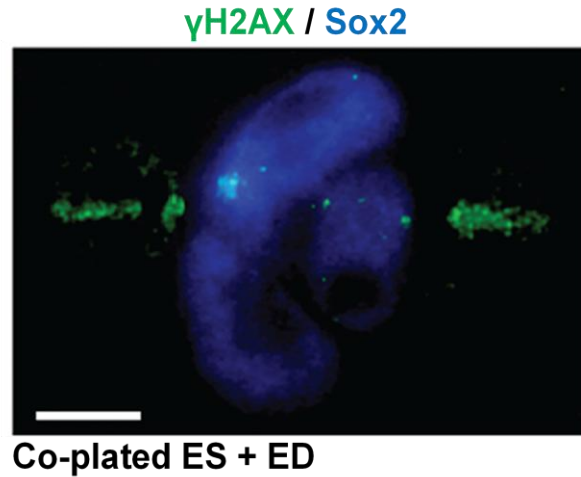


**Figure 3.6. pATM is not recruited to DSBs in cultured stem cells.** Immunofluorescence co-staining of Sox2 (blue) and pATM (green) on co-plated ES and ED cells following microirradiation. White scale bars, 10 $\mu$ m.

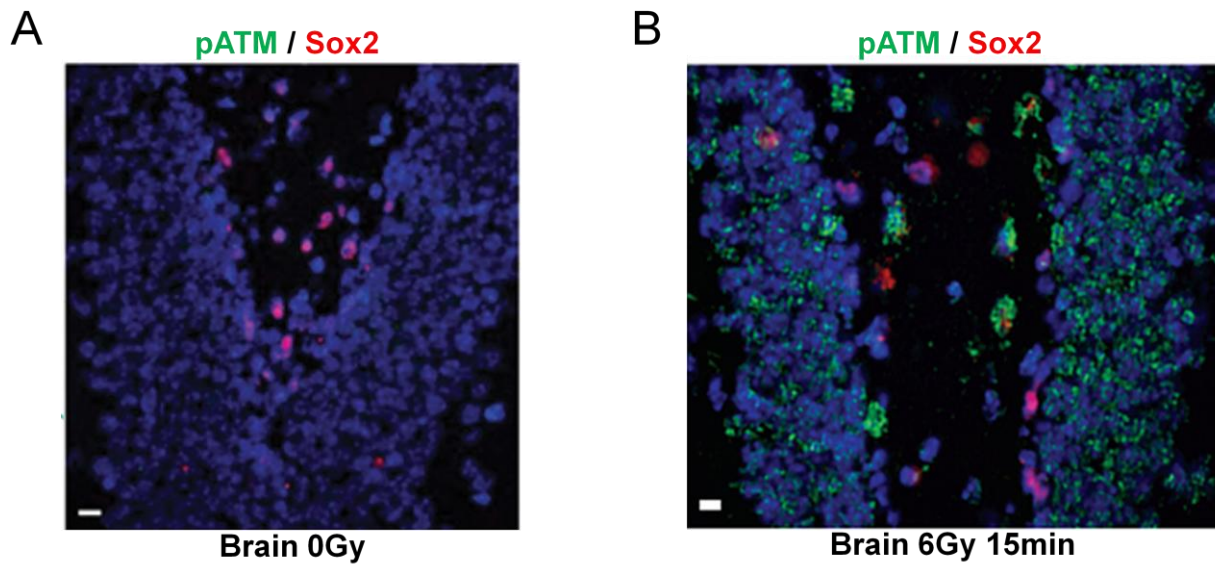


**Figure 3.7. IR-induced activation and recruitment of ATM IRIF is attenuated in stem cells *in vivo*.** Immunofluorescence co-staining of Sox2 (red) and pATM (green) in brain 15min following (A) sham or (B) 6Gy IR. DAPI=DNA. White scale bars, 10 $\mu$ m.

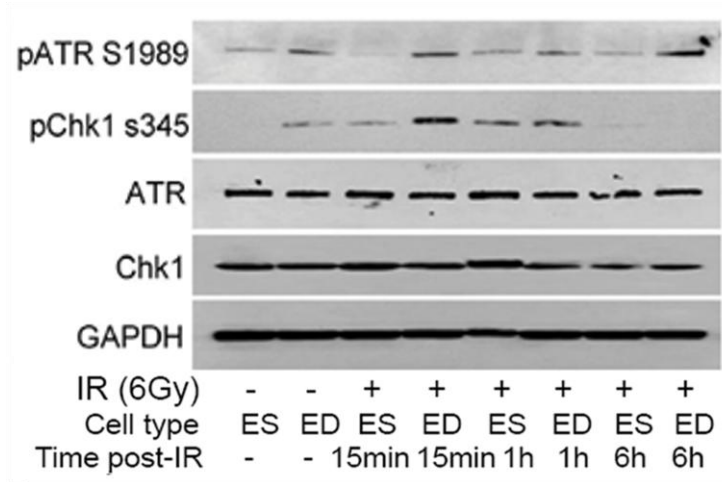


**Figure 3.8. IR-induced ATR activation is attenuated in cultured stem cells.** Western blots for pATR, total ATR, pChk1 and total Chk1 on ES and ED cells at various time points following mock or 6Gy irradiation of ES and ED cells. GAPDH served as a loading control.

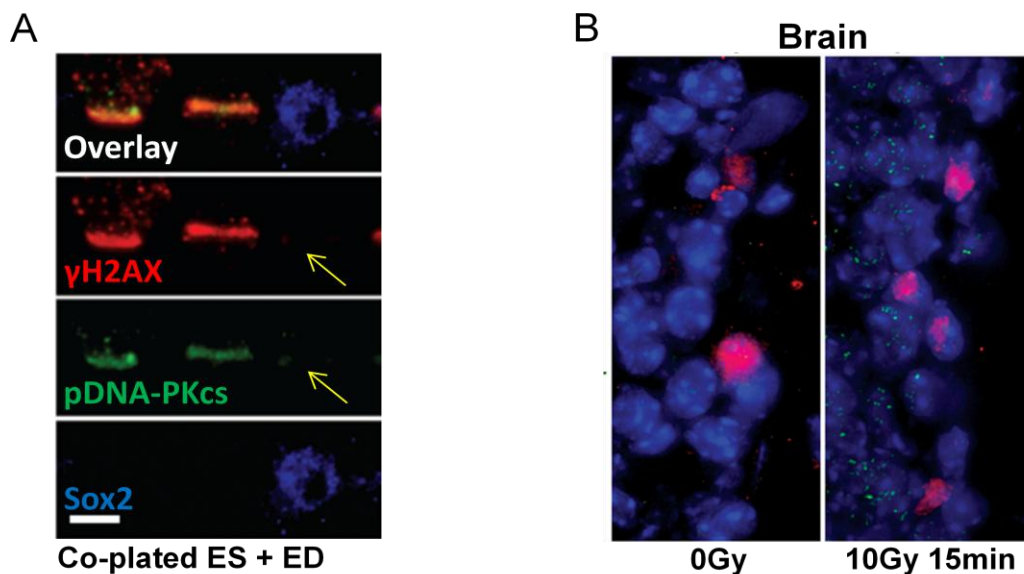


**Figure 3.9. Recruitment of pDNA-PKcs to DSBs is attenuated in stem cells both in culture and *in vivo*.** (A) Immunofluorescence co-staining of Sox2 (blue),  $\gamma$ H2AX (red) and pDNA-PKcs (green) on co-plated ES and ED cells following microirradiation. (B) Immunofluorescence co-staining of Sox2 (red) and pDNA-PK (green) in brain 4h following sham or 6Gy IR. DAPI=DNA. White scale bars, 10 $\mu$ m.

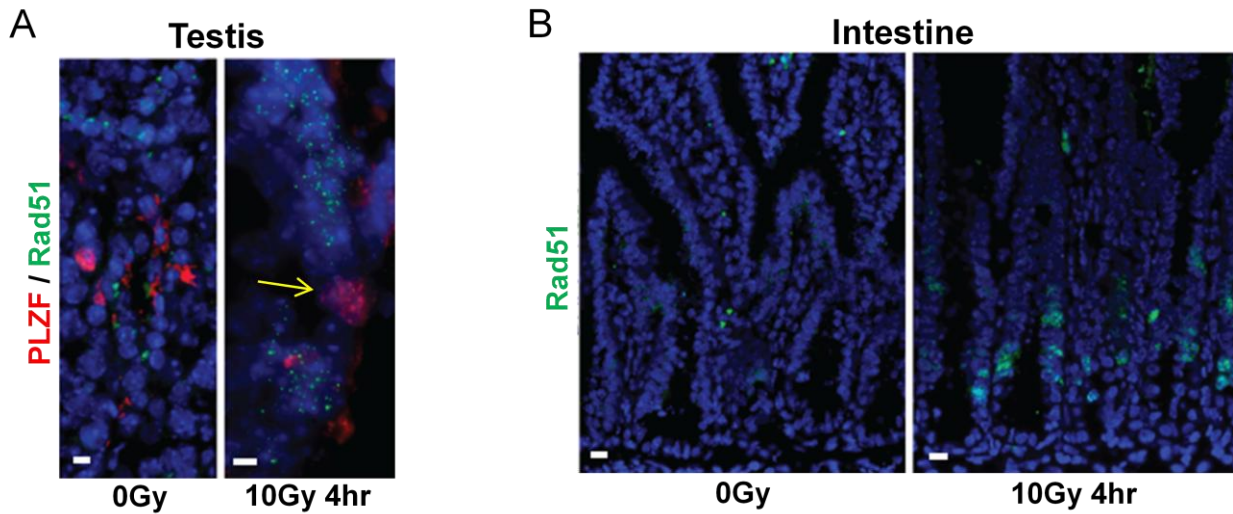


**Figure 3.10. Rad51 recruitment to IRIF is attenuated in stem cells *in vivo*.** Immunofluorescence co-staining of (A) PLZF (red) and Rad51 (green) in testis and (B) Rad51 (green) alone in intestine 4h following sham or 6Gy IR. DAPI=DNA. White scale bars, 10µm.

### 3.4.2 Stem cells display impaired cell cycle arrest compared to differentiated cells

To examine whether a difference in cell cycle control could be connected to the increased apoptosis in stem cells, the cell cycle distributions of ES and ED were analyzed after IR.

Beginning at 2 h and maximizing at 6-8 h, IR induced the accumulation of cells in G2 in both ES and ED cells (Fig. 3.11). In agreement with our previous experiments, only ES cells displayed a strong induction of a subG1 population representing the apoptotic fragmentation of DNA.

Additionally, in ES cells IR induced a greater shift in the ratio towards G2, while they show almost a complete absence of G1 accumulation. In contrast, ED cells maintained a substantial G1 population at all time points. Moreover, pulse-chase of BrdU-labeled ES and ED cells up to 8h after irradiation confirmed the lack of G1 accumulation in stem cells (Fig. 3.12). These results suggest an absence of G1 arrest in ES cells, unlike their isogenic differentiated cells. G2/M checkpoint arrest has previously been observed in ES cells<sup>10,11</sup>, however the details of G2/M arrest has not been compared between stem and differentiated cells. In order to assess both the initiation and maintenance of G2/M arrest, we quantified the percentage of cells staining positive

for the mitosis marker histone H3 serine 10 phosphorylation at multiple timepoints following irradiation. Our results showed that both stem and non-stem cells demonstrate a rapid G2/M arrest as indicated by the decrease in mitotic cells within 1h of irradiation. Contrary to differentiated cells however, ES cells were unable to fully block mitotic entry and were completely released from G2/M arrest by 9h post-irradiation (Fig. 3.13). ED cells are able to completely block cell cycle progression into mitosis and in contrast show sustained maintenance of G2/M arrest up to 12h following irradiation. Weaker cell cycle checkpoint controls in stem cells may serve as an additional contributing mechanism toward their enhanced radiosensitivity.

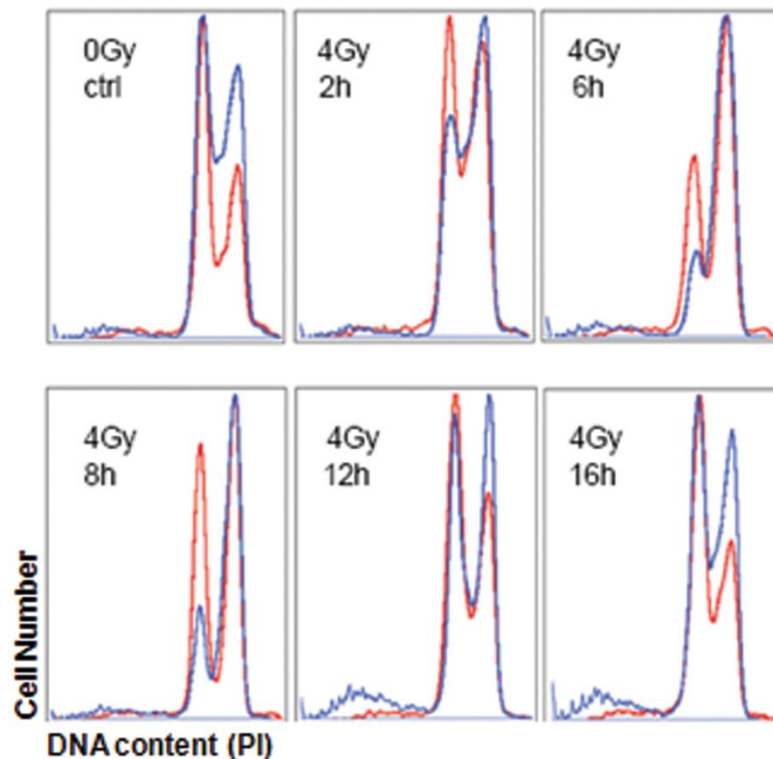


**Figure 3.11. Cell cycle profile overlays of irradiated stem and non-stem cells.** Cell cycle profiles of ES and ED cells were collected at multiple timepoints following sham or 4Gy IR. Blue outline, ES; red outline, ED. 10,000 gated cells were counted for analysis.

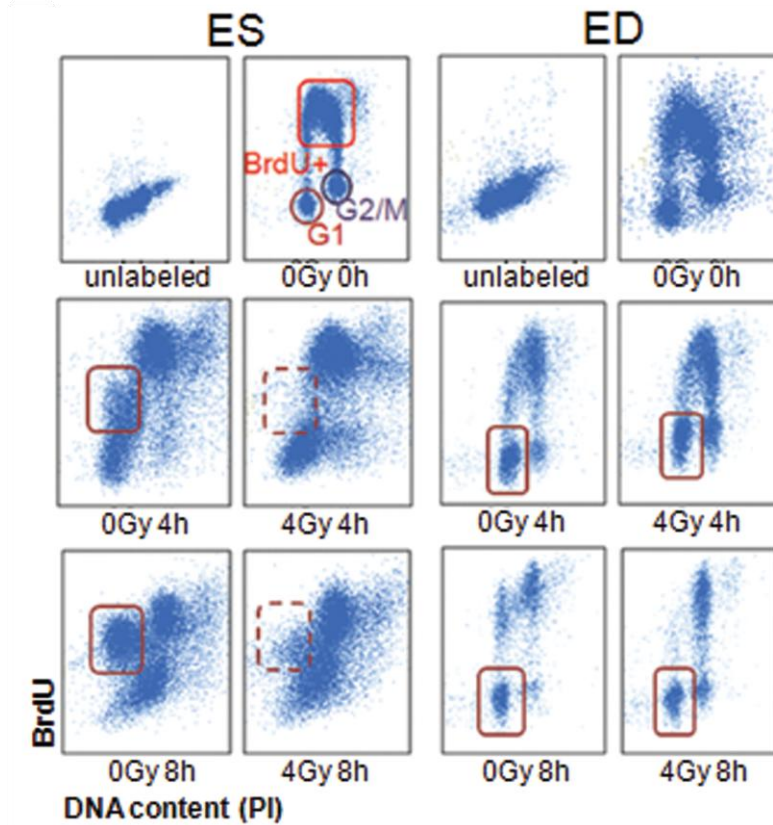


**Figure 3.12. BrdU pulse-chase profiles of irradiated stem and non-stem cells.** ES and ED cells were labeled with BrdU and chased for multiple timepoints following sham or 4Gy IR. Rectangles indicate the presence of G1, S, and G2 populations. Solid rectangle, G1 population; dotted rectangle, absence of G1 population. 20,000 gated cells were counted for analysis.

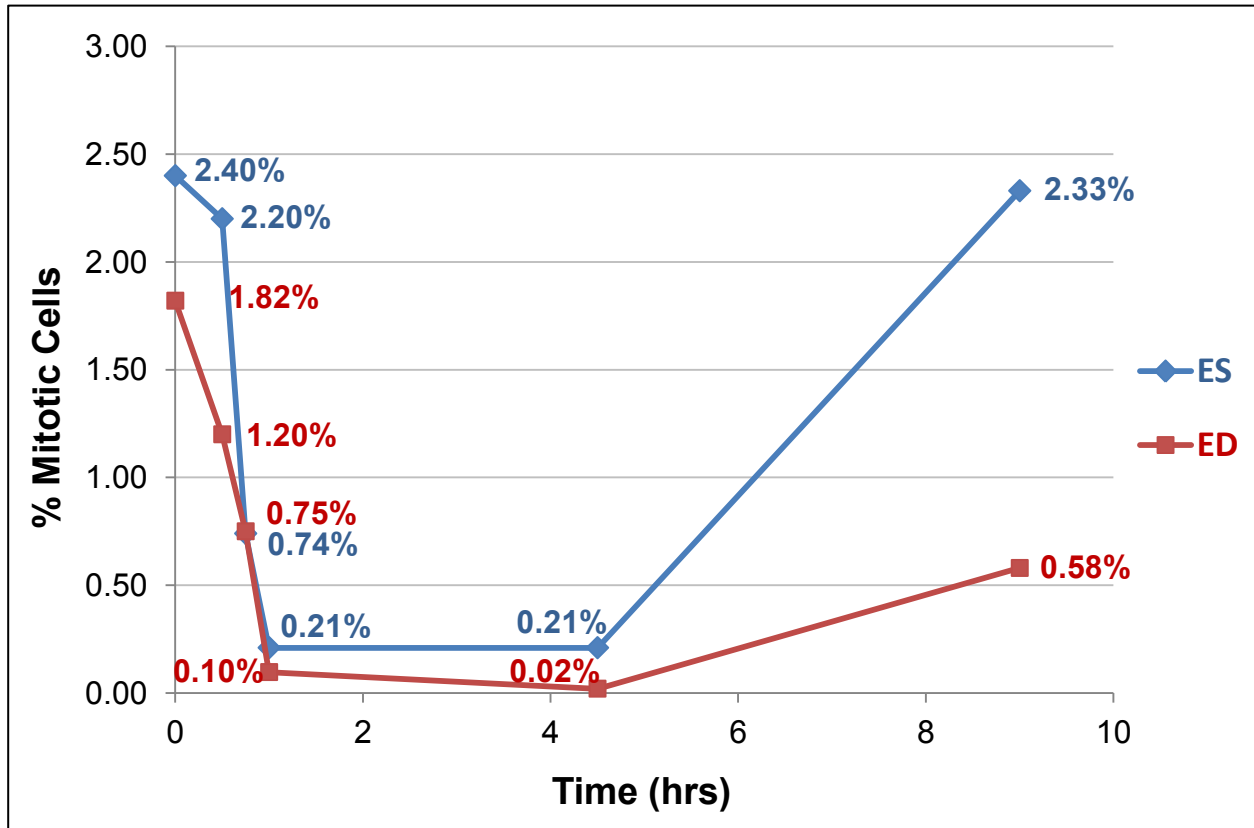


**Figure 3.13. Stem cells exhibit a shortened G2 checkpoint arrest.** ES and ED cells were collected at multiple timepoints following sham or 6Gy irradiation and mitotic cells were labeled with phospho-histone H3 (S10). G2/M arrest was measured by observed reduction in the percentage of mitotic cells in the population.

### 3.4.3 Stem cells fail to adequately repair DSBs

Differences in DNA repair proficiencies between stem and non-stem cells in culture were then quantified. The non-stem cells exhibited efficient repair as indicated by rapid reduction of DNA breaks within 1h of irradiation (Fig. 3.14). Stem cells in contrast exhibited significantly diminished repair efficiency, paralleling the repair kinetics of H2AX <sup>-/-</sup> cells <sup>12</sup>. Stem cells ultimately failed to show substantial DNA repair until 4h post-IR, when many of the radiosensitive cells had already begun dying and dropping out of the population (Fig. 2.9). Stem cells also displayed significantly higher incidences of unrepaired chromosome/chromatid breaks and fragmented/blebbing nuclei

following IR, while only minimal aberrations were seen in unirradiated controls (Fig. 3.15 A-B, 3.16). Despite attenuated DDR signaling, we did observe recruitment of the MRN complex protein Nibrin (NBS1) to microirradiation tracks in stem cells (Fig. 3.17) along with Ku80 (Fig. 3.18), another early responder to DSBs as part of the Ku70/80 heterodimer<sup>13</sup>. The presence of these factors may enable the observed low level of basal repair (Fig. 3.14). Inhibition of the DDR in stem cells thus leads to reduced DNA repair efficiency and likely relates to their reduced threshold for DNA damage-induced apoptosis.

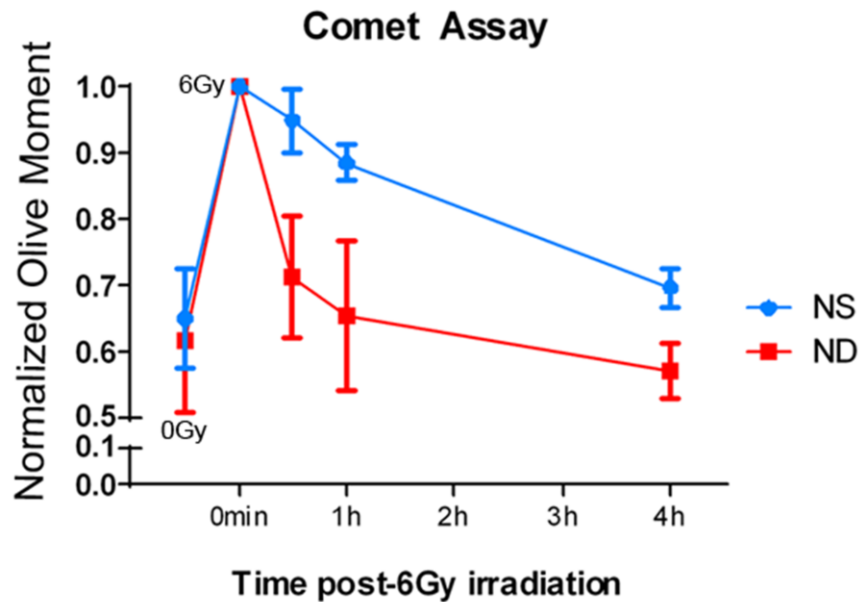


**Figure 3.14. Neutral comet assay on stem and non-stem cells to measure DNA repair.** Olive moments of NS and ND cell comet assay tails were quantified at different timepoints following sham or 6Gy IR and normalized to the irradiated 0min timepoint in order to measure DNA repair over time. The difference in olive moment across the entire timecourse was significant by ANCOVA,  $p = 0.013$ ;  $N=3$ . Error bars indicate SEM.

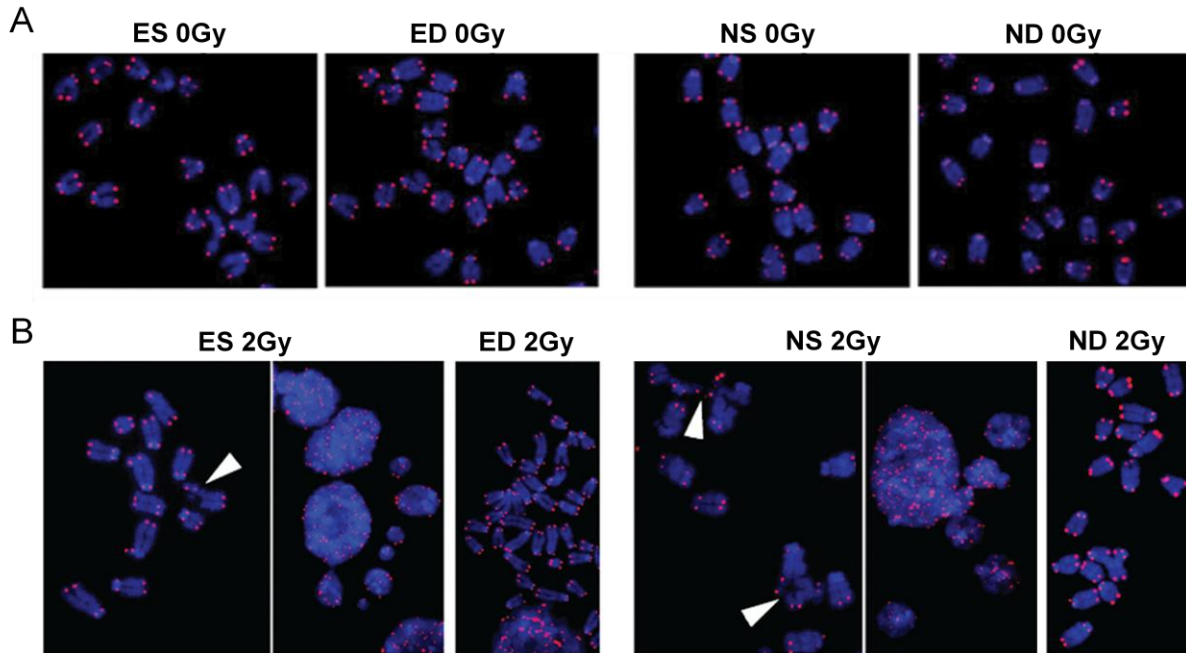


**Figure 3.15. Chromosome preparations from stem and non-stem cells.** (A) Metaphase chromosomes isolated from unirradiated ES, ED, NS and ND cells. (B) Metaphase chromosomes and fragmented nuclei isolated from ES, ED, NS and ND cells following 6Gy IR. Red, telomere; DAPI=DNA. Arrowheads indicate clusters of chromosome aberrations.

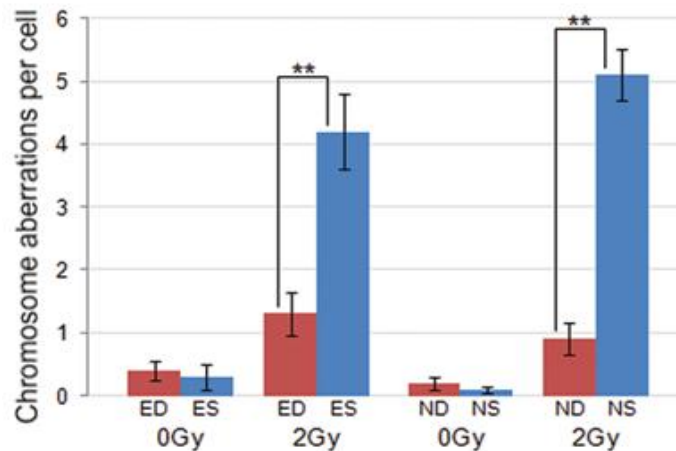


**Figure 3.16. Cultured stem cells show more residual chromosomal aberrations than non-stem cells following irradiation.** Chromosome aberrations were quantified in stem and non-stem cells following 2Gy or sham irradiation. N=3; \*\*, p < 0.01. Aberrations were scored as the sum of chromosome/chromatid breaks, translocations, and radials. Error bars indicate SEM.

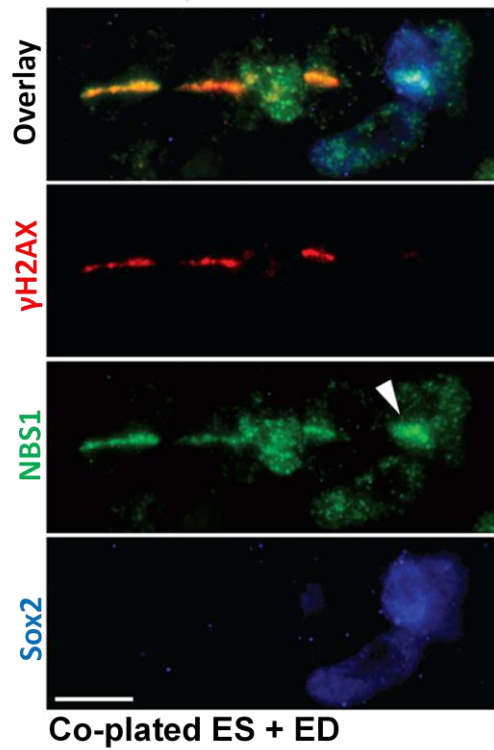


**Figure 3.17. MRN complex is recruited to DSBs in cultured stem cells.**

Immunofluorescence co-staining of Sox2 (blue),  $\gamma$ H2AX (red) and NBS1 (green) on co-plated ES and ED cells following microirradiation. Arrowhead indicates the presence of NBS1 despite attenuated induction of  $\gamma$ H2AX. White scale bar, 10 $\mu$ m.

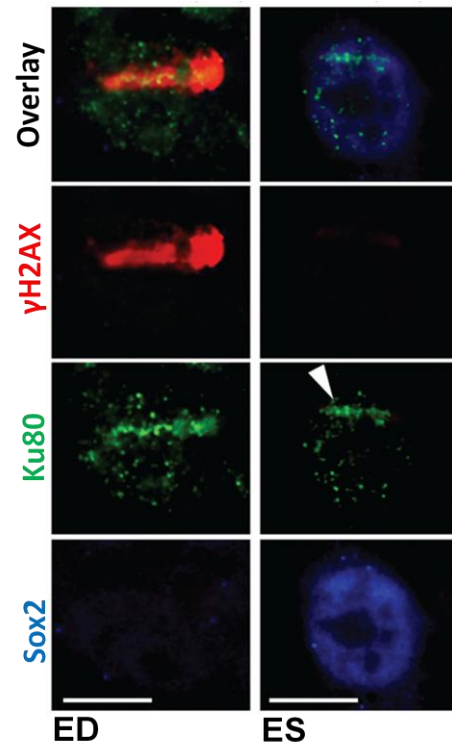


**Figure 3.18. Ku complex is recruited to DSBs in cultured stem cells.**

Immunofluorescence co-staining of Sox2 (blue),  $\gamma$ H2AX (red) and Ku80 (green) on co-plated ES and ED cells following microirradiation. Arrowhead indicates the presence of Ku80 despite attenuated induction of  $\gamma$ H2AX. Individual ES and ED pictures shown were irradiated together following co-plating. White scale bar, 10 $\mu$ m.

#### **3.4.4 IR-induced apoptosis in stem cells involves MST1-JNK-H2AX pathway**

While IR-induced apoptosis typically involves DDR signaling through ATM and p53<sup>14</sup>, stem cells underwent IR-induced apoptosis despite deficiencies in DDR signaling and DNA damage-induced apoptosis in stem cells has been shown to be p53-independent<sup>15</sup>. The ability of stem cells to apoptose despite the absence of DDR components was confirmed by observing apoptosis in the stem cell regions of DDR factor-deficient mice (Fig. 3.19). We therefore investigated potential alternative apoptotic pathways that could be active in stem cells. Once activated by caspase cleavage<sup>16</sup>, autophosphorylation<sup>17</sup> and subsequent nuclear translocation, mammalian Ste20-like kinase (MST1) pan-phosphorylates H2AX-S139 in addition to activating c-Jun N-terminal kinase (JNK)<sup>18</sup>, which can in turn also pan-phosphorylate H2AX-S139<sup>19</sup>. Despite the absence of  $\gamma$ H2AX IRIF in stem cells (Fig. 3.1, 3.3), by 6h post-irradiation they induced pan-nuclear H2AX S139 phosphorylation (H2AX-pS139) (Fig. 3.20 A-B). MST1 was phosphorylated only in stem cells following irradiation (Fig. 3.21), and pan-nuclear H2AX-pS139 signals colocalized with nuclear translocation of otherwise cytoplasmic MST1 in the SGZ at late timepoints (Fig. 3.22). Additionally, JNK was found to be activated through its phosphorylation (pJNK) only in stem cells at these late timepoints following irradiation both in culture (Fig. 3.21) and *in vivo* (Fig. 3.23 A-B). pJNK also co-stained with pan-nuclear H2AX-pS139 (Fig. 3.24) in the SGZ stem cell region. IR-induced apoptosis in stem cells therefore does not require DDR components and signals through the MST-JNK-H2AX pathway.

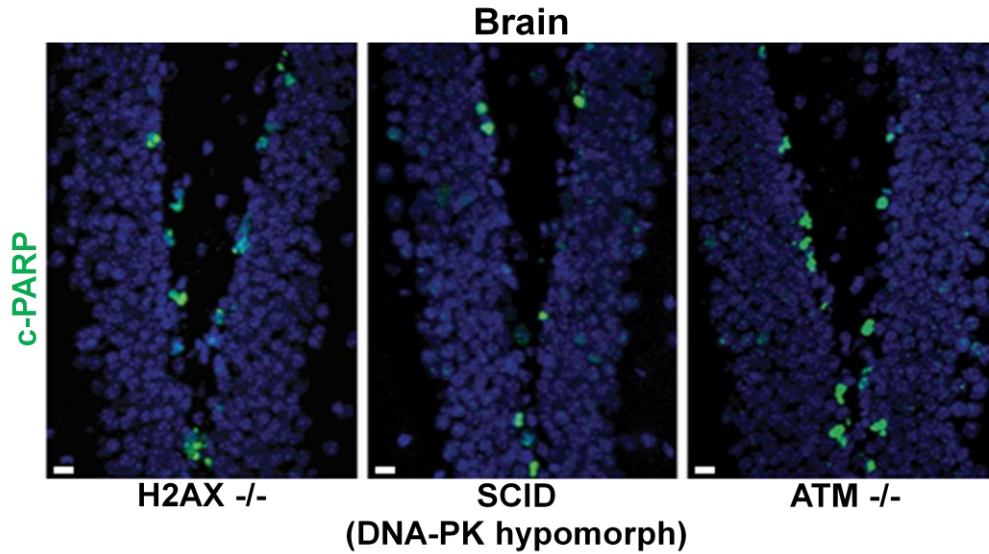


**Figure 3.19. Apoptosis in stem cell regions *in vivo* does not require DDR components.** Immunofluorescence staining of cleaved poly (ADP-ribose) polymerase (PARP) in H2AX *-/-*, SCID, and ATM *-/-* brain 6h following 6Gy IR. DAPI=DNA. White scale bars, 10 $\mu$ m.

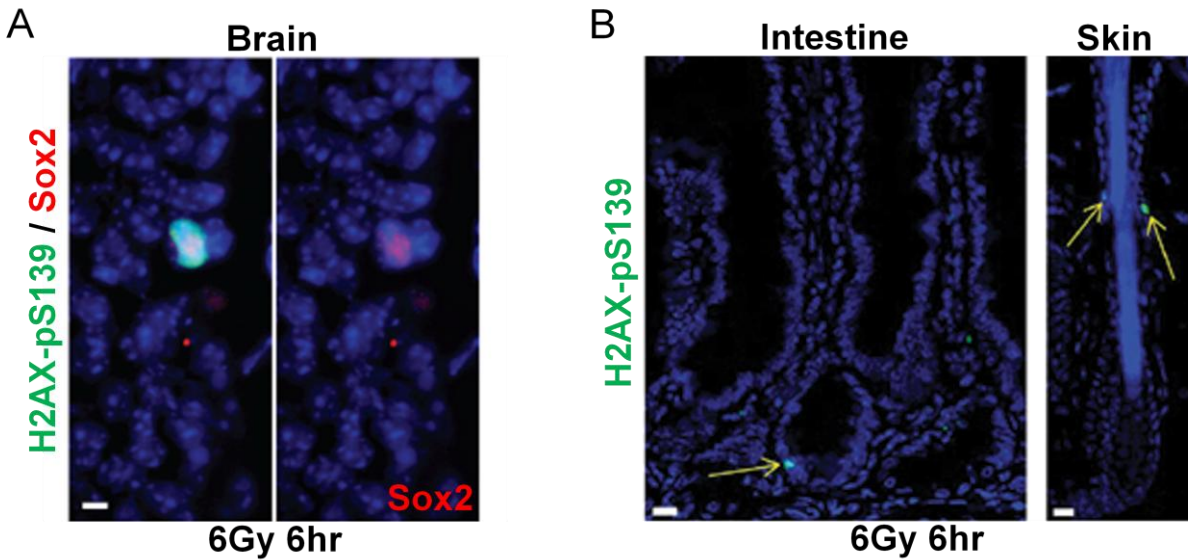


**Figure 3.20. Stem cells *in vivo* induce pan-nuclear H2AX-pS139 at late timepoints following irradiation.** (A) Immunofluorescence co-staining of Sox2 (red) and pan-nuclear H2AX-pS139 (green) in brain 6h following 6Gy IR. (B) Immunofluorescence staining of pan-nuclear H2AX-pS139 (green) in tissue niches 6h following 6Gy IR. Arrows indicate apoptotic H2AX-pS139 in stem cell regions. DAPI=DNA. White scale bars, 10 $\mu$ m.

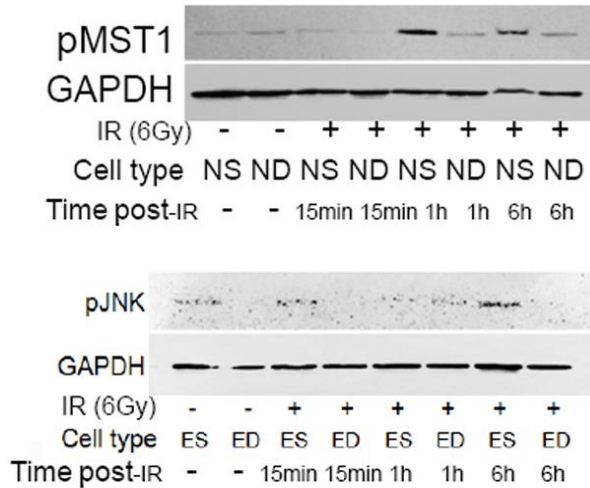


**Figure 3.21. MST1 and JNK are activated only in cultured stem cells at late timepoints following irradiation.** Western blots for pMST1 at various time points following mock or 6Gy irradiation of NS and ND cells along with western blots for pJNK at various time points following mock or 6Gy irradiation of ES and ED cells. GAPDH served as a loading control.

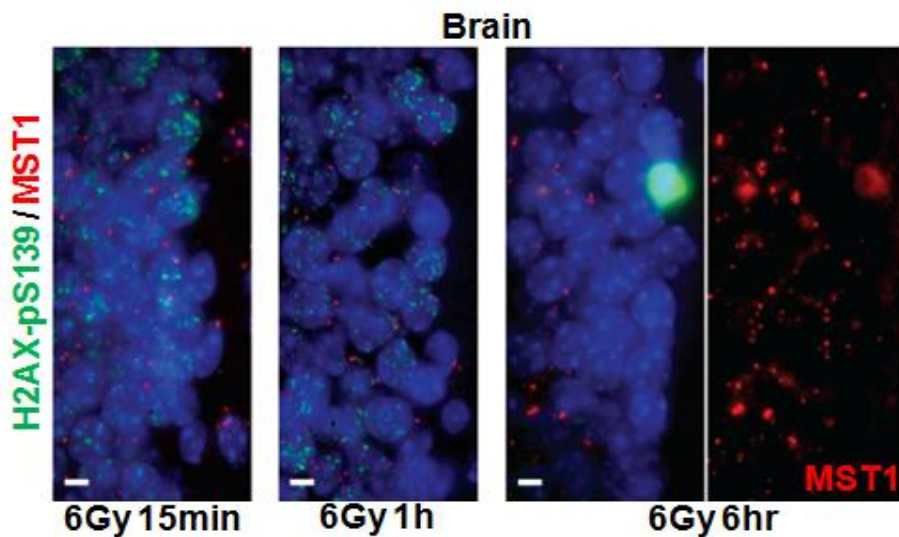


**Figure 3.22. MST1 is nuclear translocated correlating with the onset of H2AX-pS139 in stem cell regions.** Immunofluorescence co-staining of MST1 (red) and pan-nuclear H2AX-pS139 (green) in brain 15min, 1h and 6h following 6Gy IR. DAPI=DNA. White scale bars, 10µm.

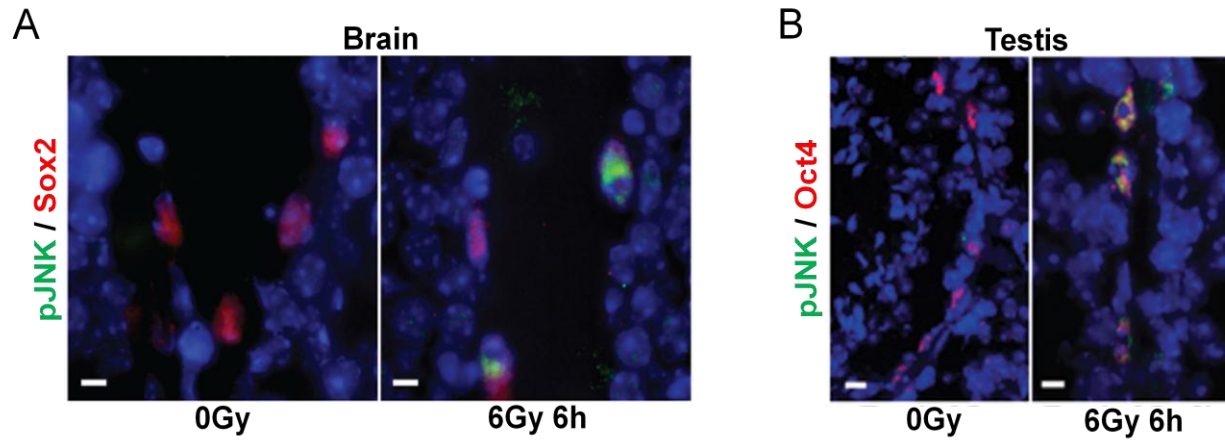


**Figure 3.23. pJNK is activated in stem cells *in vivo* at late timepoints following irradiation.**

Immunofluorescence co-staining of (A) pJNK (green) and Sox2 (red) in brain and (B) pJNK (green) and Oct4 (red) in testis 6h following either sham or 6Gy IR. DAPI=DNA. White scale bars, 10 $\mu$ m.

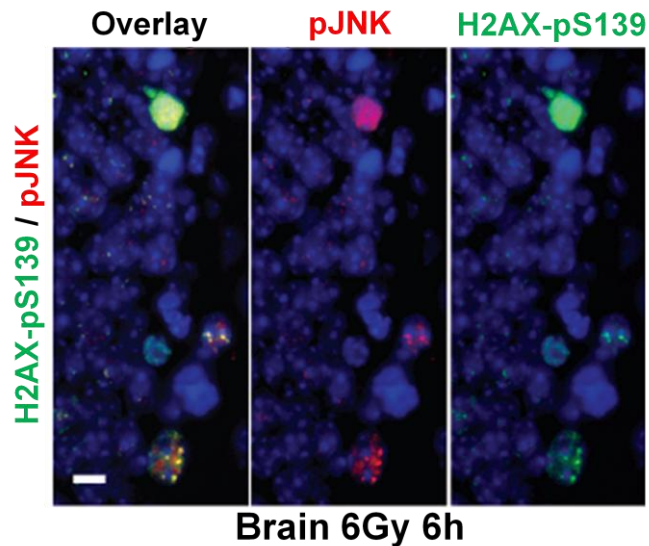


**Figure 3.24. pJNK colocalizes with H2AX-pS139 in stem cell regions.** Immunofluorescence co-staining of pJNK (red) and pan-nuclear H2AX-pS139 (green) in brain 6h following 6Gy IR. DAPI=DNA. White scale bar, 10 $\mu$ m.

### 3.5 DISCUSSION

This work demonstrates that normal stem cells *in vivo* as well as in culture exhibit an aberrant DDR and are deficient in repairing DNA DSBs compared with their isogenic differentiated non-stem progeny. Our most striking finding is the austere lack of IRIFs in stem cells, including pATM and  $\gamma$ H2AX. Stem cells therefore appear to be unique in their inability to activate the DDR, demonstrating stark heterogeneity in the molecular responses to DNA damage among cells of varying differentiation status. This suggests that not all cells respond similarly to DNA damage, challenging existing assumptions about the ubiquitous nature of the DDR and its generalizability to all cell types.

While stem cells are unable to induce IRIFs, they are able to sense DNA breaks through the recruitment of Nbs1 and Ku80, in agreement with previous studies demonstrating that MRN recruitment does not require H2AX or its phosphorylation<sup>20-22</sup>. The MRN complex is sufficient for promoting DNA repair independent of H2AX<sup>22,23</sup>, which may explain how stem cells are able to repair endogenous physiological levels of damage despite an attenuated DDR. The kinetics of DSB repair in stem cells are similar to H2AX<sup>-/-</sup> murine embryonic fibroblasts<sup>12</sup>, further indicating that stem cells are essentially a naturally-occurring DDR-null cell type. This similarity also causally links their attenuated DDR and muted DNA repair. Additionally, the radiosensitivity of ATM and H2AX-deficient cells has been attributed to their DSB repair defects<sup>24,25</sup>, suggesting that the inhibited DDR signaling and DSB repair capacity of stem cells may directly influence their radiosensitivity.

There are conflicting reports on the relative efficiency of cultured stem cells in repairing DNA damage<sup>26-31</sup>, and DDR activation in stem cells has also been observed by several groups<sup>11,32-34</sup>. However, many of these studies did not emphasize the use of early passage, primary cultures or isogenic direct differentiation as our study does, and prolonged passage of stem cells in culture results in epigenomic changes<sup>35</sup> that lead to modified radiation responses [unpublished observations]. Additionally, mouse and human ES cells appear to differ in their radiation responses<sup>36</sup>. In agreement with our studies, murine ES cells (albeit not human ES cells) have been reported as deficient in repairing DNA breaks<sup>36</sup> and murine induced pluripotent stem cells have recently been found to exhibit inadequate H2AX phosphorylation and

DNA repair<sup>37</sup>. Unirradiated ES cell lines have been found to exhibit high basal  $\gamma$ H2AX levels that are believed to be important for self-renewal<sup>38</sup>, but this basal  $\gamma$ H2AX appears to be independent of DDR signaling<sup>39</sup>. These discrepancies also reinforce the significance of corroborating work with *in vivo* tissue niches when possible, as was done in our study.

Studies on intestinal crypts<sup>40,41</sup> have observed the presence of IRIFs in stem cells but also demonstrated IR-induced cell death in those same cells. Stem cells within the hair follicle have been shown to sufficiently activate the DDR<sup>42</sup>, however it appears that the hair follicle may contain distinct stem cell populations<sup>43</sup> with varying biological radiation responses. Our observations in testicular stem cells agree with previous studies showing abrogated  $\gamma$ H2AX induction following IR<sup>44</sup> (however again with contradictory radiosensitivity data). Variability among this data is likely due to the presence of different stem cell populations within these niches as well as developmental heterogeneity related to the continual turnover of each tissue compartment. All of our work on brain stem cells is novel, as radiation responses in brain have only been previously studied in a developmental context without the use of specific stem cell markers<sup>45,46</sup>.

While ED cells appear to arrest at both G1 and G2 checkpoints after irradiation, ES cells accumulate in G2, suggesting a lack of G1 checkpoint activation and subsequent arrest. This result agrees with existing reports suggesting that stem cells lack a functional G1 checkpoint<sup>11,15,47</sup>, which is in part due to both a nonfunctional p21 pathway<sup>48</sup> and improper Chk2 localization<sup>49</sup>. Restoration of the G1 checkpoint has been shown to significantly reduce IR-induced apoptosis<sup>50,51</sup>, supporting the idea that an absent G1 checkpoint may contribute to stem cell hypersensitivity. The length of IR-induced G2 arrest among cells typically correlates with cell cycle time<sup>52</sup>. ES cells do not have a substantially longer cell cycle than ED cells however, yet employ a unique cell cycle response to radiation. ES cells rapidly activated IR-induced G2/M arrest similar to ED cells, however ED cells showed a much more gradual release from arrest. This shortened length of G2/M arrest in stem cells is likely due to their reduced activation of ATR and Chk1<sup>10,53,54</sup>. We also cannot ignore the possibility that by later timepoints many radiosensitive stem cells may have already died, whereby the observed restoration of the basal mitotic ratio merely represents an

artifact of the remaining survivor population. Interestingly, while the length of G2/M entry delay among different cell types following DNA damage-induced S-phase arrest may directly correlate with radiosensitivity<sup>55</sup>, the relationship between G2/M arrest and radiosensitivity is less clear<sup>56</sup>. Nonetheless, reduced length of G2/M arrest in stem cells may hamper proper completion of DNA repair and limited evidence does correlate reduced G2/M arrest with radiosensitivity, especially in cells already lacking G1 arrest<sup>57,58</sup>.

We observed apoptotic signaling through the JNK-MST1-H2AX pathway only in stem cells both in culture and *in vivo*. While MST1 activation was a downstream result of apoptosis signaling, evidence suggests that it may also directly promote apoptosis by blocking Bcl-xL<sup>59</sup>. MST1-mediated H2AX pan-phosphorylation at S139 is required for completion of apoptosis through DNA fragmentation<sup>16,19</sup>. Our work suggests that stem cells do not require DDR signaling for apoptosis, in agreement with another report which found that ATM deficiency only prevented IR-induced apoptosis in differentiated neuronal cells while stem cells remained radiosensitive<sup>60</sup>. The JNK-MST1-H2AX pathway may represent an alternative mechanism for IR-induced apoptosis in the absence of DDR signaling. The observation of apoptosis in H2AX<sup>-/-</sup> cells suggests that other pathways may also be active in stem cells, however H2AX-pS139 is only involved in the final “clean-up” stages of apoptosis<sup>19</sup> so upstream signaling would not be affected. It is interesting that apoptotic pan-nuclear phosphorylation of S139 occurs in stem cells, despite abrogated  $\gamma$ H2AX (ATM-mediated S139 phosphorylation around DNA break sites) immediately following DNA damage. We submit that chromatin changes induced by the onset of apoptosis may allow access to the break site and thus enable pan-nuclear S139 phosphorylation.

One may wonder how stem cells would have developed such a radiosensitive phenotype. While the decision by stem cells to undergo apoptosis in response to IR in lieu of repairing the DNA damage may be an adaptive response, wherein the long-term genomic integrity of the lineage is protected by removing damaged stem cells, these radiation responses may also be merely a coincidence of their distinctive chromatin environment and epigenetic profile. Regardless, these findings provide novel insights in the

fields of DDR and normal stem cell biology, while also identifying potential new molecular targets for preventing stem cell depletion associated with radiotherapy.

### 3.6 REFERENCES

1. Jackson, S. P. & Bartek, J. The DNA-damage response in human biology and disease. *Nature* **461**, 1071–1078 (2009).
2. Lee, J.-H. & Paull, T. T. Activation and regulation of ATM kinase activity in response to DNA double-strand breaks. *Oncogene* **26**, 7741–8 (2007).
3. Uziel, T. *et al.* Requirement of the MRN complex for ATM activation by DNA damage. *EMBO J.* **22**, 5612–21 (2003).
4. Stiff, T. *et al.* ATM and DNA-PK function redundantly to phosphorylate H2AX after exposure to ionizing radiation. *Cancer Res.* **64**, 2390–6 (2004).
5. Burma, S., Chen, B. P., Murphy, M., Kurimasa, A. & Chen, D. J. ATM phosphorylates histone H2AX in response to DNA double-strand breaks. *J. Biol. Chem.* **276**, 42462–7 (2001).
6. Paull, T. T. *et al.* A critical role for histone H2AX in recruitment of repair factors to nuclear foci after DNA damage. *Curr. Biol.* **10**, 886–95 (2000).
7. Bakkenist, C. J. & Kastan, M. B. DNA damage activates ATM through intermolecular autophosphorylation and dimer dissociation. *Nature* **421**, 499–506 (2003).
8. Liu, S. *et al.* ATR autophosphorylation as a molecular switch for checkpoint activation. *Mol. Cell* **43**, 192–202 (2011).
9. Chen, B. P. C. *et al.* Cell cycle dependence of DNA-dependent protein kinase phosphorylation in response to DNA double strand breaks. *J. Biol. Chem.* **280**, 14709–15 (2005).
10. Liu, Q. *et al.* Chk1 is an essential kinase that is regulated by Atr and required for the G2/M DNA damage checkpoint. *Genes & Dev.* **14**, 1448–1459 (2000).
11. Momcilović, O. *et al.* Ionizing radiation induces ataxia telangiectasia mutated-dependent checkpoint signaling and G(2) but not G(1) cell cycle arrest in pluripotent human embryonic stem cells. *Stem Cells* **27**, 1822–35 (2009).
12. Celeste, A. *et al.* Genomic instability in mice lacking histone H2AX. *Science* **296**, 922–7 (2002).
13. Koike, M. & Koike, A. Accumulation of Ku80 proteins at DNA double-strand breaks in living cells. *Exp. Cell Res.* **314**, 1061–1070 (2008).
14. Norbury, C. J. & Zivnotovsky, B. DNA damage-induced apoptosis. *Oncogene* **23**, 2797–808 (2004).
15. Aladjem, M. I. *et al.* ES cells do not activate p53-dependent stress responses and undergo p53-independent apoptosis in response to DNA damage. *Curr Biol* **8**, 145–155 (1998).

16. Wen, W. *et al.* MST1 promotes apoptosis through phosphorylation of histone H2AX. *J Biol Chem* **285**, 39108–39116 (2010).
17. Praskova, M., Khoklatchev, A., Ortiz-Vega, S. & Avruch, J. Regulation of the MST1 kinase by autophosphorylation, by the growth inhibitory proteins, RASSF1 and NORE1, and by Ras. *Biochem. J.* **381**, 453–62 (2004).
18. Ura, S., Nishina, H., Gotoh, Y. & Katada, T. Activation of the c-Jun N-terminal kinase pathway by MST1 is essential and sufficient for the induction of chromatin condensation during apoptosis. *Mol. Cell. Biol.* **27**, 5514–22 (2007).
19. Lu, C. *et al.* Cell apoptosis: requirement of H2AX in DNA ladder formation, but not for the activation of caspase-3. *Mol. Cell* **23**, 121–32 (2006).
20. Soutoglou, E. & Misteli, T. Activation of the cellular DNA damage response in the absence of DNA lesions. *Science* **320**, 1507–10 (2008).
21. Celeste, A. *et al.* Histone H2AX phosphorylation is dispensable for the initial recognition of DNA breaks. *Nat. Cell Biol.* **5**, 675–9 (2003).
22. Yuan, J. & Chen, J. MRE11-RAD50-NBS1 complex dictates DNA repair independent of H2AX. *J. Biol. Chem.* **285**, 1097–104 (2010).
23. Xie, A., Kwok, A. & Scully, R. Role of mammalian Mre11 in classical and alternative nonhomologous end joining. *Nat. Struct. Mol. Biol.* **16**, 814–8 (2009).
24. Kühne, M. *et al.* A double-strand break repair defect in ATM-deficient cells contributes to radiosensitivity. *Cancer Res.* **64**, 500–8 (2004).
25. Riballo, E. *et al.* A pathway of double-strand break rejoining dependent upon ATM, Artemis, and proteins locating to gamma-H2AX foci. *Mol. Cell* **16**, 715–24 (2004).
26. Tichy, E. D. *et al.* Mouse embryonic stem cells, but not somatic cells, predominantly use homologous recombination to repair double-strand DNA breaks. *Stem Cells Dev.* **19**, 1699–711 (2010).
27. Adams, B. R., Hawkins, A. J., Povirk, L. F. & Valerie, K. ATM-independent, high-fidelity nonhomologous end joining predominates in human embryonic stem cells. *Aging (Albany NY)* **2**, 582–596 (2010).
28. Saretzki, G., Armstrong, L. & Leake, A. Stress defense in murine embryonic stem cells is superior to that of various differentiated murine cells. *Stem Cells* 962–971 (2004). at <<http://onlinelibrary.wiley.com/doi/10.1634/stemcells.22-6-962/full>>
29. Maynard, S., Swistowska, A., Lee, J. & Liu, Y. Human embryonic stem cells have enhanced repair of multiple forms of DNA damage. *Stem Cells* 2266–2274 (2008). doi:10.1634/stem-cells.2007-1041
30. Lan, M. L. *et al.* Characterizing the Radioresponse of Pluripotent and Multipotent Human Stem Cells. *PLoS One* **7**, e50048 (2012).
31. Wyles, S. P., Brandt, E. B. & Nelson, T. J. Stem Cells: The Pursuit of Genomic Stability. *Int. J. Mol. Sci.* **15**, 20948–20967 (2014).

32. Chuykin, I. A., Lianguzova, M. S., Pospelova, T. V & Pospelov, V. A. Activation of DNA damage response signaling in mouse embryonic stem cells. *Cell Cycle* 2922–2928 (2008).
33. Acharya, M. M. *et al.* Consequences of ionizing radiation-induced damage in human neural stem cells. *Free Radic. Biol. Med.* **49**, 1846–1855 (2010).
34. Schneider, L., Fumagalli, M. & d'Adda di Fagagna, F. Terminally differentiated astrocytes lack DNA damage response signaling and are radioresistant but retain DNA repair proficiency. *Cell Death Differ.* 1–10 (2011). doi:10.1038/cdd.2011.129
35. Diaz Perez, S. V *et al.* Derivation of new human embryonic stem cell lines reveals rapid epigenetic progression in vitro that can be prevented by chemical modification of chromatin. *Hum. Mol. Genet.* **21**, 751–64 (2012).
36. Bañuelos, C. a *et al.* Mouse but not human embryonic stem cells are deficient in rejoining of ionizing radiation-induced DNA double-strand breaks. *DNA Repair (Amst)*. **7**, 1471–83 (2008).
37. Zhang, M., Yang, C., Liu, H. & Sun, Y. Induced Pluripotent Stem Cells Are Sensitive to DNA Damage. *Genomics. Proteomics Bioinformatics* (2013). doi:10.1016/j.gpb.2013.09.006
38. Turinetto, V. *et al.* High basal  $\gamma$ H2AX levels sustain self-renewal of mouse embryonic and induced pluripotent stem cells. *Stem Cells* **30**, 1414–23 (2012).
39. Banáth, J. P. *et al.* Explanation for excessive DNA single-strand breaks and endogenous repair foci in pluripotent mouse embryonic stem cells. *Exp. Cell Res.* **315**, 1505–20 (2009).
40. Hua, G. *et al.* Crypt Base Columnar Stem Cells in Small Intestines of Mice are Radioresistant. *Gastroenterology* (2012). doi:10.1053/j.gastro.2012.07.106
41. Wang, F. *et al.* P53-participated cellular and molecular responses to irradiation are cell differentiation-determined in murine intestinal epithelium. *Arch. Biochem. Biophys.* **542**, 21–7 (2014).
42. Sotiropoulou, P. A. *et al.* Bcl-2 and accelerated DNA repair mediates resistance of hair follicle bulge stem cells to DNA-damage-induced cell death. *Nat Cell Biol* **12**, 572–582 (2010).
43. Li, L. & Clevers, H. Coexistence of quiescent and active adult stem cells in mammals. *Science* **327**, 542–5 (2010).
44. Rube, C. E., Zhang, S., Miebach, N., Fricke, A. & Rube, C. Protecting the heritable genome: DNA damage response mechanisms in spermatogonial stem cells. *DNA Repair (Amst)*. **10**, 159–68 (2011).
45. Tanori, M. *et al.* Developmental and oncogenic radiation effects on neural stem cells and their differentiating progeny in mouse cerebellum. *Stem Cells* **31**, 2506–16 (2013).
46. Gatz, S. A. *et al.* Requirement for DNA ligase IV during embryonic neuronal development. *J. Neurosci.* **31**, 10088–100 (2011).
47. Etienne, O. & Roque, T. Variation of radiation-sensitivity of neural stem and progenitor cell populations within the developing mouse brain. *Int. J. ...* **88**, 694–702 (2012).

48. Roque, T. *et al.* Lack of a p21(waf1/cip) -Dependent G1/S Checkpoint in Neural Stem and Progenitor Cells After DNA Damage in vivo. *Stem Cells* (2011). doi:10.1002/stem.1010
49. Suvorova, I. I., Katolikova, N. V & Pospelov, V. a. New insights into cell cycle regulation and DNA damage response in embryonic stem cells. *Int. Rev. Cell Mol. Biol.* **299**, 161–98 (2012).
50. Hong, Y. & Stambrook, P. J. Restoration of an absent G 1 arrest and protection from apoptosis in embryonic stem cells after ionizing radiation. *Proc Natl Acad Sci U S A* **101**, 14443–14448 (2004).
51. Hong, Y., Cervantes, R. B., Tichy, E., Tischfield, J. A. & Stambrook, P. J. Protecting genomic integrity in somatic cells and embryonic stem cells. *Mutat Res* **614**, 48–55 (2007).
52. Denekamp, J. Cell kinetics and radiation biology. *Int. J. Radiat. Biol. Relat. Stud. Phys. Chem. Med.* **49**, 357–80 (1986).
53. Lossaint, G., Besnard, E., Fisher, D., Piette, J. & Dulić, V. Chk1 is dispensable for G2 arrest in response to sustained DNA damage when the ATM/p53/p21 pathway is functional. *Oncogene* **30**, 4261–74 (2011).
54. Shaltiel, I. a, Krenning, L., Bruinsma, W. & Medema, R. H. The same, only different - DNA damage checkpoints and their reversal throughout the cell cycle. *J. Cell Sci.* **2**, 607–620 (2015).
55. Nagasawa, H., Keng, P., Harley, R., Dahlberg, W. & Little, J. B. Relationship between  $\gamma$ -ray-induced G 2 /M Delay and Cellular Radiosensitivity. *Int. J. Radiat. Biol.* **66**, 373–379 (1994).
56. Perez, A., Grabenbauer, G. G., Sprung, C. N., Sauer, R. & Distel, L. V. R. Potential for the G2/M arrest assay to predict patient susceptibility to severe reactions following radiotherapy. *Strahlenther. Onkol.* **183**, 99–106 (2007).
57. Tamamoto, T. *et al.* Correlation between gamma-ray-induced G2 arrest and radioresistance in two human cancer cells. *Int. J. Radiat. Oncol. Biol. Phys.* **44**, 905–9 (1999).
58. Russell, K. J. *et al.* Abrogation of the G2 Checkpoint Results in Differential Radiosensitization of G1 Checkpoint-deficient and G1 Checkpoint-competent Cells. *Cancer Res.* **55**, 1639–1642 (1995).
59. Del Re, D. P. *et al.* Mst1 Promotes Cardiac Myocyte Apoptosis through Phosphorylation and Inhibition of Bcl-xL. *Mol. Cell* **54**, 639–50 (2014).
60. Lee, Y., Chong, M. J. & McKinnon, P. J. Ataxia telangiectasia mutated-dependent apoptosis after genotoxic stress in the developing nervous system is determined by cellular differentiation status. *J. Neurosci.* **21**, 6687–93 (2001).

## **CHAPTER 4**

---

# **Unique Epigenetic Regulation Contributes to Stem Cell Radiosensitivity**

## 4.1 ABSTRACT

Our work has shown that stem cells are uniquely hypersensitive to IR, readily undergoing IR-induced apoptosis and failing to sufficiently activate DNA repair signaling pathways. Stem cells exhibit an attenuated DNA Damage Response (DDR), which leads to diminished DNA repair capacity and DDR-independent apoptosis. Various histone modifications have been implicated as playing an important role in the molecular responses to DNA damage. Since stem cell pluripotency is controlled by several uniquely regulated histone modifications, we investigated whether the distinctive epigenetic environment of stem cells could contribute to their radiosensitivity and abrogated DDR. We found that IR-induced apoptosis in stem cells corresponds to the persistence of H2AX-Y142 phosphorylation around break sites, which promotes apoptosis through JNK while inhibiting DDR signaling. The abrogated DDR in stem cells is also associated with constitutively elevated histone-3 lysine-56 acetylation, which may hinder retention of repair factors and directly contributes to stem cell radiosensitivity. These data establish that unique epigenetic landscapes among differing cell types can impart heterogeneity in the DDR, resulting in varying radiosensitivities.

## 4.2 METHODS

### 4.2.1 Stem Cell Culture and Differentiation:

Normal embryonic stem (ES) cells were freshly isolated directly from the inner cell mass of blastocyst stage mouse embryos (E4.5), and later procured from the Washington University Embryonic Stem Cell Core Facility or ATCC as karyotypically normal early passage ES cells (EDJ22, RW4). Cells were grown feeder-free on gelatin-coated plates and maintained in high glucose DMEM with HEPES (Invitrogen) containing 10% Fetal Bovine Serum (Invitrogen), 10% Newborn Calf Serum (Invitrogen), 0.2% beta-mercaptoethanol (Invitrogen), a nucleoside mix containing final concentrations of 80µg/ml adenosine, 85µg/ml guanosine, 73µg/ml cytidine, 73µg/ml uridine and 24µg/ml thymidine (Sigma Aldrich) and 10ng/ml LIF (Invitrogen). ES cells were passaged with 0.05% trypsin containing 0.53mM EDTA (Invitrogen) and selective isolation of independent colonies from any differentiated cells present. They were differentiated by culture

in the absence of LIF for several days. ES cells were tested bi-monthly for mycoplasma contamination.

Neural stem cells were freshly isolated by dissecting the hippocampal region of brains from P0-P2 mouse pups and were cultured in suspension after dissociation and trituration in AB2 Basal Neural Medium (Aruna Biomedical) containing 20ng/ml EGF, 10ng/ml bFGF, 1% N2-Supplement and 2% B27 (Invitrogen). Neural stem cells were differentiated by addition of 10% FBS (Hyclone) and removal of EGF/FGF from culture medium upon plating into tissue culture-treated dishes for attachment.

#### 4.2.2 Animal Models:

Mouse strain C57BL/6 was used for all animal studies. Adult 6-8 week old males were utilized for harvest of brain, intestine, skin and testis for sectioning. For breeding, 1-6 month old male and female mice of similar age were allowed to mate continuously, with pregnant females isolated independently before giving birth. P0-P2 mouse pups were sacrificed by rapid decapitation prior to dissection for neural stem cell isolation. Procedures for all studies were been approved by the Animal Studies Committee at Washington University Medical Center.

#### 4.2.3 Antibodies

Details of the antibodies used in this work are described in Table 4.1.

**Table 4.1. Antibody Information Table**

Protein Target	Species	Company	Catalog #	Assay	Conditions
Acetylated Histone 3 (K56)	rabbit	Millipore	04-1135	IF, IHC-F	1:250, 1:100
Histone H2AX	rabbit	Cell Signaling	#7631	IF, WB	1:150, 1:2000 in BSA
Histone H3	rabbit	Cell Signaling	#4499	IF	1:250
phospho-H2AX (Y142)	rabbit	Abcam	ab9045	IF, WB	1:200, 1:2000
Sox2	rabbit	Abcam	ab7959	IHC-F	1:100
Sox2	mouse	Abcam	ab79351	IF, IHC-F	1:200, 1:100
γH2AX (S139)	mouse	Millipore	05-636	WB, IHC-F	1:4000 in BSA, 1:400
γH2AX (S139)	rabbit	Cell Signaling	#7631	IHC-F	1:150

p300	rabbit	Santa Cruz		WB	1:4000 in milk
GAPDH	mouse	Sigma Aldrich	G8795	WB	1:100,000 in milk
FITC-conjugated anti-rabbit	donkey	Vector	FI-1000	IF, IHC-F	1:100
FITC-conjugated anti-mouse	horse	Vector	FI-2000	IF, IHC-F	1:100
AMCA-conjugated anti-mouse	horse	Vector	CI-2000	IF	1:75
AMCA-conjugated anti-rabbit	donkey	Vector	CI-1000	IF	1:75
Texas Red-conjugated anti-mouse	horse	Vector	TI-2000	IF, IHC-F	1:100
Texas Red-conjugated anti-rabbit	donkey	Vector	TI-1000	IF, IHC-F	1:100
HRP-conjugated anti-mouse	rabbit	Sigma Aldrich	A9044	WB	1:5000 in milk
HRP-conjugated anti-rabbit	goat	Sigma Aldrich	A0545	WB	1:5000 in milk

#### 4.2.4 X-Ray Irradiation and Tissue Sectioning:

Cells and animals were irradiated in the RS-2000 Biological Research Irradiator (Rad-Source) at room temperature, with mock/control irradiated samples brought into the room to simulate the reduction in ambient temperature and account for any stress imparted by the travel. Cells were always placed within the central circle directly under the x-ray source to maintain consistency in dose between samples. Animals were anesthetized with isoflurane and placed on their back in the machine for whole-body irradiation to properly expose all tissues of interest to the x-ray source. Accuracy of all doses was confirmed by dosimeter probe. Both cells and animals were randomly assigned to individual timepoints or sham-irradiation controls.

Following irradiation, mice were sacrificed at specific timepoints by CO<sub>2</sub> asphyxiation and cervical dislocation. Organs were harvested, placed in OCT media and frozen in liquid nitrogen. Frozen tissues were sectioned on a cryostat machine at a thickness of 10µm, placed onto adhesive slides and stored at -80°C.

#### **4.2.5 Western Blotting:**

Cellular protein lysates were collected in RIPA buffer, electrophoresed on 4-15% Tris-Glycine polyacrylamide gels (BioRad), transferred onto PVDF membranes and incubated overnight at 4°C with various primary antibodies followed by washing and secondary antibody incubation for 2hr at room temperature. Super ECL (GE/Pierce) was used as substrate for detection on autoradiography film or ChemiDoc MP digital system (BioRad).

#### **4.2.6 Immunofluorescence:**

Freshly frozen tissues were isolated from testis, brain, intestine and skin following 6Gy irradiation or 0Gy mock before embedding in OCT media and sectioning onto slides. Slides of tissue sections or coverslips of cells were fixed in 4% formaldehyde and permeabilized with 0.2% Triton-X followed by blocking with 2% BSA. Tissues were incubated with primary antibodies in 1% BSA at 37°C for 3hr, washed and then incubated with secondary fluorescently-tagged secondary antibodies for 45min at 37°C. Tissues were then mounted in place with coverslips containing mounting media with DAPI (Vector) for identification of nuclei.

Cells were similarly fixed in 4% formaldehyde and permeabilized with 0.2% Triton-X before blocking. For double-color staining, primary antibodies were incubated together for 1hr at 37°C followed by wash and incubation with fluorescently-tagged secondary antibodies for 30min at 37°C. For triple-color staining, following the original staining procedure, cells were incubated with 1:1000  $\alpha$ - $\gamma$ H2AX antibody for 15min at 37°C followed by 12min incubation at 37°C with the appropriate secondary antibody. Anti  $\gamma$ H2AX antibody was chosen to match Sox2 to avoid cross-reaction with the other target antigen of interest.

#### **4.2.7 p300 siRNA Transfection and Molecular Inhibition**

For each sample. 563nM mouse EP300 or non-targeting control siGENOME SMARTpool siRNA (Dharmacon) was incubated together with 3.75% RNAiMAX lipofectamine transfection reagent (Invitrogen) in Opti-MEM media (Invitrogen) for 5min. siRNA complex was added to cells and

incubated in media without any antibiotic for 16h prior to irradiation, at a final concentration of 51.2nM siRNA. For pharmacological inhibition of H3K56ac, bromodomain inhibitor I-CBP112 (Cayman Chemical) was incubated with cells at a final concentration of 5 $\mu$ M prior to irradiation and washed from cells 30min later (unless cells were harvested earlier).

#### **4.2.8 Neutral Comet Assay:**

To assess repair of DNA double strand breaks, neutral comet assays were performed using CometSlide assay kits (Trevigen). Cells were collected at multiple timepoints following 6 Gy irradiation or 0 Gy mock and embedded in agarose on slides at equal concentrations. Slides were electrophoresed in TAE buffer, fluorescently stained with SYBR Green (Trevigen), and visualized by fluorescent microscopy. Olive comet moment was calculated using the CometScore software (TriTek) to analyze 50-100 comets per sample, with each series of timepoints repeated at least three independent times as both biological and technical replicates. Individual comets were randomly selected for scoring from similar regions of the slide in all samples. Outliers were eliminated that fell greater than 1.5 standard deviations from the mean. Standard error was calculated for each cell type and timepoint normalized to the value of the 0min samples, while the significance of the difference between cell types over time was analyzed by Analysis of Covariance (ANCOVA) using XLStat statistical software (Addinsoft), with two-sided significance set at  $p < 0.05$ . Data from all samples was approximately normally distributed, and the standard deviation between samples within the same experiment was similar. Samples were excluded from analysis only due to technical errors from the assay or cells being visibly unhealthy.

#### **4.2.9 Laser Microirradiation**

Stem cells (ES, NS) were co-plated with non-stem cells (ED, MEF) on glass coverslips and incubated for 2 days with 30 $\mu$ M BrdU (Sigma Aldrich) to sensitize DNA for DSB induction. Prior to laser microirradiation, cells were incubated with Stem Cell cDy1 Dye (Active Motif) for 30min to fluorescently label live stem cells for identification. Coverslips were then placed in circular magnetic chambers (Quorum Technologies) with media to be properly aligned for

microirradiation. Cells were microirradiated in a defined narrow region across adjacent stem and non-stem cells with 8000-12000 iterations of 405+633nm laser on the LSM 510 Confocal Microscope (Zeiss) at 45% power output. Care was taken to include stem (cDy1 positive) as well as non-stem cells in the DNA damage tracks. Cells were microirradiated for 20-30min per sample unless otherwise stated, with 6-12 regions of microirradiation per sample.

### **3.2.10 Microscopy and Image Processing**

Micrographs were captured utilizing MetaSystems ISIS imaging software on Zeiss Axioplan2 microscope or ZEN software on Zeiss LSM510 confocal microscope with the 20x, 63x or 100x objective lenses. Minimal threshold and contrast manipulation was performed equally across entire images. Controls were processed equally with treated samples. Adobe Photoshop CS3 software was utilized for composing the collages of multiple pictures and labeling micrographs and Immunoblots in individual layers.

### **3.2.11 Statistical Analysis**

A 'two-tailed' Student's *t*-test was used to calculate the statistical significance of the observed differences. In all cases, differences were considered statistically significant when  $p < 0.05$ .

Unless otherwise indicated, values represent mean  $\pm$  SEM.

## **4.3 INTRODUCTION**

Chromosomal DNA is tightly wrapped around histone proteins to package and organize DNA into chromatin. Because DNA is so tightly bound by histones, their presence controls DNA access for biological processes such as DNA replication, gene transcription and DNA repair<sup>1</sup>. Histone modifications are often generalized into broad roles, promoting either the loosening or tightening of chromatin in order to encourage or repress nucleoprotein binding. Acetylation of lysine residues generally loosens chromatin by neutralizing the ionic charge between DNA and histones, while lysine methylations can be either activating or repressive depending on the specific residue. In addition to their broad cumulative effects on chromatin density, individual histone modifications have their own specific functions. Specific histone

modifications can serve as binding sites for recruiting proteins to DNA and controlling chromatin organization, depending on the geographical context of the residue. This series of specific functional modifications is known as the “histone code”<sup>2</sup>.

In addition to controlling DNA replication and gene transcription, many of these histone modifications are extremely important for a functioning DNA Damage Response (DDR) and effective DNA repair<sup>3,4</sup>. Histone modifications are involved in every step of the DDR, from chromatin opening to signaling and restoration of the basal state. While numerous histone modifications have been implicated in a broad range of DDR processes<sup>5</sup>, much is still unknown about the complexity of chromatin dynamics in response to DNA damage and during DNA repair. Additionally, all that is known about the epigenetics of the DDR comes from studies on cancer cells or transformed differentiated cells. To our knowledge there have not been any studies performed investigating the influence of particular histone modifications on the cellular response to DNA damage in stem cells. Stem cell pluripotency is regulated by unique chromatin organization along with distinctive expression of various histone modifications<sup>6-9</sup>. It is very likely that these same epigenetic marks which dictate gene expression also influence DNA access for repair factors and DDR signaling components.

We established in previous chapters that normal stem cells exhibit a severely attenuated DDR resulting in insufficient DNA repair and promoting ionizing radiation (IR)-induced apoptosis. Here we examine the association between these radiation responses and unique epigenetic regulation. H2AX Y142 phosphorylation status has been shown to influence cellular DNA damage sensitivity and the DDR<sup>10-12</sup>, and we demonstrate that failure to dephosphorylate H2AX Y142 around break sites in stem cells is strongly related to their radiosensitive phenotype. Moreover, the diminished DDR in stem cells is also associated with enhanced constitutive acetylation of histone 3 lysine 56 (H3K56ac), an epigenetic mark that may hinder the binding and retention of repair factors around double-strand breaks (DSBs)<sup>13,14</sup>. Reduction of H3K56ac through knockdown and inhibition of the acetyltransferase p300 protected stem cells from IR-induced apoptosis and restored DDR signaling. Our findings therefore indicate that stem cells exhibit an attenuated DDR through a unique regulation of chromatin structure. We deduce that

pluralistic epigenetic mechanisms act in concert to impede the DDR in normal stem cells, thus promoting their radiosensitivity.

## 4.4 RESULTS

### 4.4.1 DDR attenuation in stem cells is associated with a failure to dephosphorylate H2AX Y142 following DNA damage

Tyrosine 142 (Y142) of histone H2AX is constitutively maintained in a phosphorylated state in chromatin, but dephosphorylation of H2AX-pY142 upon DNA damage has been determined to be required for recruitment of mediator of DNA damage checkpoint protein 1 (MDC1) to nearby H2AX-pS139 ( $\gamma$ H2AX) and subsequent downstream DDR signaling<sup>10,15</sup>. In the absence of Y142 dephosphorylation, DDR signaling is blocked while apoptotic signaling is activated through binding of JNK<sup>14</sup>. We therefore investigated if the selective activation of apoptosis coincident with an attenuated DDR in stem cells could be explained by unique regulation of H2AX Y142 phosphorylation. The presence of H2AX-pY142 was found mutually exclusive from  $\gamma$ H2AX-labeled microirradiation tracks of DNA damage in differentiated non-stem cells, while Y142 remained prominently phosphorylated in stem cells where  $\gamma$ H2AX was abrogated (Fig. 4.1 A-B). Immunoblotting also confirmed that Y142 is dephosphorylated at the break sites only in non-stem cells following IR (Fig. 4.2) MDC1 was also found not to be recruited to the tracks of DNA damage in stem cells (Fig. 4.3A) and H2AX-pY142 was absent from MDC1-labeled tracks only in non-stem cells (Fig. 4.3B). These data surmise that stem cells are primed to apoptose in lieu of DNA repair signaling by the maintenance of constitutive H2AX Y142 phosphorylation following DNA damage.

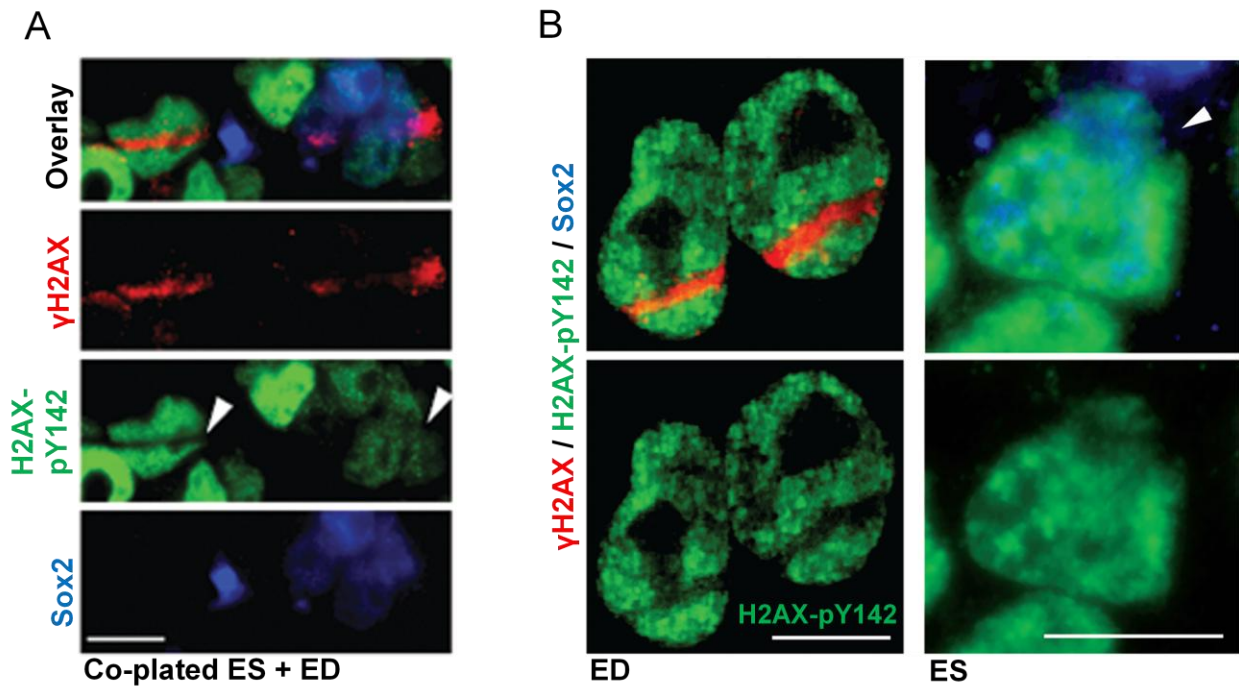


**Figure 4.1. H2AX-pY142 persists along DSBs only in cultured stem cells.** Immunofluorescence co-staining of Sox2 (blue) H2AX-pY142 (green), and  $\gamma$ H2AX (red) on co-plated ES and ED cells following microirradiation. (A) White arrowheads indicate H2AX-pY142 dephosphorylation at  $\gamma$ H2AX-labeled DNA breaks only in non-stem cells. (B) Arrowhead marks the path of microirradiation across the stem cell. Individual ES and ED pictures shown were irradiated together following co-plating. White scale bars, 10 $\mu$ m.

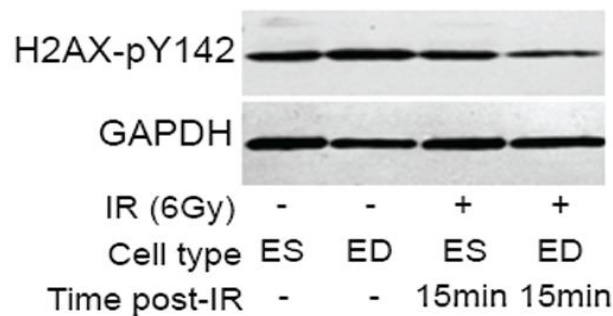


**Figure 4.2. Global H2AX-pY142 is reduced following irradiation only in non-stem cells.** Western blots for phosphorylated H2AX-pY142 at 15min following mock or 6Gy irradiation of ES and ED cells. GAPDH served as a loading control.

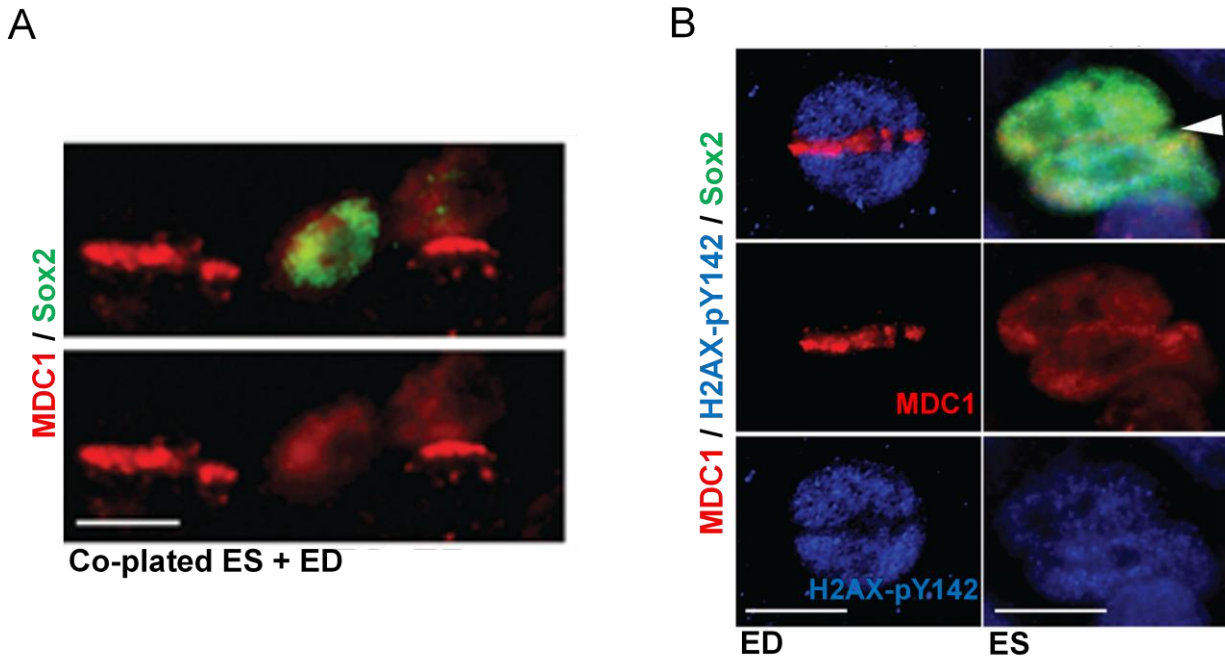


**Figure 4.3 MDC1 is not recruited to DSBs in cultured stem cells.** Immunofluorescence co-staining of (A) Sox2 (green) and MDC1 (red) or (B) Sox2 (green), MDC1 (red), and H2AX-pY142 (blue) on co-plated ES and ED cells following microirradiation. Individual ES and ED pictures shown were irradiated together following co-plating. White scale bars, 10 $\mu$ m.

#### 4.4.2 The absence of IRIFs inversely correlates with high H3K56ac levels in stem cells

Chromatin structure has been shown to have a major influence on DNA repair<sup>3</sup>. Our screening for histone modifications implicated in DDR using blastocyst stage embryos and isogenic stem/ non-stem cells, identified histone H3 lysine 56 acetylation as a potential epigenetic regulator of stem cell radiation response. H3K56ac has been implicated as a DNA damage-responsive histone modification<sup>13,14,16-18</sup>, is known to be directly involved in maintaining the pluripotent state of embryonic stem cells<sup>7,19</sup>, and is elevated in undifferentiated cells<sup>17</sup>. We therefore investigated whether enhanced H3K56ac levels in stem cells may be related to the observed attenuation DDR signaling. We elucidated that H3K56ac levels were dramatically enhanced within the inner cell

mass of embryos where stem cells are located (Fig. 4.4 A), and high H3K56ac levels in cultured ES cells sharply decreased upon differentiation (Fig. 4.4 B). Interestingly, high H3K56ac levels were associated with an absence of  $\gamma$ H2AX foci following irradiation of culture cells (Fig. 4.5). This phenomenon was also observed *in vivo*, where high H3K56ac levels in stem cells corresponded to strongly abrogated DDR signals (Fig. 4.6).

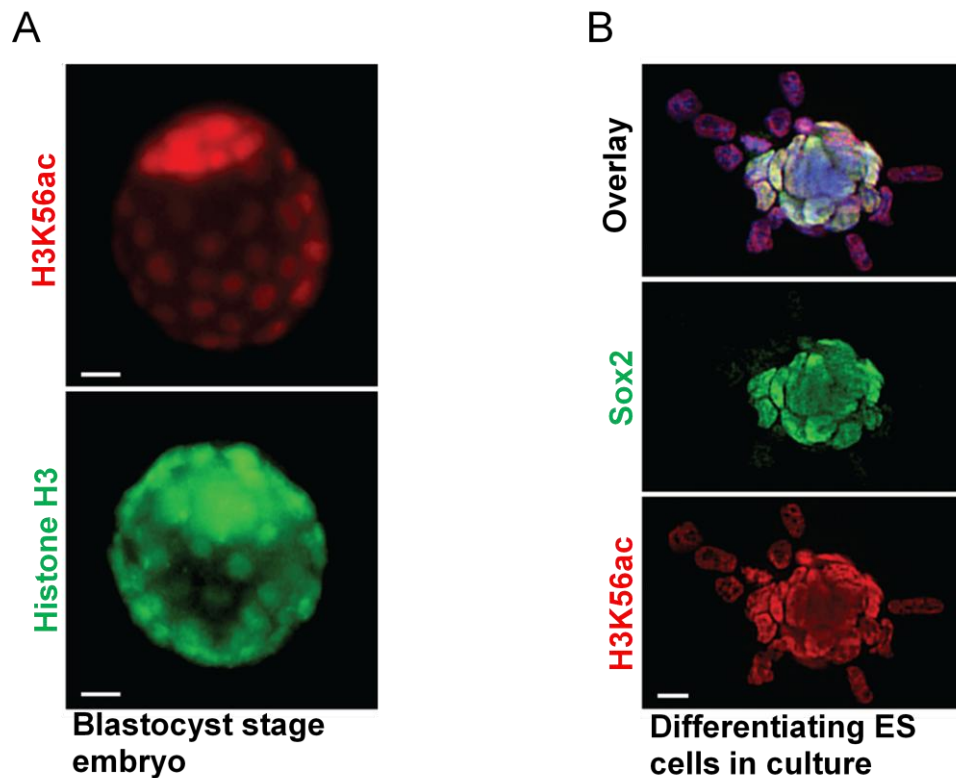


**Figure 4.4. H3K56ac is enhanced in ES cells compared to differentiated progeny.**

(A) Immunofluorescence staining for H3K56ac (red) or total histone H3 (green) on unirradiated E4.5 day mouse embryos. (B) Immunofluorescence co-staining of Sox2 (green) and H3K56ac (red) on an unirradiated, partially differentiated ES cell colony. DAPI=DNA. White scale bars, 10 $\mu$ m.

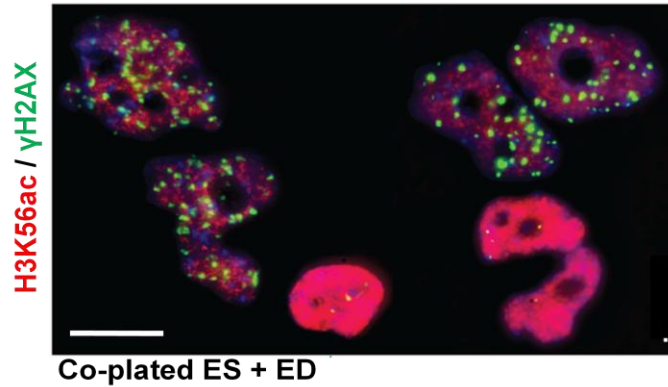


**Figure 4.5. Elevated H3K56ac levels in culture cells correlates with attenuated  $\gamma$ H2AX induction.** Immunofluorescence co-staining of  $\gamma$ H2AX (green) and H3K56ac (red) on co-plated ES and ED cells 15min following 2Gy IR. DAPI=DNA. White scale bars, 10 $\mu$ m.

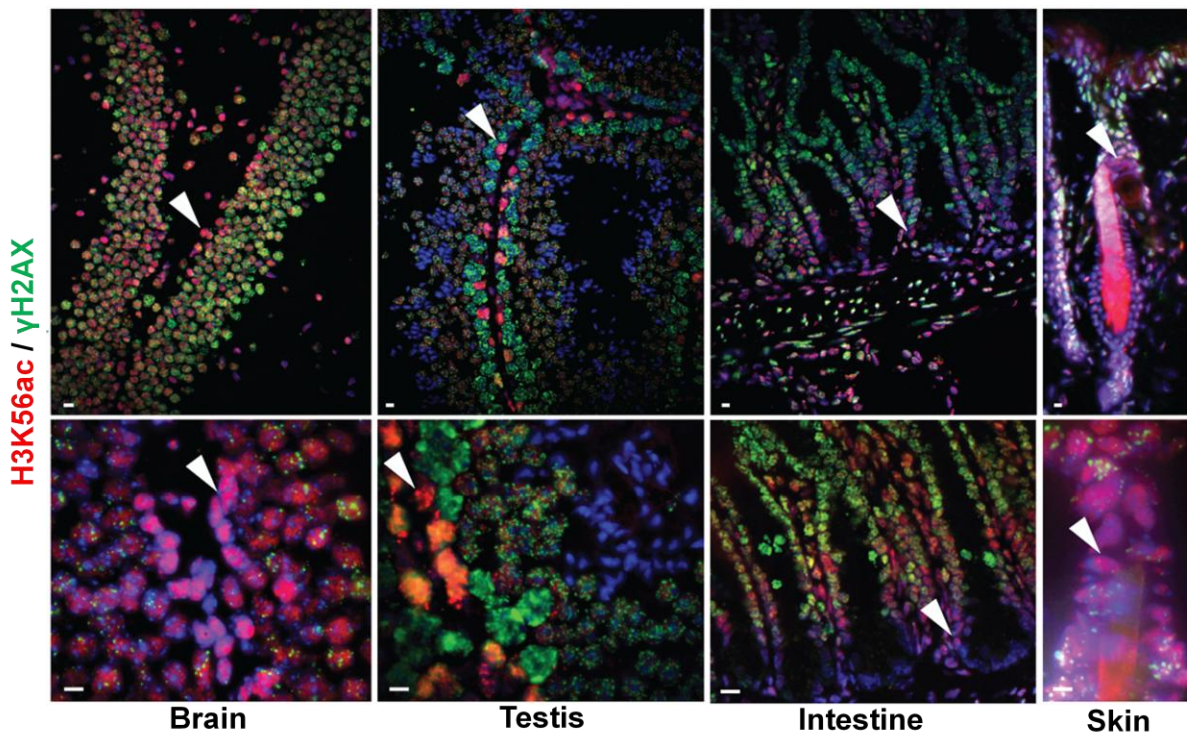


**Figure 4.6. Elevated H3K56ac levels in stem cell regions correlates with attenuated  $\gamma$ H2AX induction.** Immunofluorescence co-staining of H3K56ac (red) and  $\gamma$ H2AX (green) in tissue niches 15min following 6Gy IR. DAPI=DNA. Arrowheads indicate cells expressing high H3K56ac and an absence of  $\gamma$ H2AX foci. White scale bars, 10 $\mu$ m.

#### **4.4.3 Stem cells lack transient reduction of H3K56ac in chromatin around DSB sites**

We utilized microirradiation tracks to investigate any differential kinetics of H3K56ac changes around DNA break sites in stem and non-stem cells at different timepoints after induction of DNA damage. Our results revealed that acetylation of H3K56ac was significantly reduced along the  $\gamma$ H2AX tracks within minutes of DNA damage only in non-stem cells, while in stem cells attenuated  $\gamma$ H2AX corresponded with constitutively elevated H3K56ac levels that did not substantially change in the region of DNA damage (Fig. 4.7 A-B). H3K56ac reduction was due to decreased acetylation and not eviction of histones from the break site, as histone H3 levels did not change along the track of DNA damage (Fig. 4.8). This reduction in H3K56ac at break sites in non-stem cells that display robust DDR signaling was found to be transient in nature. No alteration was observed in either stem or non-stem cells at 30min or 1h following microirradiation (Fig. 4.9 A-B), indicating that alteration of chromatin structure may only be necessary for initial induction and maintenance of the DDR immediately following DNA damage. Constitutively enhanced H3K56ac in stem cells without any reduction at break sites is therefore associated with hampered recruitment/ retention of DDR factors to DNA breaks.

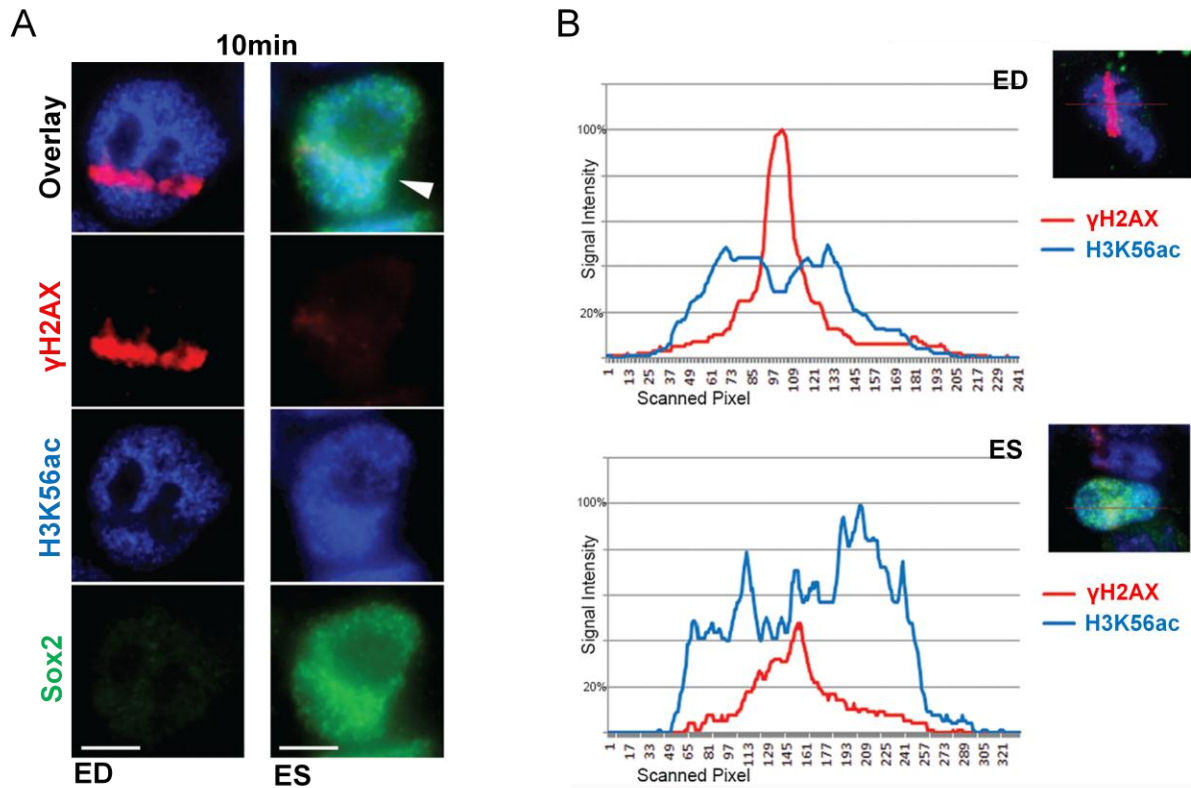


**Figure 4.7. H3K56ac is reduced in non-stem but not stem cells along DSBs.**

(A) Immunofluorescence co-staining of Sox2 (green),  $\gamma$ H2AX (red) and H3K56ac (blue) on co-plated ES and ED cells 10min following microirradiation. Arrowhead marks the path of laser microirradiation across the stem cell. (B) Signal intensity profiles of microirradiated ES and ED cells demonstrate the relationship between H3K56ac (blue) and  $\gamma$ H2AX (red) across the break site. Red lines across the nuclei indicate the path of signal intensity measurements. Sox2=green. Individual ES and ED pictures shown were irradiated together following co-plating. White scale bars, 10 $\mu$ m.

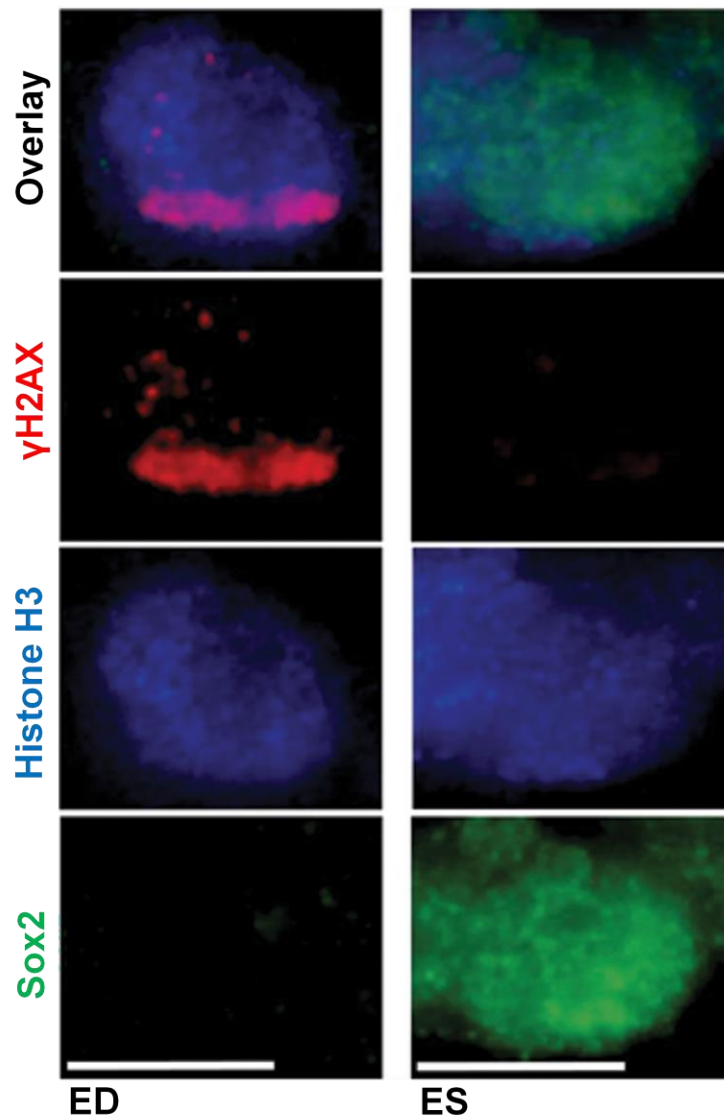


**Figure 4.8. Histones are not evicted from chromatin along DSBs in stem or non-stem cells.**

Immunofluorescence co-staining of Sox2 (green),  $\gamma$ H2AX (red) and histone H3 (blue) on co-plated ES and ED cells 10min following microirradiation. Individual ES and ED pictures shown were irradiated together following co-plating. White scale bars, 10 $\mu$ m.

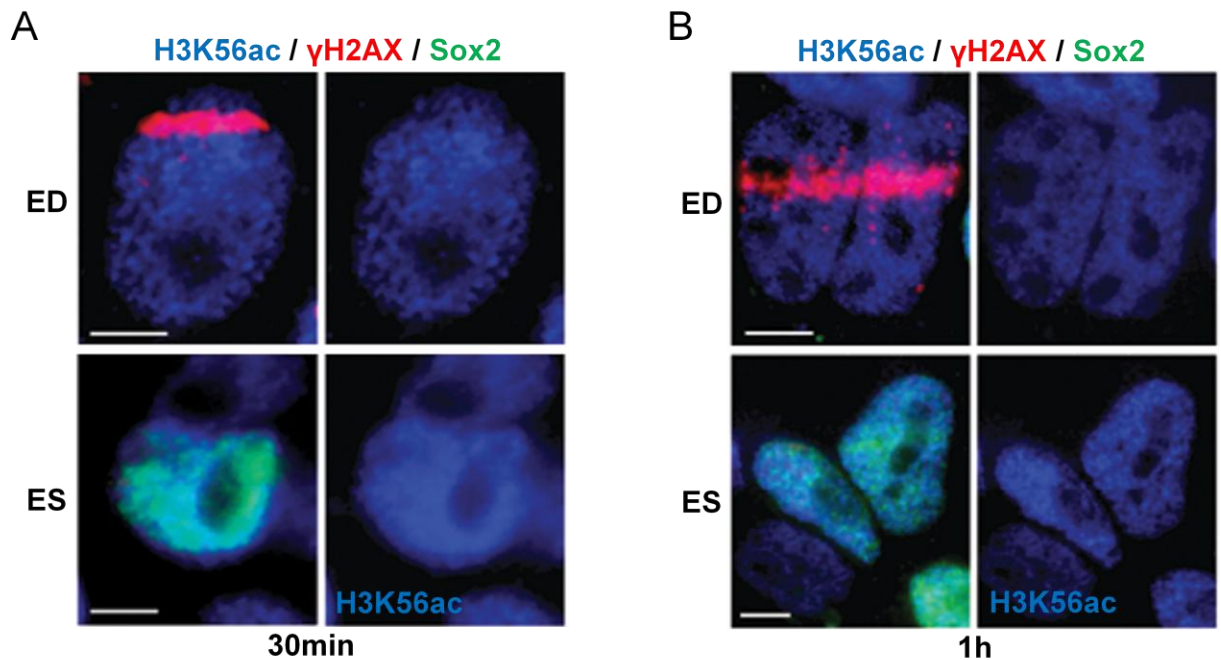


**Figure 4.9. Baseline H3K56ac levels are restored along DSBs in non-stem cells within 30min of microirradiation.** Immunofluorescence co-staining of Sox2 (green),  $\gamma$ H2AX (red) and H3K56ac (blue) on co-plated ES and ED cells (A) 30min or (B) 1h following microirradiation. Individual ES and ED pictures shown were irradiated together following co-plating. White scale bars, 10 $\mu$ m.

#### 4.4.4 Knockdown and inhibition of p300 acetyltransferase reduces H3K56ac levels

Having established a negative correlation between H3K56ac expression and  $\gamma$ H2AX induction, we wanted to determine whether we could modulate H3K56ac levels in order to more directly assess its effect on radiosensitivity and the DDR in stem cells. The H3K56ac acetyltransferase p300 was extremely elevated in both unirradiated and irradiated stem cells in culture (Fig. 4.10-11), only displaying minimal observable expression in differentiated cells. p300 expression also paralleled elevated H3K56ac levels in mixed culture (Fig. 4.12). siRNA knockdown substantially reduced H3K56ac levels (Fig. 4.13), although the reduction was transient likely due to compensatory effects from other acetyltransferases. We therefore confirm that p300 is an acetyltransferase for H3K56ac, and its knockdown provides a suitable method for H3K56ac downregulation.

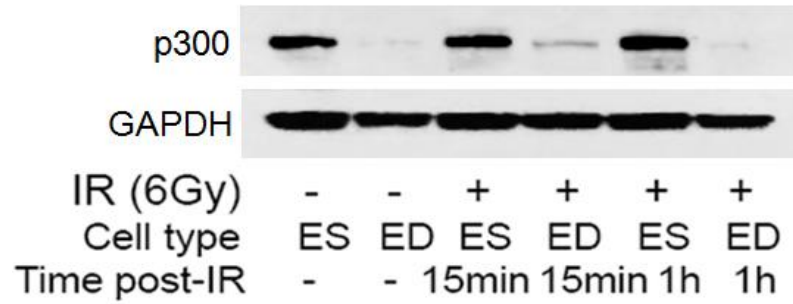


**Figure 4.10** Expression of p300 acetyltransferase is substantially higher in stem cells as compared to non-stem cells. Western blots for p300 at multiple timepoints following mock or 6Gy irradiation of ES and ED cells. GAPDH served as a loading control.

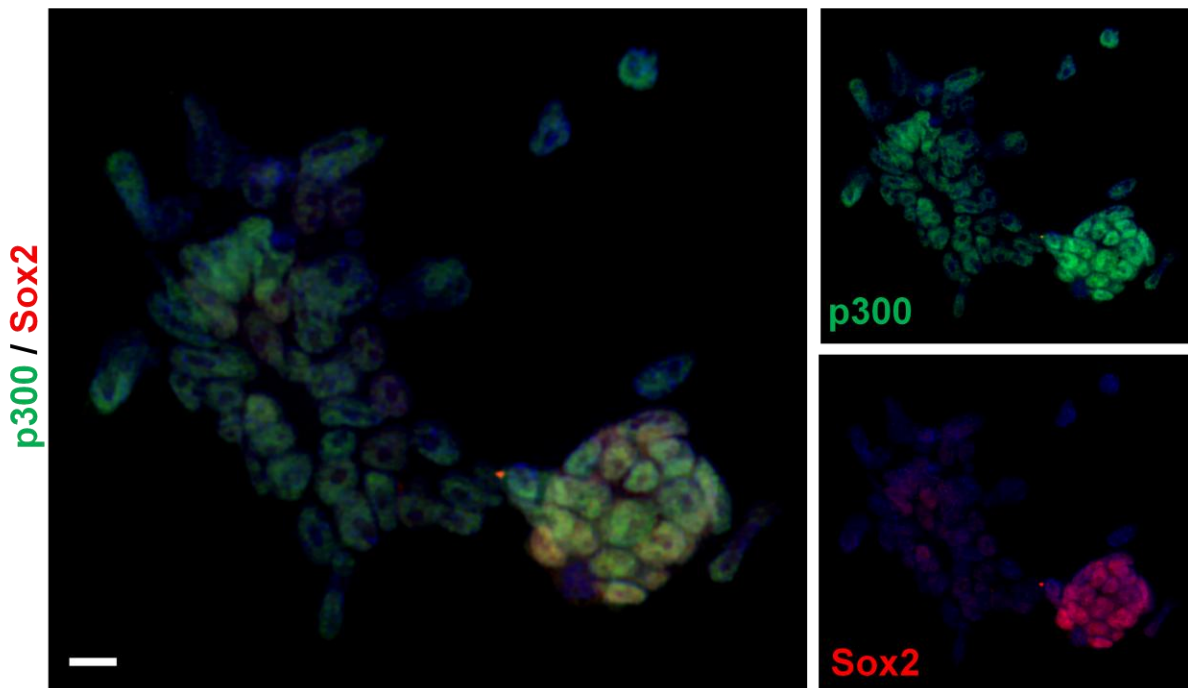


**Figure 4.11.** Elevated p300 expression corresponds with Sox2 expression in ES colonies. Immunofluorescence co-staining of p300 (green) and Sox2 (red) on an unirradiated, partially differentiated ES cell colony. DAPI=DNA. White scale bars, 10µm.

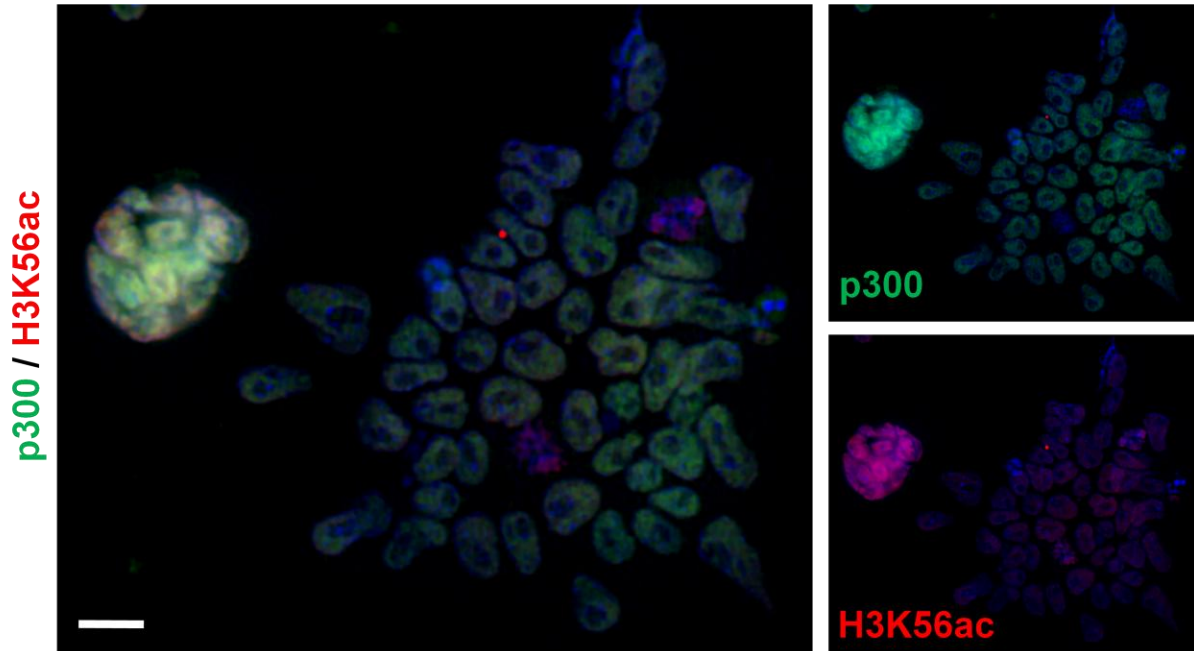


**Figure 4.12. Elevated p300 expression corresponds with elevated H3K56ac in ES colonies.** Immunofluorescence co-staining of p300 (green) and H3K56ac (red) on an unirradiated, partially differentiated ES cell colony. DAPI=DNA. White scale bars, 10µm.

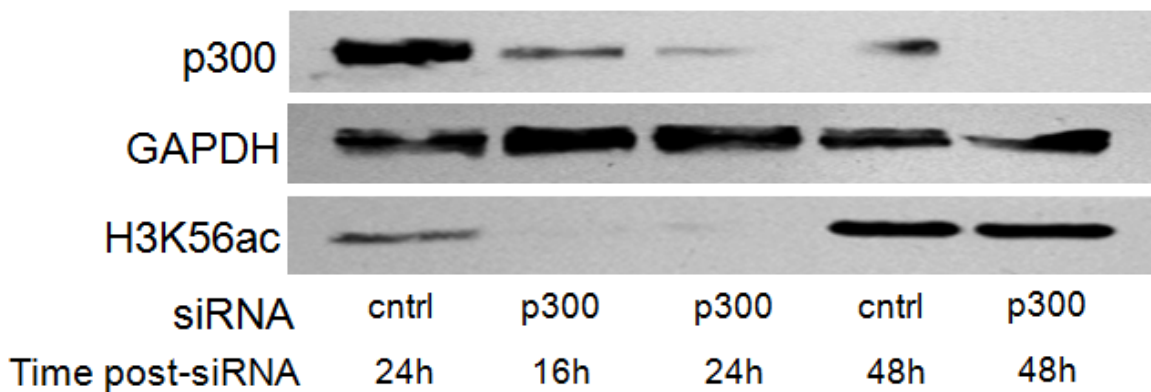


**Figure 4.13. siRNA knockdown of p300 transiently downregulates H3K56ac in cultured stem cells.** Western blots for p300 and H3K56ac at multiple timepoints in ES cells following 16h incubation with negative control or p300 siRNA. GAPDH served as a loading control.

#### 4.4.6 Reducing H3K56ac levels imparts radioprotection on stem cells through restoration of the DDR

Being able to downregulate H3K56ac allowed us to determine whether enhanced H3K56ac levels are truly responsible for the abrogation of the DDR in stem cells. p300 knockdown (and associated H3K56ac reduction) in stem cells increased global induction of  $\gamma$ H2AX (Fig 4.14) following irradiation. We then performed a comet assay to assess whether an enhanced DDR due to decreased H3K56ac levels could successfully improve DNA repair proficiency. Knockdown of p300 in stem cells resulted in significant improvement in DNA repair efficacy as indicated by a hastened reduction in DNA breaks (Fig. 4.15). We then examined whether this improved DNA repair through increased DDR signaling was sufficient to reduce stem cell radiosensitivity. IR-induced apoptosis was significantly reduced in stem cells following p300 knockdown (Fig. 4.16), determining that constitutively elevated H3K56ac in stem cells is indeed a major contributor to their IR hypersensitivity. p300 knockdown had no effect on either baseline or IR-induced cell death in non-stem cells, indicating that H3K56ac modulation can be utilized to specifically regulate radiosensitivity in stem cells without unintended effects on other cell types.

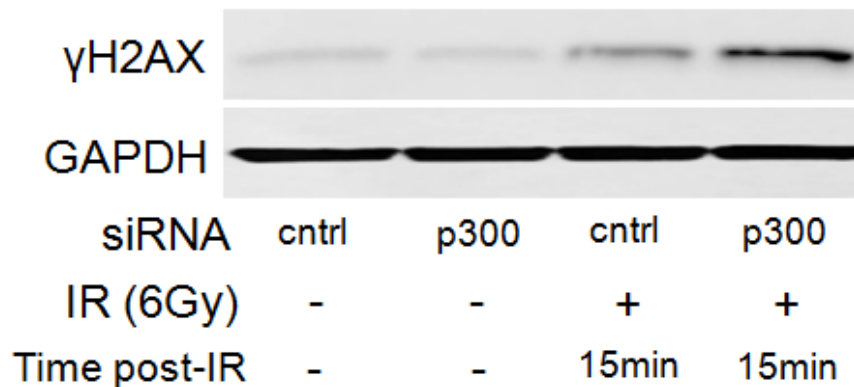


**Figure 4.14. p300 knockdown increases  $\gamma$ H2AX induction in cultured stem cells following irradiation.** Western blot for  $\gamma$ H2AX at 15min following either sham or 6Gy IR of ES cells after 16h incubation with negative control or p300 siRNA. GAPDH served as a loading control.

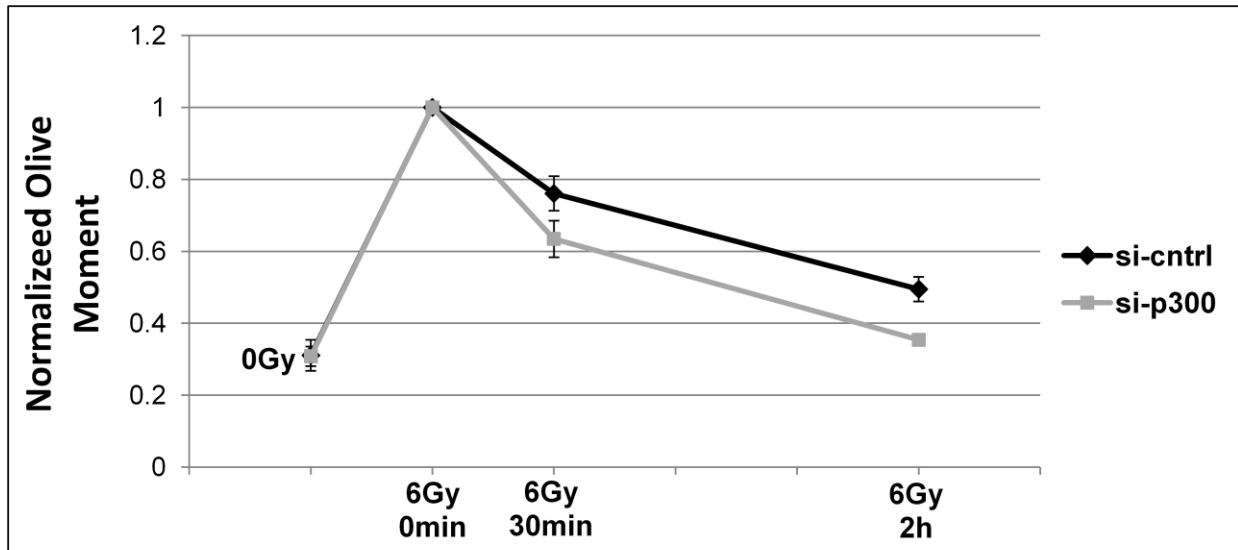


**Figure 4.15. p300 knockdown improves DNA repair in cultured stem cells.** Olive moments of NS and ND cell comet assay tails were quantified at different timepoints following sham or 6Gy IR after 16h incubation with negative control or p300 siRNA. Olive moments were normalized to the irradiated 0min timepoint in order to measure DNA repair over time. N=3. Error bars indicate SEM.

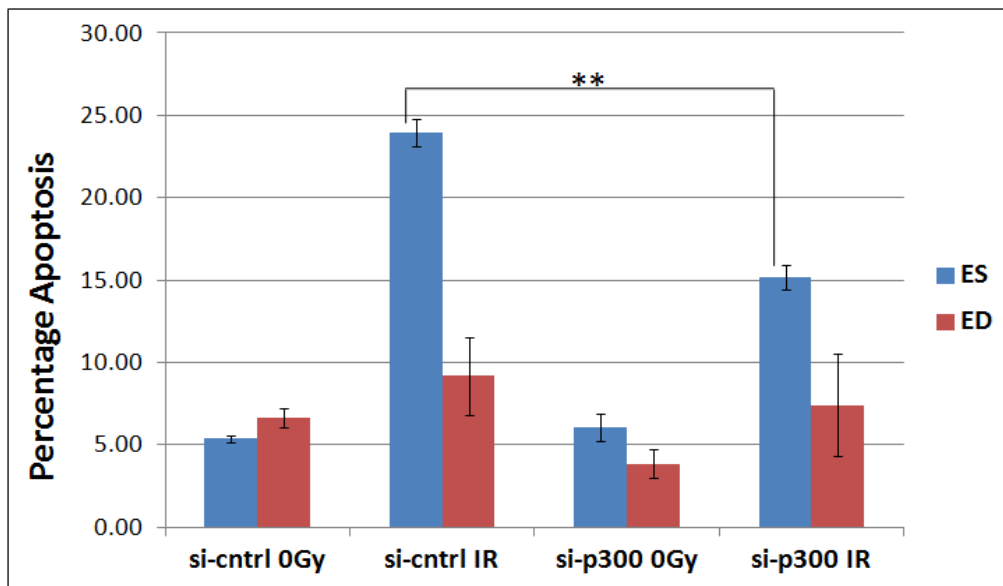


**Figure 4.16. p300 knockdown reduces IR-induced apoptosis in stem cells without any effect on non-stem cells.** Flow cytometric analysis of apoptosis comparing ES and ED cells by Annexin-V labeling 16h following sham or 6Gy IR after 16h incubation with negative control or p300 siRNA. N=3; \*\* =  $p < 0.01$ ; Error bars indicate SEM.

## 4.5 DISCUSSION

Our work from previous chapters showed that despite being able to sense DSBs through the Mre11-Nbs1-Rad50 (MRN) complex, downstream DDR signaling is abrogated in stem cells. Since stem cells are able to sense broken DNA, they must have some inhibitory mechanism(s) blocking DDR factors from accessing/ accumulating around DSBs. Our data suggests that the failure of stem cells to dephosphorylate H2AX-pY142 following DNA damage blocks DDR signaling and instead induces apoptosis through c-Jun N-terminal kinase (JNK). This epigenetic mechanism explains how stem cells can undergo IR-induced apoptosis without active DDR signaling (Supplementary Fig. 4b). In addition to providing novel evidence that unique regulation of H2AX Y142 phosphorylation status in stem cells may regulate their radiosensitivity, this study also suggests that H2AX-pY142 may directly inhibit S139  $\gamma$ H2AX phosphorylation. While it is unclear whether H2AX-pY142 is directly blocking the initial phosphorylation of H2AX-S139 in stem cells or if Y142 phosphorylation merely prevents MDC1-mediated amplification of  $\gamma$ H2AX<sup>20</sup> along the break site; regulation of H2AX-pY142 appears to influence cellular responses to DNA damage. We propose that the close proximity of H2AX-pY142 sterically hinders access to the H2AX-S139 site, therefore blocking  $\gamma$ H2AX phosphorylation and/or MDC1 binding.

H2AX-pY142 is also related to the apoptotic induction of mammalian sterile 20-like kinase-1 (MST1) and pan-nuclear H2AX-pS139. MST1 is required for imatinib-mediated apoptosis through H2AX-pY142<sup>21</sup> (likely involving pJNK). Additionally, apoptotic H2AX-pS139 has been directly linked to both MDC1 inhibition<sup>22</sup> and enhanced Y142 phosphorylation<sup>21</sup>. Our work suggests that H2AX-pY142 may directly inhibit  $\gamma$ H2AX at S139, although it is unclear whether H2AX-pY142 is directly blocking the initial phosphorylation of H2AX-S139 in stem cells or merely preventing MDC1-mediated amplification of  $\gamma$ H2AX along the break site. We propose that the close proximity of H2AX-pY142 sterically hinders access to the S139 site, therefore blocking  $\gamma$ H2AX induction and/or MDC1 binding. This mechanism explains how DDR signaling is inhibited in stem cells despite proper sensing of DSBs.

We also elucidated that continuously elevated H3K56ac in stem cells is associated with abrogated induction of the DDR following DNA damage. Existing literature has primarily only assessed global

changes in H3K56ac, with contradictory results concerning whether levels increase<sup>16,17</sup> or decrease<sup>13,14,23</sup> following genotoxic stress. In one of the few studies that assessed local H3K56ac changes around break sites, however, Miller et al. demonstrated that H3K56ac is absent from  $\gamma$ H2AX within microirradiated regions of DNA damage in cancer cells<sup>14</sup>, providing rationale to investigate whether enhanced levels of H3K56ac in stem cells are mechanistically associated with an abrogated DDR. These inconsistencies may result from the dynamic nature of the H3K56ac radioresponse<sup>14,24</sup>, and our results confirm that DNA damage-induced depletion of H3K56ac occurs only transiently during the early stages of DDR signaling. H3K56ac is required for chromatin reassembly at the end of DSB repair in yeast<sup>25</sup>, however this may merely explain why H3K56ac levels are so quickly restored to baseline following transient reduction. Histone deacetylation at specific sites may also be the mechanism responsible for the transient compaction of chromatin locally surrounding DSBs that has been found to be important for proper DDR signaling<sup>26</sup>. The temporal response of H3K56ac to DNA damage suggests dynamic interplay of associated histone deacetylases and acetyltransferases around DNA break sites. While histone acetylation is generally associated with the overall loosening of chromatin, acetylation at specific residues such as H3K56 may create a non-permissive chromatin environment for DNA repair, either blocking access for recruitment of repair factors or allowing binding of repressor proteins that could restrict IRIF maturation.

While several acetyltransferases<sup>13,16,17</sup> and deacetylases<sup>14,17,18,27</sup> have been shown to effect mammalian H3K56ac levels<sup>13,16,17</sup>, we chose to target p300 acetyltransferase for modulation of H3K56ac levels. p300 has been implicated in H3K56ac regulation by many studies and mirrors H3K56ac recruitment to ES-specific genes<sup>7,19,28</sup>. In addition to its role as an acetyltransferase, p300 and the related CREB-binding protein (CBP) also act as transcriptional coactivators by directing assembly of transcriptional machinery at promoter regions<sup>29,30</sup>. p300 and CBP also play a role in the induction of apoptosis, primarily through their regulation of p53. p300 binding to p53 may promote its degradation under basal conditions, but upon cellular stress p300/CBP acetylation of p53 promotes p53 transcriptional activation of target genes<sup>29,31-34</sup>. Additionally, p300 and CBP are also mutated in many cancers<sup>35</sup> and p300 (but not CBP) loss has been shown to impair apoptosis in culture cells<sup>36</sup>. It is therefore plausible that p300 knockdown could reduce

radiosensitivity independent of H3K56ac. Several lines of evidence suggest that reduced p53 activation is not responsible for improved radioresponses in stem cells following p300 knockdown, however. Neither p53<sup>37</sup> or its upstream kinase ataxia telangiectasia mutated (ATM) (Fig. 3.19) is required for DNA damage-induced apoptosis in stem cells. Additionally, p300 knockdown only affected radiosensitivity in stem cells where enhanced H3K56ac levels are the most predominant p300-related phenotype. These data suggests that there may be a threshold level of H3K56ac expression during DDR signaling above which the recruitment of repair factors is inhibited. H3K56ac reduction therefore has no effect in differentiated cells with basally low levels of H3K56ac and the ability to downregulate H3K56ac along DSBs, however it has a substantial effect on the radiation responses of stem cells. Based on the large difference in p300 expression between stem and non-stem cells, it is also possible that H3K56ac regulation in stem cells is more p300-dependent than other cell types, and therefore p300 knockdown only has a significant effect on stem cells. Either way, these possibilities postulate that H3K56ac modulation may be used to specifically radioprotect stem cells without any effect on differentiated or cancer stem cells.

Successful restoration of DDR signaling and the associated reduction in IR-induced apoptosis in stem cells following H3K56ac downregulation indicates that elevated H3K56ac directly contributes to stem cell radiosensitivity by preventing proper recruitment and retention of DDR factors. Because H3K56ac modulation only affected the radiosensitivity of stem cells, p300 and other H3K6ac regulators may serve as useful pharmacological targets for preventing stem cell dropout during radiation therapy. Protecting stem cells will minimize clinical consequences of radiation therapy and allow the use of higher doses for more effective cancer treatment.

## 4.6 REFERENCES

1. Zentner, G. E. & Henikoff, S. Regulation of nucleosome dynamics by histone modifications. *Nat. Struct. Mol. Biol.* **20**, 259–66 (2013).
2. Jenuwein, T. & Allis, C. D. Translating the histone code. *Science* **293**, 1074–80 (2001).
3. Lukas, J., Lukas, C. & Bartek, J. More than just a focus: The chromatin response to DNA damage and its role in genome integrity maintenance. *Nat. Cell Biol.* **13**, 1161–9 (2011).

4. Rossetto, D., Truman, A. W., Kron, S. J. & Côté, J. Epigenetic modifications in double-strand break DNA damage signaling and repair. *Clin. Cancer Res.* **16**, 4543–52 (2010).
5. Deem, A. K., Li, X. & Tyler, J. K. Epigenetic regulation of genomic integrity. *Chromosoma* **121**, 131–151 (2012).
6. Chia, N.-Y. *et al.* A genome-wide RNAi screen reveals determinants of human embryonic stem cell identity. *Nature* **468**, 316–320 (2010).
7. Xie, W. *et al.* Histone h3 lysine 56 acetylation is linked to the core transcriptional network in human embryonic stem cells. *Mol. Cell* **33**, 417–27 (2009).
8. Armstrong, L. Epigenetic control of embryonic stem cell differentiation. *Stem Cell Rev.* **8**, 67–77 (2012).
9. Meshorer, E. *et al.* Hyperdynamic plasticity of chromatin proteins in pluripotent embryonic stem cells. *Dev. Cell* **10**, 105–16 (2006).
10. Cook, P. J. *et al.* Tyrosine dephosphorylation of H2AX modulates apoptosis and survival decisions. *Nature* **458**, 591–6 (2009).
11. Singh, N. *et al.* Dual recognition of phosphoserine and phosphotyrosine in histone variant H2A.X by DNA damage response protein MCPH1. *Proc. Natl. Acad. Sci. U. S. A.* **109**, 14381–6 (2012).
12. Brown, J. a L., Eykelenboom, J. K. & Lowndes, N. F. Co-mutation of histone H2AX S139A with Y142A rescues Y142A-induced ionising radiation sensitivity. *FEBS Open Bio* **2**, 313–7 (2012).
13. Tjeertes, J. V, Miller, K. M. & Jackson, S. P. Screen for DNA-damage-responsive histone modifications identifies H3K9Ac and H3K56Ac in human cells. *EMBO J* **28**, 1878–1889 (2009).
14. Miller, K. M. *et al.* Human HDAC1 and HDAC2 function in the DNA-damage response to promote DNA nonhomologous end-joining. *Nat Struct Mol Biol* **17**, 1144–1151 (2010).
15. Xiao, A. *et al.* WSTF regulates the H2A.X DNA damage response via a novel tyrosine kinase activity. *Nature* **457**, 57–62 (2009).
16. Vempati, R. K. *et al.* p300-mediated acetylation of histone H3 lysine 56 functions in DNA damage response in mammals. *J. Biol. Chem.* **285**, 28553–64 (2010).
17. Das, C., Lucia, M. S., Hansen, K. C. & Tyler, J. K. CBP/p300-mediated acetylation of histone H3 on lysine 56. *Nature* **459**, 113–7 (2009).
18. Yuan, J., Pu, M., Zhang, Z. & Lou, Z. Histone H3-K56 acetylation is important for genomic stability in mammals. *Cell Cycle* **8**, 1747–1753 (2009).
19. Tan, Y., Xue, Y., Song, C. & Grunstein, M. Acetylated histone H3K56 interacts with Oct4 to promote mouse embryonic stem cell pluripotency. *Proc. Natl. Acad. Sci. U. S. A.* **110**, 11493–8 (2013).
20. Lou, Z. *et al.* MDC1 maintains genomic stability by participating in the amplification of ATM-dependent DNA damage signals. *Mol. Cell* **21**, 187–200 (2006).

21. Zhang, Y. *et al.* Imatinib induces H2AX phosphorylation and apoptosis in chronic myelogenous leukemia cells in vitro via caspase-3/Mst1 pathway. *Acta Pharmacol. Sin.* **33**, 551–7 (2012).
22. Solier, S. & Pommier, Y. MDC1 cleavage by caspase-3: a novel mechanism for inactivating the DNA damage response during apoptosis. *Cancer Res.* **71**, 906–13 (2011).
23. Maroschik, B. *et al.* Radiation-induced alterations of histone post-translational modification levels in lymphoblastoid cell lines. *Radiat. Oncol.* **9**, 15 (2014).
24. Battu, A., Ray, A. & Wani, A. a. ASF1A and ATM regulate H3K56-mediated cell-cycle checkpoint recovery in response to UV irradiation. *Nucleic Acids Res.* **39**, 7931–7945 (2011).
25. Chen, C.-C. *et al.* Acetylated lysine 56 on histone H3 drives chromatin assembly after repair and signals for the completion of repair. *Cell* **134**, 231–43 (2008).
26. Burgess, R. C., Burman, B., Kruhlak, M. J. & Misteli, T. Activation of DNA Damage Response Signaling by Condensed Chromatin. *Cell Rep.* **9**, 1703–17 (2014).
27. Yang, B., Zwaans, B. M. M., Eckersdorff, M. & Lombard, D. B. The sirtuin SIRT6 deacetylates H3 K56Ac in vivo to promote genomic stability. *Cell Cycle* **8**, 2662–3 (2009).
28. Chen, X. *et al.* Integration of external signaling pathways with the core transcriptional network in embryonic stem cells. *Cell* **133**, 1106–17 (2008).
29. Giordano, A. & Avantaggiati, M. L. p300 and CBP: partners for life and death. *J. Cell. Physiol.* **181**, 218–30 (1999).
30. Kalkhoven, E. CBP and p300: HATs for different occasions. *Biochem. Pharmacol.* **68**, 1145–55 (2004).
31. Avantaggiati, M. L. *et al.* Recruitment of p300/CBP in p53-dependent signal pathways. *Cell* **89**, 1175–84 (1997).
32. Grossman, S. R. p300/CBP/p53 interaction and regulation of the p53 response. *Eur. J. Biochem.* **268**, 2773–8 (2001).
33. Brooks, C. L. & Gu, W. The impact of acetylation and deacetylation on the p53 pathway. *Protein Cell* **2**, 456–62 (2011).
34. Mujtaba, S. *et al.* Structural Mechanism of the Bromodomain of the Coactivator CBP in p53 Transcriptional Activation. *Mol. Cell* **13**, 251–263 (2004).
35. Iyer, N. G., Ozdag, H. & Caldas, C. p300/CBP and cancer. *Oncogene* **23**, 4225–31 (2004).
36. Yuan, Z. M. *et al.* Function for p300 and not CBP in the apoptotic response to DNA damage. *Oncogene* **18**, 5714–7 (1999).
37. Aladjem, M. I. *et al.* ES cells do not activate p53-dependent stress responses and undergo p53-independent apoptosis in response to DNA damage. *Curr Biol* **8**, 145–155 (1998).

## **CHAPTER 5**

---

### **Conclusions and Ongoing Work**

## 5.1 SUMMARY

Radiation therapy utilizes targeted ionizing radiation (IR) to induce double-strand breaks (DSBs) in cancer cells, leading to destruction of the tumor. While every effort is made to spare normal tissue, nevertheless patients often experience detrimental clinical consequences following radiation therapy as a result of damaged normal tissue. There are several mechanisms of long-term radiation injury; this project focused on the loss of regenerative capacity in proliferative tissues resulting in functional sequelae following normal tissue turnover. Due to the loss of regenerative capacity and observable damage to the stem cell compartment, this form of radiation injury has been attributed to stem cell dropout. Despite this association, conflicting evidence exists concerning the true radiosensitivity of stem cells themselves compared to surrounding differentiated cells within their respective tissue niche. Previous studies have only investigated specific stem cell compartments or individual cell culture models. Stem cell culture models typically involve high-passage, established cell lines and do not compare stem cells with their directly differentiated isogenic progeny. In order to identify conserved molecular mechanisms underlying stem cell radiation responses, we investigated stem cell radiosensitivity in four clinically relevant stem cell niches as well as two primary, early passage culture models from mice. *In vivo* stem cell compartments assayed in this project included the subventricular zone within the dentate gyrus of brain, the seminiferous tubules of testis, the hair follicle in skin and intestinal crypts. For culture models, embryonic stem (ES) cells were isolated from the inner cell mass of blastocyst-stage embryos and neural stem (NS) cells were freshly dissected from the hippocampus of P0-P2 mouse pups. Both culture models were directly differentiated by removal of growth factors from media and assayed in parallel with their differentiated progeny.

Whole-body irradiation of mice induced apoptosis exclusively within individually labeled stem cells of all four tissue niches and this differential radiosensitivity was recapitulated in both culture models. Dose curves determined that stem cells are radiosensitive at as low as 2Gy while differentiated cells only begin to apoptose above 8Gy. While the long-held tenet of radiobiology known as the Law of Bergonié and Tribondeau states that radiosensitivity is directly related to proliferation rate, we found no association between proliferation status and radiosensitivity among our stem cell models. While radiosensitivity

differences among differentiated cell populations correlated with proliferation status, enhanced radiosensitivity in stem cells was not associated with enhanced proliferation. Radiation responses did differ between stem and non-stem cells across the cell cycle however, as stem cells apoptosed much more broadly across the cell cycle. Stem cells are therefore hypersensitive to IR independent of their proliferation status, in contrast with their radioresistant differentiated progeny.

Investigation of DDR signaling among stem and differentiated cells elucidated that stem cells both *in vivo* and in culture exhibit a strongly attenuated DDR as indicated by substantially reduced induction of  $\gamma$ H2AX as well as reduced activation and recruitment of phosphorylated ATM. Muted DDR signaling in stem cells was associated with inadequate DNA repair and improper cell cycle checkpoint arrest. Despite the absence of  $\gamma$ H2AX foci, at late timepoints stem cells exhibited apoptotic pan-nuclear H2AX phosphorylation at the same S139 as part of the MST1-JNK-H2AX pathway. Diminished DDR signaling in stem cells is therefore associated with their radiosensitivity.

Stem cells also showed a unique persistence of H2AX Y142 around break sites, resulting in hindered recruitment of the DDR factor MDC1 and instead prompting JNK-mediated apoptosis. Failure to dephosphorylate H2AX Y142 may thus direct stem cells toward apoptosis in lieu of DNA repair. Histone 3 lysine 56 acetylation (H3K56ac) was found to be elevated in stem cells and was inversely correlated with robust induction of  $\gamma$ H2AX foci both *in vivo* and in culture. H3K56ac was reduced along break sites in differentiated but not stem cells, and H3K56ac downregulation reduced IR-induced apoptosis in stem cells through restoration of the DDR. Unique epigenetic regulation can thereby promote heterogeneous radiation responses among different cell types. Therapeutic modulation of these histone modifications may protect stem cells from IR and thus allow more efficient treatment of cancer patients.

## **5.2 ONGOING WORK AND FUTURE DIRECTIONS**

### **5.2.1 H3K56ac**

We are continuing to investigate the contribution of H3K56ac toward stem cell radiosensitivity.

Preliminary evidence suggests that the presence of elevated H3K56ac and its persistence along

DSBs is hindering DDR signaling. It is unclear at which step H3K56ac might be interrupting DDR progression. H3K56ac may prevent initial ATM kinase recruitment to DSBs, blocking its activation and phosphorylation of H2AX at S139. H3K56ac may also be acting through its effect on H2AX-pY142, blocking recruitment of EYA phosphatase which is responsible for H2AX Y142 phosphorylation<sup>1</sup>. H3K56ac could even itself be inhibiting expansion of  $\gamma$ H2AX around the DSB and thereby blocking DDR amplification. A whole series of experiments will be required to parse apart the specific locations in the pathway at which H3K56ac is acting.

#### **5.2.1.1 Targeting ASF1 and the p300/CBP bromodomain**

Current experiments are focusing on alternative methods for reducing H3K56ac levels aside from p300 knockdown. In addition to its acetyltransferase activity, p300 also functions as a transcriptional co-activator<sup>2</sup>, so it would be useful to parse apart these functions. The bromodomain of p300 and its sister protein CBP binds acetylated lysines on target proteins<sup>3,4</sup> and is necessary for efficient acetylation of these proteins as well. While p300/CBP can promote aggregation of transcription factors at promoter regions through a distinct activation domain<sup>2</sup>, its transcriptional coactivation function is often acetylation-dependent for proteins such as p53<sup>3</sup>. Acetylation of H3K56 may possibly be more precisely targeted by modulation of the interaction with ASF1, a histone chaperone that promotes p300/CBP mediated acetylation of H3K56<sup>5-8</sup>. ASF1 mutually interacts with the bromodomain and H3K56ac to conformationally promote histone acetylation. While the bromodomain can bind various acetylated lysines, CBP bromodomain binding has been found to most strongly interact with H3K56ac. Additionally, ASF1 specifically promotes acetylation of H3K56ac. We have therefore begun experiments utilizing I-CBP112, a p300/CBP-specific bromodomain inhibitor that has been shown to selectively reduce H3K56ac, potentially acting through disruption of the ASF1-bromodomain-H3K56 interaction. In addition to potentially improving specificity towards H3K56ac, pharmacological inhibition will also allow more precise temporal control of H3K56ac modulation. Genetic knockdowns of ASF1 may also produce H3K56ac-specific

downregulation, although this may prove less effective for improving repair as ASF1-mediated H3K56ac is required for DDR recovery through  $\gamma$ H2AX dephosphorylation and basal chromatin reassembly<sup>6,9</sup>.

### **5.2.1.2 H3K56ac upregulation and targeted chromatin modulation**

In parallel with downregulation of H3K56ac in stem cells, we would like to investigate whether upregulation of H3K56ac can impart enhanced radiosensitivity to differentiated cells. This could be performed through overexpression of p300 by plasmid transfection, pharmacological molecular activators, or newly-developed CRISPR-based transcriptional activation (Santa Cruz). Similarly, knockout and inhibition of various histone deacetylases could be used, although multiple deacetylases have been shown to act on H3K56ac<sup>7,8,10,11</sup> and they are unlikely to exhibit much specificity. Reversing the radiosensitivity phenotype in both directions would thoroughly confirm the hypothesis and provide insights into both radioprotection and radiosensitization. H3K56ac and its relationship to the DDR is likely complicated however, and simple upregulation may not be sufficient to modify radiation responses. Additionally, the dynamic influence of the various acetyltransferases and deacetylases on H3K56ac may differ among stem and differentiated cells. Nonetheless, attempting H3K56ac upregulation in differentiated cells will be a worthwhile experiment.

A major issue with existing epigenetics research is the difficulty of modulating chromatin at designated sites. Knockdown or inhibition of an acetyltransferase or deacetylase will affect global acetylation levels, producing pleiotropic effects that may be hard to directly attribute to changes specifically at the break site. New technologies however enable tethering and recruitment of chromatin modifying enzymes to DNA DSBs. The Misteli Lab has developed an effective system utilizing I-Sce1 endonuclease recognition sites bordered by LacO/TetO sequences. Integrated I-Sce-I will only cut at the inserted recognition site to produce a site-specific DSB, and chromatin modifiers can be tethered

to additionally transfected LacR/TetR repressor which will recruit them to the DSB at the LacO/TetO sites<sup>12,13</sup>. A similar procedure can be performed using CRISPR technology with catalytically-inactive Cas9 endonuclease<sup>14</sup>. These methods could allow more precise analysis of H3K56ac effects specific to the region around DSBs.

### 5.2.2 Cancer Stem Cells

Cancer stem cells (CSCs) are a unique cell type that while still debated are generally believed to exist at the core of many tumors. Similar to normal stem cells, cancer stem cells are capable of regenerating all other cells of a tumor and therefore must be destroyed in order to prevent recurrence<sup>15</sup>. It is unclear whether cancer stem cells originate from the de-differentiation of radioresistant differentiated cells or the transformation of normal stem cells, but either way the majority of evidence suggests that they are extremely radioresistant<sup>15-17</sup> yet exhibit an undifferentiated stem cell-like phenotype. Several factors contribute to impart complex and often unique concerted mechanisms of radioresistance in CSCs<sup>15-20</sup>, and it would be extremely interesting to compare their radiation responses to those in normal stem and differentiated cells. While an elevated DDR has been implicated in cancer stem cell radioresistance<sup>17</sup>, a failure to induce  $\gamma$ H2AX has been shown in breast CSCs<sup>21</sup>. Parallel comparison of the IR-responsive mechanisms and epigenetic regulation examined in this project among stem, differentiated, and cancer stem cells would provide additional context for the uniqueness of stem cell radiation responses and how to best target radioprotective therapies.

## 5.3 REFERENCES

1. Cook, P. J. *et al.* Tyrosine dephosphorylation of H2AX modulates apoptosis and survival decisions. *Nature* **458**, 591–6 (2009).
2. Giordano, A. & Avantaggiati, M. L. p300 and CBP: partners for life and death. *J. Cell. Physiol.* **181**, 218–30 (1999).
3. Mujtaba, S. *et al.* Structural Mechanism of the Bromodomain of the Coactivator CBP in p53 Transcriptional Activation. *Mol. Cell* **13**, 251–263 (2004).
4. Chen, J., Ghazawi, F. M. & Li, Q. Interplay of bromodomain and histone acetylation in the regulation of p300-dependent genes. *Epigenetics* **5**, 509–15 (2010).

5. Das, C. *et al.* Binding of the histone chaperone ASF1 to the CBP bromodomain promotes histone acetylation. *Proc. Natl. Acad. Sci. U. S. A.* **111**, E1072–81 (2014).
6. Battu, A., Ray, A. & Wani, A. a. ASF1A and ATM regulate H3K56-mediated cell-cycle checkpoint recovery in response to UV irradiation. *Nucleic Acids Res.* **39**, 7931–7945 (2011).
7. Das, C., Lucia, M. S., Hansen, K. C. & Tyler, J. K. CBP/p300-mediated acetylation of histone H3 on lysine 56. *Nature* **459**, 113–7 (2009).
8. Yuan, J., Pu, M., Zhang, Z. & Lou, Z. Histone H3-K56 acetylation is important for genomic stability in mammals. *Cell Cycle* **8**, 1747–1753 (2009).
9. Chen, C.-C. *et al.* Acetylated lysine 56 on histone H3 drives chromatin assembly after repair and signals for the completion of repair. *Cell* **134**, 231–43 (2008).
10. Miller, K. M. *et al.* Human HDAC1 and HDAC2 function in the DNA-damage response to promote DNA nonhomologous end-joining. *Nat Struct Mol Biol* **17**, 1144–1151 (2010).
11. Yang, B., Zwaans, B. M. M., Eckersdorff, M. & Lombard, D. B. The sirtuin SIRT6 deacetylates H3 K56Ac in vivo to promote genomic stability. *Cell Cycle* **8**, 2662–3 (2009).
12. Roukos, V., Burgess, R. C. & Misteli, T. Generation of cell-based systems to visualize chromosome damage and translocations in living cells. *Nat. Protoc.* **9**, 2476–92 (2014).
13. Burgess, R. C., Burman, B., Kruhlak, M. J. & Misteli, T. Activation of DNA Damage Response Signaling by Condensed Chromatin. *Cell Rep.* **9**, 1703–17 (2014).
14. Gilbert, L. A. *et al.* CRISPR-mediated modular RNA-guided regulation of transcription in eukaryotes. *Cell* **154**, 442–51 (2013).
15. Baumann, M., Krause, M. & Hill, R. Exploring the role of cancer stem cells in radioresistance. *Nat. Rev. Cancer* **8**, 545–54 (2008).
16. Vlashi, E., McBride, W. H. & Pajonk, F. Radiation responses of cancer stem cells. *J. Cell. Biochem.* **108**, 339–42 (2009).
17. Alison, M. R., Lin, W.-R., Lim, S. M. L. & Nicholson, L. J. Cancer stem cells: In the line of fire. *Cancer Treat. Rev.* **38**, 589–598 (2012).
18. Abdullah, L. N. & Chow, E. K.-H. Mechanisms of chemoresistance in cancer stem cells. *Clin. Transl. Med.* **2**, 3 (2013).
19. Cojoc, M., Mäbert, K., Muders, M. H. & Dubrovskaja, A. A role for cancer stem cells in therapy resistance: cellular and molecular mechanisms. *Semin. Cancer Biol.* **31**, 16–27 (2014).
20. Hittelman, W. N., Liao, Y., Wang, L. & Milas, L. Are cancer stem cells radioresistant? *Future Oncol.* **6**, 1563–76 (2010).
21. Phillips, T. M., McBride, W. H. & Pajonk, F. The response of CD24(-/low)/CD44+ breast cancer-initiating cells to radiation. *J. Natl. Cancer Inst.* **98**, 1777–85 (2006).

**KEITH JACOBS**  
kmjacobs@wustl.edu  
516-457-1859

**Home Address:**

4336 W Pine Blvd Rear  
St. Louis, MO 63108

**Work Address:**

Campus Box 8224  
4511 Forest Park Ave  
St. Louis, MO 63108

---

**PROFESSIONAL PROFILE**

Ph.D. Candidate in Molecular Cell Biology, researching mechanisms for stem cell radiosensitivity in the laboratory of Dennis Hallahan and Girdhar Sharma. Diverse research experience in cell biology, tissue dissection and DNA damage studies. Identified unique epigenetic regulators of stem cell radioresponses.

**HIGHLIGHTS**

- Upon graduation will have one first author review, one first author research publication and two second author publications, with another first author publication in progress.
- Extensive laboratory mentoring and educational outreach experience.
- Voted as 2<sup>nd</sup> best research presentation by faculty at 2014 MCB Program Annual Retreat.

**EDUCATION**

**Ph.D. Candidate – Molecular Cell Biology** (Expected Thesis Defense March 2015) Aug 2009 – present  
*Division of Biology and Biomedical Sciences (DBBS), Washington University in St. Louis*  
Current GPA: 3.62/4.00

**B.S. in Chemistry with specialization in Biochemistry (Minor in Biology)** Aug 2005 – May 2009  
*Graduated with Highest Distinction – University of Virginia (UVA)*  
Overall GPA: 3.69/4.00

**RESEARCH EXPERIENCE**

**Washington University PhD Thesis Lab** Aug 2010 – present  
*Laboratory of Dennis Hallahan / Girdhar Sharma, Department of Radiation Oncology*

- Determining the mechanisms responsible for the hypersensitivity of stem cells to ionizing radiation.

**Washington University DBBS Laboratory Rotations** Aug 2009 – Aug 2010  
*Laboratory of:*

- *Jason Weber* – examined the effect of the mTOR pathway on cellular growth and proliferation.
- *Daniel Link* – created and optimized a miRNA northern blot protocol for the lab.
- *Craig Micchelli* – investigated intestinal and muscle stem cells in *Drosophila*.
- *David Holtzman* – studied the effect of specific proteins on neonatal hypoxic injury in neonatal mice and Alzheimer's Disease.

**University of Virginia Medical School** Sep 2006 – Apr 2009  
*Laboratory of Dr. Roy Ogle, Department of Regenerative Medicine*

- Compared differentiation efficiency of adipose stem cells (ASCs) as opposed to bone marrow cells (BMCs) in order to show that ASCs are a better stem cell source than previously believed.

**Gerstner Sloan Kettering Graduate School** Jun 2007 – Aug 2007  
*Laboratory of Dr. Andrew Koff, Department of Cell and Molecular Biology*

- Researched the effect of p21 on glioma tumorigenesis and its interaction with PDGF signaling.

## **TEACHING EXPERIENCE**

- WU-CIRTL (Center for the Integration of Research, Teaching, and Learning) Community Member – completed four STEM Pedagogies Teaching Workshops Spring 2015
- Topic instructor – “Laser Microirradiation for Detecting Localized DNA Repair” – Washington University BIO 4933-Molecular Biology at the Cutting Edge. Feb 2015
- Lab Mentoring – multiple undergraduate students and summer technicians. 2011 – present
- Guest lecturer – Harris-Stowe State University BIO 0312-Introduction to Microbiology. Jan 2014
- Teaching Assistant – Washington University BIO 2960-Principles of Biology I. Jan 2011 – May 2011
- Tutoring – various biology and chemistry courses at UVA. 2006 – 2009

## **PRESENTATIONS**

- Talk – DBBS Molecular Cell Biology Program Annual Retreat. Oct 2013, 2014
- Talk – Multiple journal clubs and student research seminar series. 2009-2014
- Poster – 1<sup>st</sup> annual DBBS Cell and Molecular Biology Programs Symposium. Sep 2013
- Poster - 104th Annual Meeting of the American Association for Cancer Research. Apr 2013
- Poster – DBBS Developmental Biology Program Annual Retreat. Jun 2011, 2012, 2013
- Poster – DBBS Molecular Cell Biology Program Annual Retreat. Oct 2011, 2012
- Talk – UVA Chemistry Distinguished Majors Program Thesis Symposium. May 2009

## **AWARDS/RECOGNITION**

- Voted by faculty as 2<sup>nd</sup> best research talk at 2014 MCB Program Annual Retreat. Oct 2014
- Was one of only 17 applicants selected nationwide to attend the Fall 2014 American Society for Biochemistry and Molecular Biology (ASBMB) Hill Day – participated in active lobbying with congressman for increased science funding. Sep 2014
- Awarded Highest Distinction (summa cum laude) as a participant in the UVA Chemistry Distinguished Majors Program based on undergraduate thesis and research presentation. May 2009
- Received the Merck Index Award for exceptional performance in chemistry at UVA. May 2009
- Was among 3% of applicants accepted into the Summer Undergraduate Research Program at Memorial Sloan-Kettering Cancer Center. June 2007
- Obtained Dean’s List recognition 6 out of 8 semesters at UVA. Dec/May 2005-2009

## **OTHER ACADEMIC/LEADERSHIP EXPERIENCE**

### **Washington University Young Scientist Program (YSP) (<http://ysp.wustl.edu/>)**

- Director of Human Resources – Manage volunteer recruitment and participation, attend executive board meetings and implement new YSP programs. Jan 2013 – present
- Team leader for various programs and events – classroom visits, summer internship program, teacher lab experience program, teaching kits. May 2010 – Jan 2013

### **The Biotechnology and Life Sciences Advising Group (BALSA) (<http://www.thebalsagroup.org>)**

- Consultant and Project Manager – consulting for professors and biotech startups on technology patentability, market assessment, competitor analysis and pricing. July 2013 – present

### **Washington University DBBS Genetics Program Student Research Seminar**

- Co-coordinator – Organized and managed a weekly student seminar series. Sep 2010 – May 2011

## **CURRENT/EXPECTED PUBLICATIONS AND ACADEMIC CONTRIBUTIONS**

### **Research Papers**

- Jacobs KM**, Misri S, Meyer B, Raj S, Zobel CL, Sleckman BP, Hallahan DE, Sharma GG. Concerted epigenetic and signaling mechanisms regulate normal stem cell radiosensitivity. [Submitted].
- Zhao DY, **Jacobs KM**, Hallahan DE, Thotala D. Silencing the Egr1 transcription factor attenuates radiation-induced apoptosis in normal mouse tissues while killing cancer cells. Molecular Cancer Therapeutics. [In Review]
- Jacobs KM**, Meyer B, Zeng K, Zobel CL, Hallahan DE, Sharma GG. Inhibition of acetyltransferase p300 protects stem cells from IR-induced apoptosis. [In Progress]

### **Reviews**

- Jacobs KM**, Bhave SR, Ferraro, DJ, Jaboin, JJ, Hallahan DE, Thotala D. GSK-3 $\beta$ : A Bifunctional Role in Cell Death Decisions. Int J Cell Biol. 2012:930710, 2012.

### **Conference Abstracts**

- Jacobs KM**, Misri S, Meyer B, Raj S, Zobel CL, Sleckman BP, Hallahan DE, Sharma GG. Concerted epigenetic and signaling mechanisms regulate normal stem cell radiosensitivity. In: Proceedings of the 106th Annual Meeting of the American Association for Cancer Research. 2015 Apr 18-22; Philadelphia, PA. Abstract nr 3300.
- Meyer B, **Jacobs KM**, Raj S, Zobel CL, Sleckman BP, Hallahan DE, Sharma GG. The role of H3K9 acetylation and tri-methylation in stem cell radiosensitivity. In: Proceedings of the 106th Annual Meeting of the American Association for Cancer Research. 2015 Apr 18-22; Philadelphia, PA. Abstract nr 3299.
- Jacobs KM**, Misri S, Hallahan DE, Sharma GG. DNA Damage Response Contrasts in Stem and Differentiated Cells Contributing to Differential Radiosensitivities. In: Proceedings of the 104th Annual Meeting of the American Association for Cancer Research. 2013 Apr 6-10; Washington, DC. Abstract nr 1585.
- Zhao YD, **Jacobs KM**, Karvas R, Hallahan DE, Thotala D. Early growth response 1 is required for radiation-induced apoptosis in normal tissues. In: Proceedings of the 104th Annual Meeting of the American Association for Cancer Research. 2013 Apr 6-10; Washington, DC. Abstract nr 5945.
- Misri S, **Jacobs KM**, Hallahan DE, Sharma GG. Epigenetic regulation of normal stem cell radiosensitivity: A role for Long NonCoding RNAs. In: Ninth AACR-Japanese Cancer Association Joint Conference: Breakthroughs in Basic and Translational Cancer Research.
- Misri S, **Jacobs KM**, Hallahan DE, Sharma GG. Normal Stem Cells Elicit Hypersensitivity and Cell Death in Response to Ionizing Radiation. In: Proceedings of the 103rd Annual Meeting of the American Association for Cancer Research; 2012 Mar 31-Apr 4; Chicago, IL. Abstract nr 4350.

### **Database Contributions**

- Misri S, **Jacobs KM**, Hallahan DE, Sharma GG. Differential transcriptional responses of stem and differentiated non-stem cells to ionizing radiation exposure. NCBI Gene Expression Omnibus 2013. Series GSE44780.

## **PERSONAL INTERESTS**

- Science blogging – <http://blabberingbiologist.blogspot.com/>
- Playing various sports – tennis, soccer, golf
- Musical theater